

IEROM Image Processing Pipeline and 3D Real-Time Interactive Visualization Methods for Teravoxel Volumes

A thesis submitted in partial fulfillment of the

requirements for the degree of

Master of Science

in

Computer Engineering

by

Akanksha Ashwini

Kettering University, Flint, MI

Fall 2016

This thesis is approved for recommendation to the Graduate Council.

Jungme Park, Thesis Director

Assistant Professor (ECE Dept., Kettering University)

Jaerock Kwon, Committee Member

Assistant Professor (ECE Dept., University of Michigan Dearborn)

Giuseppi Turini, Committee Member

Associate Professor (CE Dept., Kettering University)

**IEROM Image Processing Pipeline and 3D Real-Time Interactive Visualization
Methods for Teravoxel Volumes**

Copyright 2016
by
Akanksha Ashwini

Abstract

IEROM Image Processing Pipeline and 3D Real-Time Interactive Visualization Methods for Teravoxel Volumes

With high-throughput and high-resolution imaging technologies such as Knife-Edge Scanning Microscopy (KESM), it is possible to acquire teravoxel sized three-dimensional neuronal and microvascular images of the whole mouse brain with sub-micrometer resolution. It is imperative to be able to visualize and share these teravoxel volumes efficiently, to facilitate group efforts from research communities. However, due to the immense size of the data sets, sharing and managing them have always been a big challenge. This thesis describes an image processing pipeline for a real-time 3D visualization framework that allows research groups to work in collaboration. The proposed work can visualize and share terabyte-sized three-dimensional images for study and analysis of mammalian brain morphology. Although the image processing pipeline used a KESM data set to show the feasibility of it, the proposed pipeline can also be used for other larger data sets. We believe that this novel framework for Web-based real-time 3D visualization can facilitate data sharing of teravoxel volumes across research communities.

The whole mouse brain vasculature data acquired by the IEROM is a motley bunch of interconnected blood vessels. To properly study and analyze the architecture of such data sets, there is a need of sophisticated visualization methods which can deduce even minor morphological details accurately. With the advancement of Virtual Reality (VR) in the field of biomedical image visualization, it is now possible to design VR frameworks to visualize and interact with 3D biomedical images. The idea is to use VR to visualize and comprehend large and complex biomedical datasets for better detailed understanding. Therefore, in this thesis, I will explain my approach to create such a VR framework for the study and analysis of mouse brain vascular networks through better visualization and interaction techniques. The aim is to load the mouse brain vascular data (teravoxel volumes) created using the image processing pipeline (explained in this thesis) in a virtual reality space and be able to walk-through the structure and interact with it. The proposed framework supports multi-resolution data switching and proposes a novel data mapping method to select and load the teravoxel volume from the local disk space at run-time.

*I dedicate this thesis
to my strength, my mother,
Mrs. Rashmi Sinha,
to my inspiration, my father,
Late Dr. Ashwini Sinha
and my sister & brother-in-law
Mrs. Annie Sinha & Mr. Neeraj Kumar.
Thank you all, for the unconditional love and support.*

Contents

Contents	ii
List of Figures	v
List of Tables	vii
I Introduction	1
1 Introduction	2
1.1 Background	3
1.2 Related Work	4
1.3 Overview and Thesis Structure	7
II Image Processing Pipeline : Principles and Methods	10
2 Image Processing Pipeline for IEROM Dataset	11
2.1 Overview	11
2.2 Image Processing Pipeline Design	11
2.3 Tools and Software used to design the Image Processing Pipeline	14
2.4 Controller-Worker Model	15
3 Stitching of Column Images	16
3.1 Overview	16
3.2 Input for Image Stitcher	16
3.3 Image Sticher	17
3.4 Output of Image Stitcher	20
3.5 Challenge	20
4 Sub-Sampling of Image Stacks	22
4.1 Overview	22
4.2 Input for Sub-Sampler	22

4.3	Sub-Sampler	23
4.4	Output of the Sub-Sampler	24
4.5	Challenges	25
5	Unit-Volume Creation	27
5.1	Overview	27
5.2	Input for Unit-Volume Creator	28
5.3	Unit-Volume Creator	28
5.4	Output of the Unit-Volume Creator	30
5.5	Challenges	33
6	Making 3D Models and Meshes	34
6.1	Overview	34
6.2	Input for the 3D Model Maker	34
6.3	3D Model Maker	35
6.4	Output of the 3D Model Maker	37
6.5	Challenges	37
III Web-Based 3D Visualization Framework : Implementation		40
7	<i>3D Brain Atlas: Web-Based Real-Time 3D Visualization Framework</i>	41
7.1	Overview	41
7.2	Tools and Environment Settings	42
7.3	Input Data Set	43
7.4	Graphical User Interface Design	43
7.5	Results	46
7.6	Challenges	46
IV Virtual Reality Framework : Methods and Implementation		48
8	Virtual Reality for Mouse Brain Vascular Network Study	49
8.1	Overview	49
8.2	Tools and Environment Settings	50
8.3	Input Data Preparation	65
8.4	Mouse Brain as a GameObject in Unity	65
8.5	Challenges	71
9	Gesture Controlled Navigation Method	72
9.1	Overview	72
9.2	Required Input	72
9.3	Basics of Scripting in Unity	73

9.4	Gesture Controller	75
10	User-Interface for the Virtual Reality Framework	80
10.1	Overview	80
10.2	Required Input	80
10.3	Basics of UI Designing in Unity	81
10.4	Walk-Through the User-Interface Design	81
10.5	Challenges	88
V	Conclusion and Future Work	90
11	Conclusion and Future Work	91
11.1	Image Processing Pipeline Improvement	91
11.2	Web-Based Framework Additions	91
11.3	Virtual Reality Framework Additions	92
11.4	Conclusion	92
VI	Appendix	94
A	Image Processing Pipeline Code	95
A.1	Image Stitcher block	95
A.2	Sub Sampler block	95
A.3	Unit Volume Maker Block	95
A.4	3D Model Maker Block	96
B	Web-based GUI Code	97
B.1	3D Brain Atlas	97
C	Virtual Reality Framework Code	98
	Bibliography	99

List of Figures

1.1	Knife edge tissue sectioning in KESM. (Adopted from [8])	3
1.2	Optic train and knife assembly. (Referred in [32])	5
2.1	The four steps of the image processing pipeline creates 3D unit images out of the scanned raw column images acquired by IEROM. (Image Acquisition image adopted from [32])	12
3.1	Image stitcher block overview.	17
3.2	Tiling order of the column images.	19
3.3	Tiled image binarized to get clear tissue-areas and low background artifacts. . .	19
3.4	Dummy image appended after stitching of the images from different columns. . .	21
4.1	Sub-sampler block overview.	23
4.2	Theoretical representation of the sub-sampler output.	25
4.3	Overcrowding of data caused by binarization and sub-sampling seen during volume visualization.	26
5.1	Unit-images created from an input image.	29
5.2	Unit-volume image stack creation.	31
5.3	Creation of one temporary directory and corresponding unit-stack directories. . .	32
6.1	Unequal spacing observed in the 3D STL meshes.	38
6.2	Iso-surface selection for the multiple resolution <i>unit-volumes</i>	39
7.1	3D Brain Atlas loaded with the smallest resolution volume file.	44
7.2	STL meshes of different resolutions loaded according to the region of interest selected by the user.	47
8.1	Unity default setup with different views and windows [36].	52
8.2	A default scene in <i>Unity</i> with the <i>main camera</i> and <i>directional light</i> [36].	53
8.3	A sample gameobject in <i>Unity</i> called <i>Cube</i> and its inspector window options [36].	54
8.4	Oculus Rift Kit [30].	55
8.5	Oculus <i>Remote Controller</i> specifications [14].	57
8.6	Oculus Sensor and its field of view [30].	58

8.7	Combined optimal tracking volume when two sensors can see the headset controller [30].	59
8.8	Oculus Headset Specifications [30].	60
8.9	Leap Motion Controller Setup [19].	61
8.10	Leap Motion Controller mounting on the Oculus Rift [37].	62
8.11	Enabling VR option in Unity [36].	63
8.12	Using the Leap Motion core assets in Unity [18].	65
8.13	Imported mouse brain model settings.	68
8.14	Unity breaks up any high-poly model prefab into sub-models based on the maximum vertex limit.	70
8.15	Transform settings of the imported mouse brain model.	70
9.1	Gesture Controller Component options open in the inspector window.	75
9.2	Right hand gesture change required to activate the 3D joystick.	76
9.3	Different gestures used to navigate inside the unit volume loaded to the VR framework.	79
10.1	Canvas options appearing on the detection of left hand gesture change from closed fist to open palm.	82
10.2	UI Controller component options and the main canvas options.	83
10.3	Object Manager component options for the lowest resolution volume loaded in the scene in Unity.	84
10.4	Obj Reader component options selected for the unit volume loaded.	86
10.5	Reset Camera component options in the inspector window.	89

List of Tables

2.1	Results of the image stitcher block used for the vascular networks dataset	13
2.2	Results of the sub-sampler block used for the vascular networks dataset	14
3.1	Vascular networks dataset input for the image stitcher block	18
3.2	Output of the image stitcher block for the vascular networks dataset	20
4.1	Output of the sub-sampler block for the vascular networks dataset.	24
5.1	Common terms used with respect to volume maker block	28
5.2	Output of the unit-volume maker for the vascular networks dataset.	33
6.1	Results of the 3D model maker block for the vascular network dataset.	37
7.1	List of mouse control modes used for interacting with the renderer. I used the above mouse control modes for panning, zooming in and zooming out operations.	45
7.2	List of keyboard control modes used for interacting with the renderer. When multiple renderers exist in the document, the one under the mouse listens to the keyboard interaction.	46
8.1	List of Unity Utilities to support Oculus VR devices.	51
8.2	List of Oculus Remote button's functionalities.	56
8.3	System Specifications of a computer required to power-up the connected Oculus VR device.	61
8.4	Leap Motion Core Asset Prefabs and their Use Cases.	66
8.5	3D space translation of the user's movement in virtual reality framework.	67
9.1	Execution order of some editable event functions while scripting in Unity.	74
10.1	The 8 split parts of the lower resolution mapped to the 8 unit volume models in the higher resolution.	85

Acknowledgments

I wish to express my sincere appreciation to Prof. Jaerock Kwon for his guidance throughout my research term at Kettering, I am thankful for the opportunity he gave me. I had a great learning experience while working as a research assistant at Kettering. I learned about biomedical research work, concerning the human brain study, which was a new field to experience. However, Prof. Kwon understood my interests and helped me channel them into meaningful work. He provided me with very valuable lessons on how to write research papers and be a better researcher.

I would like to pay my special regards to Prof. Giuseppi Turini for his constant support during my thesis. I am thankful to him for teaching me application development for the virtual reality framework and helping me create the split dataset for the Unity game engine, which was required for this thesis experiment. I would like to offer my special thanks to Prof. Ravi Warriar, for his support and encouragement throughout my Kettering journey, and Prof. Jungme Park, for agreeing to be my primary advisor in the absence of Prof. Jaerock Kwon.

The technical contributions of the Brain Networks Laboratory at Texas A&M University are truly appreciated. They laid the foundation for the imaging technique that made the instrument possible. I wish to acknowledge the help provided by my lab-mate Mrs. Shruthi Raghavan, for me to better understand the research work and pre-process the raw images acquired by the instrument.

I am grateful for the encouragement and great love of my family, my mother, Mrs. Rashmi Sinha; my sister, Mrs. Annie Sinha; and my brother-in-law, Neeraj Kumar. They kept me going and this work would not have been possible without their support. I also want to express my gratitude to my beloved husband, Mr. Mahesh Kabra, for believing in me and being extremely supportive in all my endeavors.

I want to thank Mrs. Shruthi Raghavan and her husband Mr. Rahul Rangarajan, who welcomed me as a family member and made my transition to the new country very easy. I also want to thank Mr. Pratin Naik, who helped me stay sane during stressful times, with his encouraging words and witticism.

Part I

Introduction

Chapter 1

Introduction

Today researchers have implemented numerous ways to study the mammalian brain. It is believed that many of the human brain illness and diseases can be cured by understanding the abnormalities in the brain morphology. Accurate microvascular morphometric information from the brain has significant implications in fields including the quantification of angiogenesis in cancer research, the study of immune response for neural prosthetics, and predicting the nature of blood flow as it relates to stroke.

For decades, scientists have routinely used mice as a primary model for brain research. Rodents can be a good model for humans because a lot of the structure and connectivity that exists in human brains also exists in rodents. It is said that Rodents are genetically similar to humans, they have shorter lifespans, enabling scientists to study their brain structure across generations if desired. Therefore, a lot of research performed today for the study of the human brain uses a mouse brain for experiments.

Connectomics[38] aims to map the full connection matrix of the brain. A vast variety of methods and approaches have been developed for vascular extraction, analysis, and modeling with increasing complexity[21]. Knife-Edge Scanning Microscopy (KESM) being the first instrument of this technique allows imaging of the whole mouse brain microvascular system at resolutions sufficient to perform accurate morphometry. With such high-throughput and high-resolution imaging technologies, it is possible to acquire teravoxel sized three-dimensional neuronal and microvascular images of the whole mouse brain with sub-micrometer resolution. Besides having such efficient image acquisition system available. It is also imperative to be able to visualize and share these teravoxel volumes efficiently, to facilitate group efforts from research communities. However, due to the immense size of the data sets, effectively visualizing, sharing and managing them have always been a big challenge.

This thesis describes an image processing pipeline for handling such huge teravoxel volumes, a web-based real-time 3D visualization framework that allows research groups to work in collaboration and a virtual reality framework for fully-interactive scientific visualization of the mouse brain data. The proposed work can visualize and share terabyte-sized three-dimensional images for study and analysis of mammalian brain morphology. Although the

image processing pipeline used a KESM data set to show the feasibility of it, the proposed system can also be used for other larger biomedical data sets. The virtual reality application provides researchers a novel way to be able to step into the 3D visualization framework to explore and fully interact with the mouse brain data.

1.1 Background

Knife-Edge Scanning Microscopy

KESM is one of the first instruments to achieve whole-mouse-brain-scale imaging at sub-micrometer resolution [26][17][24]. KESM is the technique of concurrently slicing and imaging tissue samples at sub-micrometer resolution with a high resolution and high sensitivity digital line camera.

Three-dimensional light microscopy in medical imaging needs continuous automated sectioning method to automate the process. This can be achieved by either optical sectioning or physical sectioning using a suitable sample and movement stage. However, to obtain high-resolution volumetric tissue structure data at high throughput, it is preferred to use physical sectioning. Optical sectioning is disadvantageous because of the depth resolution limitation and the trade-off between signal quality and disruptive background noise such as tissue data from out-of-focus imaging planes.

Since the slicing and imaging happens simultaneously in KESM, the overall throughput of the system is high. Each slice is an aggregation of multiple line images. It also preserves image registration throughout the depth of the tissue block and eliminates undesirable events such as back-scattering of light and bleaching of fluorescent-stained tissue below the knife. The tissue is stained and embedded in either LR-White or Araldite to make it stiff, as it is

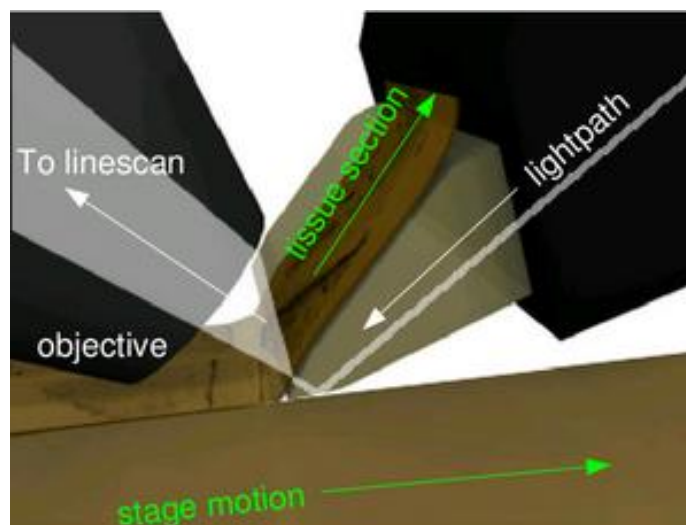


Figure 1.1: Knife edge tissue sectioning in KESM. (Adopted from [8])

important to have the tissue rigid and wrinkle-free during cutting to achieve sub-micrometer thickness. The tissue sample being sliced by the knife is imaged just above the knife edge by a powerful line scan camera (See Fig.1.1). The image capture mechanism is triggered based on the encoded position of the tissue being sliced, which ensures that every sectioning results in an image capture. The KESM can image a 1cm^3 tissue block in approximately 50 hours at a voxel resolution of $0.6\mu\text{m}\times 0.7\mu\text{m}\times 1.0\mu\text{m}$. While sectioning and imaging, the width of the tissue slice is not exactly as the field of view of the objective. Thus, there are additional non-tissue areas that appear as dark regions on either side of the tissue in every image. The additional region causes a significant increase of memory required to store the images and process them. Each tissue sample imaged by the KESM can generate up to around 80,000 images (the tissue is laterally sectioned several times, and each column has around 10,000 images). Thus, to extract tissue region manually requires a lot of time and effort and is inefficient. With an aim to automate this process, a template-matching based method was proposed for tissue extraction from the KESM image stacks [8] and was later improved [32]. After the tissue region extraction, intensity levels are normalized, and the clean images are stored in the column stacks.

Internet Enabled Robotic Microscopy

The Internet Enabled Robotic Microscope (IEROM) (see Fig. 1.2), the second generation of microscope based on KESM, is a low-cost and more robust version of the first prototype. It aims to overcome the limitations of the first generation prototype by making the instrument less expensive, flexible, less bulky and occupy a smaller footprint. The cost is reduced by changes such as using LED illumination instead of laser illumination. The optics train design is modular and flexible. This provides an easily operable, flexible platform for biomedical researchers across different domains such as neuroscience and vascular research. The IEROM promises to be commercially viable and indispensable to biomedical researchers.

1.2 Related Work

With high-throughput and high-resolution imaging technologies such as KESM, it is possible to acquire teravoxel sized three-dimensional neuronal and microvascular images of the whole mouse brain with sub-micrometer resolution. The Web-based framework explained in this thesis, is a real-time platform for the 3D visualization and sharing of such teravoxel volumes, facilitating group efforts from research communities. The proposed work can visualize and share terabyte-sized three-dimensional images for study and analysis of mammalian brain morphology. To show the feasibility of it, the image processing pipeline for the framework uses the KESM data set, but the proposed system can use any other larger data sets.

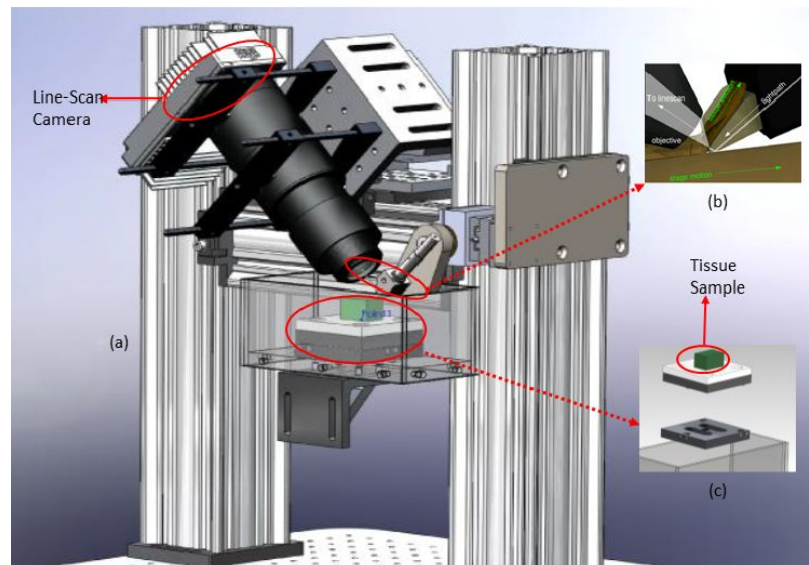


Figure 1.2: Optic train and knife assembly. (Referred in [32])

(a) shows the entire setup of the optic train resting on a stable platform supported by dense-sand filled pillars. (b) The light from the LED passes through the diamond knife that acts as a collimator with the help of ball lenses and enables imaging of the tissue as it is being sectioned. (c) It has fiducials to register the position of tissue and ensures registration even in case of removal during slicing or any other interruptions by magnetic coupling to the bottom plate.

The Mouse Atlas Project (MAP)

Mackenzie Graham developed a probabilistic atlas of the adult and developing C57BL/6J mouse. The MAP consists of not only data from Magnetic Resonance Microscopy (MRM) and histological atlases, but also a suite of tools for image processing, volume registration, volume browsing, and annotation. The MAP will produce an imaging framework to house and correlate gene expression with anatomic and molecular information drawn from traditional and novel imaging technologies. This digital atlas of the C57BL/6J mouse brain is composed of volumes of data acquired from μ MRI, block-face imaging, histology, and immunohistochemistry. MAP technology provides the infrastructure for the development of the Allen Brain Atlas [23]. Also, see the related Mouse BIRN (Biomedical Informatics Research Network)[16][3].

Allen Brain Atlas

The Allen Brain Atlas contains detailed gene expression maps for $\approx 20,000$ genes in the C57BL/6J mouse [20]. A semi-automated procedure was used to conduct in situ hybridization and data acquisition on $25\mu\text{m}$ thick sections (z-axis) of the mouse brain. The x-y axis

resolution of the images ranges from $0.95\mu\text{m}$ to $8\mu\text{m}$. The Allen Brain Atlas is the first comprehensive gene expression map at the whole-brain level and is currently accessed over 4 million times per month, with over 250 scientists browsing the data on a daily basis.

The Mouse Brain Library (MBL)

MBL is developing methods to construct atlases from celloidin-embedded tissue to guide registration of MBL data into a standard coordinate system, by segmenting each brain in its collection into 1,200 standard anatomical structures at a resolution of $36\mu\text{m}$ [34]. Algorithms are to be designed to segment each brain in the MBL into a set of standard anatomical structures like those defined in the rat atlas produced by Computer Vision Laboratory for Vertebrate Brain Mapping at Drexel College of Medicine, whose computerized 3D atlas was built from stained sections for the mouse brain that reconstructs Nissl-stained sectional material, a $17.9\mu\text{m}$ isotropic 3D data set, from a freshly frozen brain of an adult male C57BL/6J mouse.

BrainMaps.org

Brain Maps.org is an internet-enabled, high-resolution brain map [27]. The map contains over 10 million megapixels (35terabytes) of scanned data, at a typical resolution of $\approx 0.46\mu\text{m}/\text{pixel}$ (in the x-y plane). The atlas provides an intuitive Web-based interface for easy and bandwidth efficient navigation, through the use of a series of sub-sampled (zoomed out) views of the data sets, similar to the Google Maps interface. Even though the x-y plane resolution is below $1\mu\text{m}$, the z-axis resolution is orders of magnitude lower (for example, one coronal brain set has 234 slides in it, corresponding to a sectional thickness of $25\mu\text{m}$). The database also serves serial sections from electron microscopy, cryosections, and immunohistochemistry, and hosts a total of 135 data sets (as of March 2, 2011).

Whole-Brain Catalog (WBC)

WBC is a 3D virtual environment for exploring multiple sources of brain data (including mouse brain data), e.g., Cell Centered Database (CCDB), Neuroscience Information Framework (NIF), and the Allen Brain Atlas (see above). WBC has native support for registering to the Waxholm Space, a rodent standard atlas space [15]. It supports multiple functionalities including visualization, slicing, animations, and simulations. In summary, there are several mouse brain atlases available, with data from different imaging modalities, but their resolution is not high enough in one or more of the x , y , or z axes to show the morphological detail of neurons.

Knife-Edge Scanning Microscopy Brain Atlas (KESMBA)

KESMBA [9] framework has been designed and implemented to allow the widest dissemination of KESM mouse brain circuit data by overlaying transparent layers of images with distance attenuation. Overlaying image stacks containing two intertwining objects to get minimum intensity projection results in the loss of 3D information. Although, interleaving each image with semi-opaque blank images brings out the 3D information. Still, KESMBA provides a pseudo 3D visualization as it stacks the semitransparent image slices for not more than 30 layers at once.

Terafly - Vaa3D plugin

Terafly is a Vaa3D plugin [5] for real-time 3D visualization of terabyte sized volumetric images. Vaa3D, which is an open-source, cross-platform system, extended its powerful 3D visualization and analysis capabilities to images of potentially unlimited size with this plugin. When used with large volumetric images up to 2.5 Terabyte in size, Vaa3D-TeraFly exhibited real-time (sub-second) performance that consistently scaled on image size. TeraFly can generate a 3D region of interest (ROI) by subsequent fetching and rendering of image data at higher resolutions, thus enabling fast (sub-second) visualization of Terabyte-size images. It exhibits real-time performance regardless of image size when used on both high and medium-end computers. However, the performance is constrained on a local computer and cannot be directly used to share 3D visualization results of terabyte-sized data sets among research groups.

1.3 Overview and Thesis Structure

Modern high-throughput and high-resolution 3D bioimaging technologies such as Knife-Edge Scanning Microscopy (KESM) have enabled imaging and reconstruction of the whole mouse brain architecture at sub-micrometer resolution. The KESM performs simultaneous serial sectioning and imaging of the whole mouse brain and generates data sets that include: neuronal circuits (Golgi stained), soma distribution (Nissl stained), and vascular networks (India ink-stained). The data sets are multi-scaled images, ranging from sub-cellular ($< 1\mu\text{m}$) to the whole organ scale ($\approx 1\text{cm}$). The KESM scans a 1cm^3 tissue block in approximately 50 hours at a resolution of $0.6\mu\text{m}\times 0.7\mu\text{m}\times 1.0\mu\text{m}$. It then stores the scanned biological tissue data digitally in the form of stacked 2D images, the size for which is $\approx 2\text{TB}$. Then, through a processing pipeline, these stacked 2D images are converted into volumes composed of terabytes of voxels, referred as *Teravoxel Volumes*. Due to immense size and multi-scale nature of the data set, efficiently visualizing and sharing them among research communities for analytical studies have always imposed challenges on researchers.

3D visualization helps users to understand the morphology of the biological organ. At the same time, efficiently sharing the data across research communities is also essential for review

and feedback. Terafly [31][5] is an open-source Vaa3D [22] plug-in to support 3D visualization of immensely sized biomedical images. Although the tool is efficient in visualizing terabyte-scale images, the plug-in toolkit is a stand-alone software package that is required to be installed on local computers. Also teravoxel data must reside on the same computer or local network resources. This hinders the research communities to work in collaboration with data sets. On the other hand, there have been efforts to develop web-based applications to visualize neuronal circuits and microvascular data sets (e.g., The Mouse Atlas Project, Allen Brain Atlas [20] and Knife-Edge Scanning Microscopy Brain Atlas (KESMBA) [9]). These applications allow centralization of data sets and facilitate sharing of visualization results. Yet they are not efficient real-time 3D visualization methods. For instance, Allen Brain Atlas based on the Mouse Atlas Project does not support high-resolution data visualization (details will be in the next section). KESMBA provides pseudo-3D visualization through stacking of semitransparent image slices. The maximum number of layers is 30. It takes time for KESMBA load all the layers before it displays. Also, it is just layered and attenuated 2D image stacks. This creates a need for the development of technologies which facilitate efficient 3D visualization along with centralization of teravoxel volumes.

In this thesis, I will discuss the implementation of an image processing pipeline for a Web-based real-time framework for 3D visualization of teravoxel volumes, such as the microvascular data set obtained by the KESM. This pipeline is capable of visualizing both terabyte volumes in real-time. Since the proposed framework is Web-based, visualization is entirely independent of the underlying operating system. Through the framework, 3D visualized data sets can be accessed easily so that it facilitates sharing of results across research communities. It even overthrows the necessity of downloading large data sets or installing any software. Out of the several other advantages of using Web technology, one of the most important features is the great level of interoperability achieved that results in faster switching and visualization of multi-resolution volumes. The web-based framework is currently implemented using a mouse brain vascular dataset from KESM. Also, since we intend to share and study KESM dataset only, we do not require any spatial database to manage them. However, the approach can be implemented for any other biomedical dataset of any size. The visualization of a volume of a region of interest (ROI) currently depends on the manual selection input from the user. But the process of switching between different resolution volumes through user's mouse scroll input can be automated later as a part of future work. The graphical user interface is designed to display a polygon mesh from a $256 \times 256 \times 256$ volume. The user can explore the dataset by selecting a region of interest to display at a particular resolution. Thus, different sections of the whole-mouse-brain at various resolutions can be visualized in real-time. This kind of visualization will be similar to one obtained in the Vaa3D [22] plugin: Terafly [31][5] or the Google Earth application.

Another major part of this thesis discusses the implementation of a virtual reality framework for a fully-interactive and immersive 3D visualization experience with the mouse brain. Effective data visualization is the demand of the era of *big data* and immersive virtual reality provides benefits beyond the traditional desktop visualization tools. Understanding the complex microvascular network of the brain in such a platform leads to better perception of

the morphology, more intuitive data understanding and a better retention of the perceived relationships in the data structure. With the VR framework designed for the KESM data, it is possible to navigate inside the mouse brain structure and load different resolution data set prepared by the image processing pipeline.

This thesis has been divided into three logical parts. The first part describes the image processing pipeline implemented, the second part discusses the web-based 3D visualization framework design, and the third part introduces the virtual reality framework for the KESM data set. The mouse brain data-set used in this thesis are those imaged by the Brain Tissue Scanner in the Brain Networks Laboratory at Texas A&M University in 2008 and is from a C57/BL6 mouse specimen. It is a *India Ink* stained vascular network data set, labeled with the mouse brain id: MOU1_BRA_IND_2008_04.

Part II

Image Processing Pipeline : Principles and Methods

Chapter 2

Image Processing Pipeline for IEROM Dataset

2.1 Overview

The imaging techniques implemented in the IEROM can reconstruct the mouse brain with microscopic resolution. However, the architecture of a Mammalian Brain cannot be understood properly in a single-cell resolution. So, I designed the Image Processing Pipeline for IEROM to create multi-resolution unit volumes which can help visualize and study the structure of the biological organ efficiently.

During the image acquisition stage, the IEROM scans a 1cm^3 tissue block in approximately 50 hours, at a resolution of $0.6\mu\text{m}\times 0.7\mu\text{m}\times 1.0\mu\text{m}$. It then stores the scanned biological tissue data digitally in the form of stacked 2D images, the size for which is $\approx 2\text{TB}$. However, the dataset obtained from the automated microscope cannot be directly used for visualization or feature extraction. The images contain background noise and additional artifacts that needs to be alleviated, before it can be clearly visualized and further processed. Therefore, after the acquisition of images, initial pre-processing steps are executed to remove any unwanted noise or artifacts from the images. [32].

After the pre-processing of images, I got 2D column stacks of clean images containing only tissue areas from the mouse brain. Through the image processing pipeline explained in this chapter, these stacked 2D images are then converted into volumes composed of terabytes of voxels, referred as *Teravoxel Volumes*.

2.2 Image Processing Pipeline Design

The complete implementation of the image processing pipeline for IEROM[2] is divided into four stages (see Fig. 2.1):

- Stitching of 2D images across column stacks to create a single 2D image stack of microscopic resolution images.
- Sub-sampling of the images in the stack (created after stitching), to generate multiple resolution image stacks.
- Creating unit-image stacks of 256 images, where a unit is defined as a resolution of 256×256 . These unit-image stacks are pre-requisite for making 3D models of unit-volumes.
- Making 3D models of different formats from the unit-image stacks.

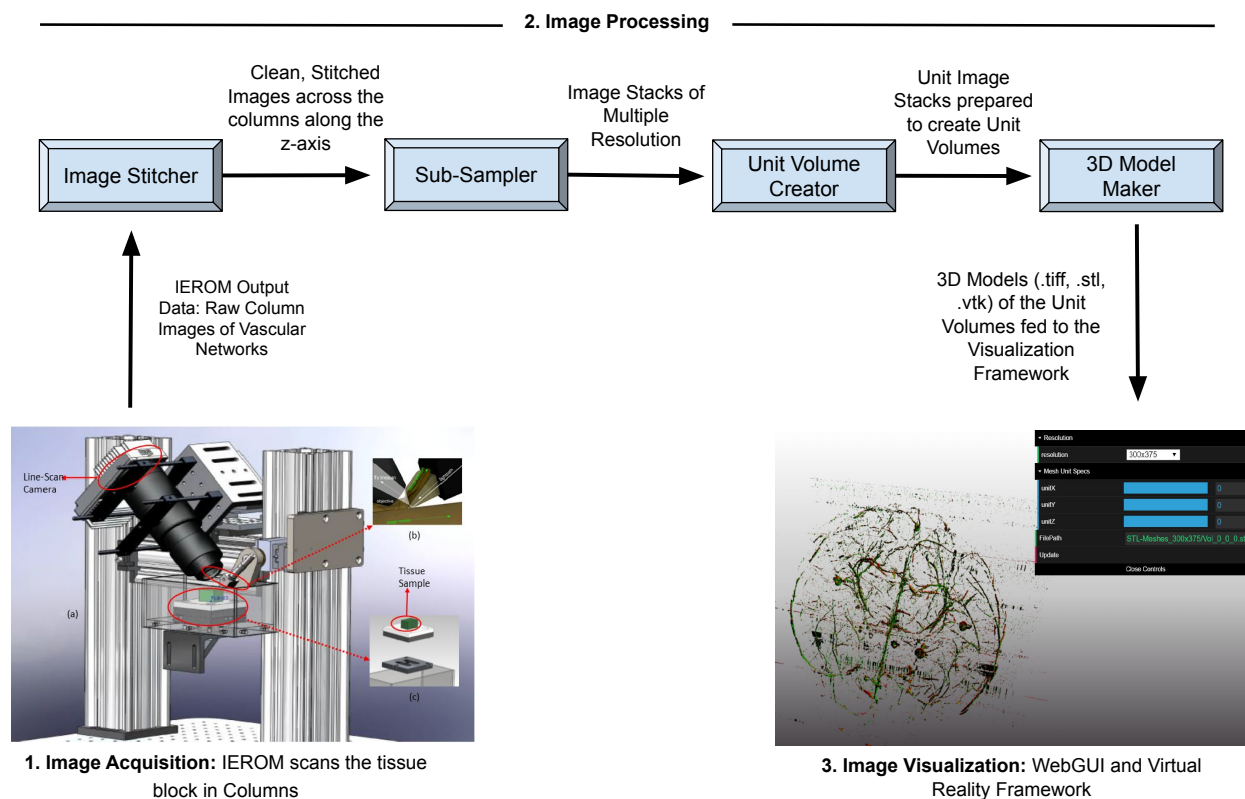


Figure 2.1: The four steps of the image processing pipeline creates 3D unit images out of the scanned raw column images acquired by IEROM. (Image Acquisition image adopted from [32])

Image Stitcher Block

The images received after the acquisition and pre-processing steps are clean, without any artifacts and noise, with only tissue areas, but are in the form of column stacks. Each column

store images for a specific section of the tissue. Since during IEROM serial sectioning, the images scanned for a particular part of the tissue are stored in a single column stack. So each column stack is from a different starting point along the y -axis. Although, the width and height of the images in each column stack remains same.

To test this pipeline, I used the scanned data set created by the KESM in the year 2008. The scanned files are saved in the column stacks and are named in such a manner that they provide information about the year and date of scanning, x-position, y-position, z-position, time, the speed of sectioning, and orientation of the knife. As a part of the pre-processing step, the images in the columns are filtered for the non-tissue areas and the files with no tissue areas are removed. This process reduced the number of column stacks eventually (from six to four, in my case for the vascular networks dataset).

The Image Stitcher block will stitch the images across the columns along the z -axis. The image files with the same z -position value are tiled together to form a larger image. Table 2.1 summarizes my experiment results, where the sliced images from the four columns were tiled together for a particular z value.

Each Column Image Resolution	2400×12000
Tiled Image Resolution	9600×12000

Table 2.1: Results of the image stitcher block used for the vascular networks dataset

Sub-Sampler Block

This block will create multi-resolution image stacks from the original microscopic resolution image stack. The image stack created by the Image Stitcher block has images of the highest possible resolution for the images acquired by the IEROM. The only way to create multiple resolution images without hampering the quality of images is to sub-sample them.

The sub-sampler block will create image stacks of resolution half of the input image stack. For example, if I sub-sample the original stitched images of resolution $x \times y$, I will end up in an image stack with images of resolution $x/2 \times y/2$. The sub-sampler block will continuously sub-sample the image stack till the smallest resolution image stack is achieved.

For example, in my case, the sub-sampling was performed five times to achieve the smallest resolution. This process created six different resolution image stacks, summarized in Table 2.2.

Unit Volume Creator Block

The higher resolution volumes are difficult to visualize together, due to their immense size. Breaking such large volume data set into smaller volumes makes it easier and efficient for the user to visualize and study the sections of the mouse brain.

Original Image Resolution	9600 × 12000
First Sub-sampled Image Resolution	4800 × 6000
Second Sub-sampled Image Resolution	2400 × 3000
Third Sub-sampled Image Resolution	1200 × 1500
Fourth Sub-sampled Image Resolution	600 × 750
Fifth Sub-sampled Image Resolution	300 × 375

Table 2.2: Results of the sub-sampler block used for the vascular networks dataset

This block basically creates unit-image stacks where a unit is a predefined chosen size of 256. The idea is to create image stacks which can be used to directly create volumes of equal dimensions across all three axes, i.e., $256 \times 256 \times 256$. So the unit-image stacks have 256 image files, each of resolution 256×256 . The unit-image stacks are extracted and cropped out from all the different resolution image stacks.

3D Model Maker Block

As the name suggests this block creates the 3D models out of the unit-volumes. The methods implemented so far is capable of creating 3D models and meshes in .tiff, .stl, and .vtk formats. However, the approach can be extended to create other visualization formats as well.

2.3 Tools and Software used to design the Image Processing Pipeline

The Insight Segmentation and Registration Toolkit (ITK)

ITK is an open-source software toolkit, implemented in C++, that provides algorithms for performing registration and segmentation to multidimensional data. Segmentation is the process of identifying and classifying data found in a digitally sampled representation. Registration is the task of aligning or developing correspondences between data. ITK is widely used for medical image processing. However, It does not include methods for displaying images, nor a development environment or an end user application for exploring the implemented algorithms.

The Visualization Toolkit (VTK)

VTK is an open-source, freely available software system for scientific visualization, information visualization, 3D computer graphics, modeling, image processing, and volume rendering. VTK is implemented as a C++ toolkit, requiring users to build applications by combining various objects into an application.

2.4 Controller-Worker Model

All the above methods were implemented using a *controller-worker* model. Each block explained above has its own *controller* and *worker*. A *worker* is the one which make changes; execute functions utilizing ITK and VTK libraries. Whereas, a *controller* is the one which decides what files are to be passed to the *worker* and even controls the *worker* execution. This model has been applied to avoid time delays, generally caused due to looping over the same task. Here, each time a task is to be executed, the *controller* code simply calls the *worker* application which performs that task. Since all the *controllers* are written in Qt and do not use any ITK/VTK libraries, the complete design is a cross-platform solution.

Chapter 3

Stitching of Column Images

3.1 Overview

After the serial sectioning performed in IEROM, the raw data set of 2D images is stored in the form of stacks and columns. The tissue area from each raw image is automatically cropped and saved, so each column contains images of only tissue area from the mouse brain. The images in each column are further processed; the noise is removed, and image intensity is normalized for each cropped image. Then the images at the same z coordinate are stitched across the columns in an image sheet. ITK filters are utilized to perform the stitching algorithm. we implemented the image intensity normalization algorithm, previously proposed for KESM image stacks[32].The outcome of this process is a single stack of 2D images with clean prominent tissue areas.

For the course of this thesis, the raw images of vascular networks of the mouse brain were initially scanned and further cleaned to result in four columns (stacks of images).The resolution of each image of a column stack was 2400×12000 (this number could vary depending upon the data set used and the scanner setup). After the stitching operation, I finally got a stack of 9626 images each of resolution 9600×12000 (See Fig.3.1).

3.2 Input for Image Stitcher

The IEROM performs serial sectioning of the whole mouse-brain tissue. The thin slices of the tissue are simultaneously cut and imaged. All the serially scanned images are then stored digitally in the form of stacks and columns. Each serially cut section is of the same width as that of the knife edge. The line scan camera scans and stores the images with their x and y coordinate information. The images with same x and y coordinates are stored in a column stack. So, each column stack has images with same x and y coordinates but different z coordinates. These images are further cropped and normalized. The image files are finally stored across several column stacks or directories, where the number of directories

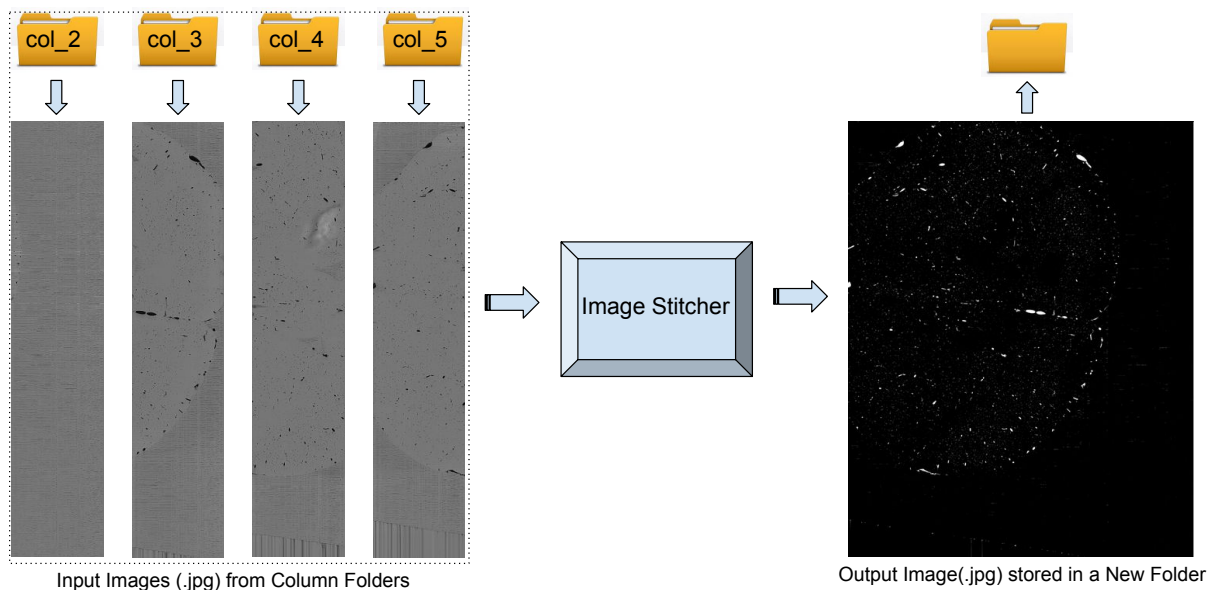


Figure 3.1: Image sticher block overview.

depends upon the type of dataset and scan setup. With reference to file system, the column directories are named as *typeofdataset_colnumber*.

The input for the Image Sticher block are those column directories with jpeg files, and a file with all the metadata information generated by the IEROM during the sectioning and imaging process.

The name of a file stored in any column directory provides information about the date of creation, x coordinate, y coordinate, z coordinate, type of staining performed, etc.

A Metadata file is created by the IEROM which specifies the information about the tissue sample used, specimen, organ, staining performed, sectioning plane, slice size, knife edge orientation, voxel resolution and the number of columns stacks created. After the pre-processing step, images with non-tissue areas are removed which reduces the number of column stacks.

To minimize the artifacts in the output images, after the cropping and normalization process, files containing images of only non-tissue areas are deleted. Such images do not retain the original architecture of the mouse brain and adversely increase the amount of processing dataset. As a result, the column directories now do not have the same number of image files. Table 3.1 summarizes the input for my experiment.

3.3 Image Sticher

For each output image, this block picks one image from each column directory, stitches them together and then applies thresholding values to each pixel in the image.

Image Stack	Image Resolution	Directory Name
First Column	2400 × 12000	Vasculature_col0002
Second Column	2400 × 12000	Vasculature_col0003
Third Column	2400 × 12000	Vasculature_col0004
Fourth Column	2400 × 12000	Vasculature_col0005

Table 3.1: Vascular networks dataset input for the image stitcher block

Image Stitcher Controller

The *Controller* decides what files are to be passed on to its *Worker*. Since the number of image files in the column directories are unequal, the *Controller* code needs to perform some searching algorithm to find the right combination of data to be stitched. The idea is to stitch together the image files extracted at the same z coordinate (which is physically the depth level inside the tissue).

First, *Image Stitcher Controller* searches for the column directory with maximum number of files, and makes it the base directory for all the z coordinate references. In my case, Column 4 had the maximum number of files, which means it had the maximum number of z coordinates.

Second, for each file in the *base directory*, the *controller* starts searching for files with the same z coordinate value in other column directories. Once it finds all the images for a particular z coordinate, it calls the *Image Stitcher Worker*, and passes all the four images obtained for that z coordinate.

Image Stitcher Worker

The *worker* tiles the input images received from the *controller*, side-by-side using a corresponding ITK library filter; **TileImageFilter()**. For example, let's say, if the input for the filter is n images each of $x \times y$ resolution, then the output is one tiled image of resolution $n \times x \times y$. The layout for the filter is specified as $[n, 0]$ which means it tiles n input images along their lengths.

Depending upon the direction of the knife set while cutting and imaging, the images stored in the consecutive columns might or might not align when directly placed together. In my case, the input images were not tiled in the same order as their column numbers. Instead, the image from the last column was the first one to be placed in the image sheet (See Fig.3.2).

The *worker* then binarizes the tiled image using Thresholding method in ITK; **Binary-ThresholdImageFilter()**. The tissue areas in the image are set to a threshold intensity value of 255 that corresponds to *white* and the non-tissue areas are set to a threshold intensity value of 0 which corresponds to *black*. The images are binarized to create a sharp

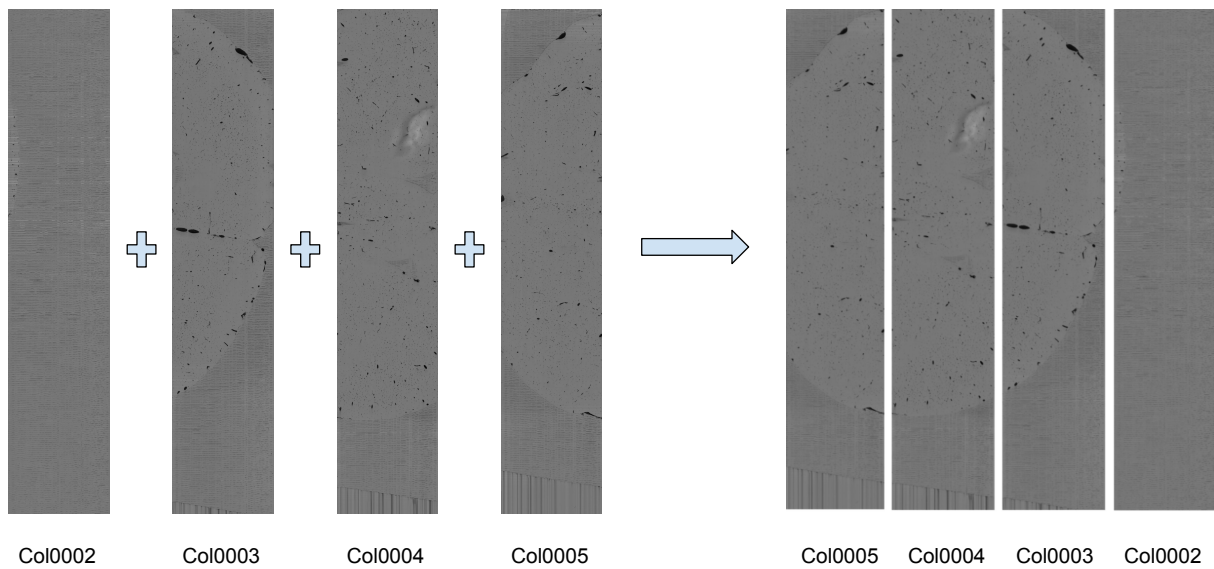


Figure 3.2: Tiling order of the column images.

contrast between the background and the tissue imprints in the foreground (See Fig.3.3). This process also eliminates knife chatter or artifact in the image, if present.

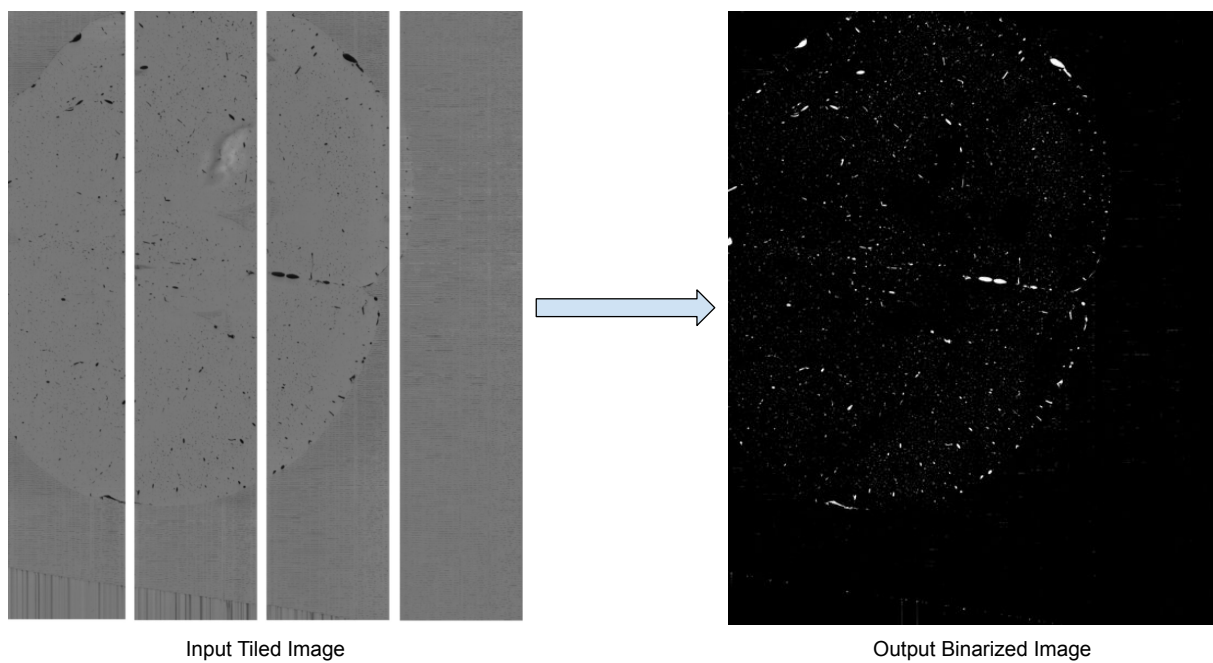


Figure 3.3: Tiled image binarized to get clear tissue-areas and low background artifacts.

The *worker* also creates an output directory for storing the stitched images, in a path

specified by the user. The metadata file information is used for labeling the directory.

3.4 Output of Image Stitcher

The stitching operation results in an output directory with all stitched and binarized images. The output directory is labeled with its metadata information to indicate the ID of the biological organ used for the experiment, type of staining, date of scanning and the resolution of the stitched image. Each output image is saved as a jpeg file and is labeled with its z coordinate information and the date when the file was created. Table 3.2 summarizes my experiment results.

Stitched Image Resolution	9600 × 12000
Total No. of Stitched Images	9626
Output Directory Name	MOU1_BRA_IND_2008_04_9600x12000
Sample Name of a Stitched File	20160414_z5.0670.jpg

Table 3.2: Output of the image stitcher block for the vascular networks dataset

3.5 Challenge

Unequal Number of Images in Column Stacks

All the serially scanned images are stored digitally in the form of stacks and columns. After that, the tissue areas are cropped and saved from each image. Since, the mouse brain is embedded in plastic, the serial sectioning and imaging data set also include images of non-tissue areas. After the removal of such images from the column stacks, we end up with unequal number of images in the column directories. For reference, we call these images as *relevant images*. It is observed that the mouse brain is embedded in the center of the plastic volume, so there are more number of images in the center column stacks than in the end column stacks. If the images were to be stitched directly, it would result in an unequal width of images in the final output image stack.

Thus, to maintain a constant width, we need to stitch the *relevant images* with *dummy images*, in cases when we do not have the corresponding images for a z level in other columns. A *dummy image* has a constant intensity value throughout, which is equal to the background intensity value of the *relevant image*. In our case, the background intensity value is θ , which results in a complete black *dummy image* (see Fig.3.4).

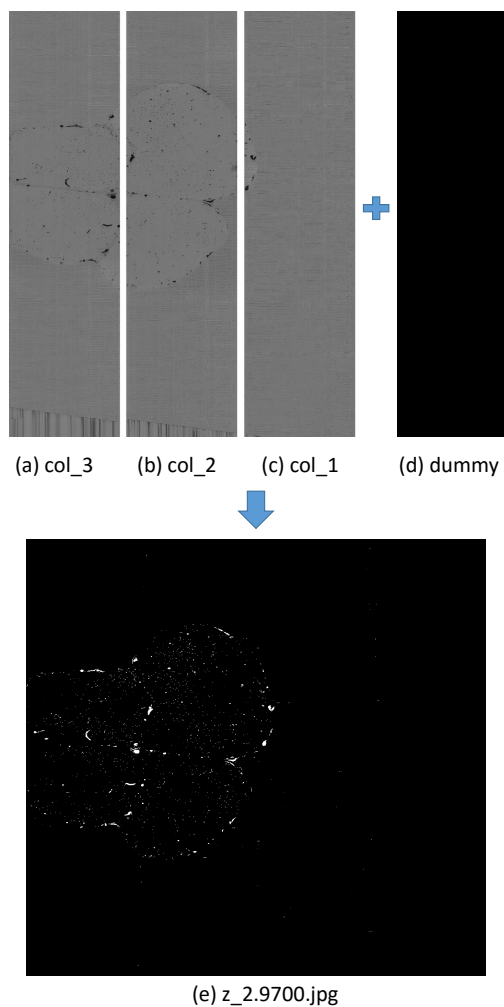


Figure 3.4: Dummy image appended after stitching of the images from different columns.

(a), (b) and (c) represent images from three columns with *relevant images* for the z coordinate. These images are processed to invert the intensity of the foreground and set a constant intensity value for the background. (d) *Dummy Image* of the same resolution as that of the column image, but having the background intensity value throughout the image. (e) Stitched image of resolution 9600×12000 .

Chapter 4

Sub-Sampling of Image Stacks

4.1 Overview

For studying the architecture of any biological organ, it is required to develop multidimensional microscopic data resources. This chapter illustrates how to create those data resources. To create multi-resolution image stacks, it is required to sub-sample the original 2D image stack obtained after the stitching process. I used ITK filters to create output image stacks, which are half the resolution of the input image stack. I shrink the 2D images in the x - y plane, and choose to keep alternate files from the original stack in the z direction. So, if the resolution of the image stack created after stitching is A , the sub-sampled image stack will be of resolution $A/2$. The method is used to create a series of image stacks of resolution till the lowest resolution is achieved: A , $A/2$, $A/4$, $A/8$, $A/16$, $A/32$... (See Fig.4.1). The sub-sampled image stacks are stored in directories labeled with its metadata information to indicate the ID of the biological organ used for the experiment, type of staining, date of scanning and the resolution of images in the stack.

For example, in my case, the original stitched image stack had 9626 images each of resolution 9600×12000 . When sub-sampled, it created a stack with 4813 images each of resolution 4800×6000 . I continuously sub-sampled the image stacks until an image resolution lesser than 512×512 was achieved. Finally, I ended up creating image stacks of resolution: 9600×12000 , 4800×6000 , 2400×3000 , 1200×1500 , 600×750 , 300×375 .

4.2 Input for Sub-Sampler

The cutting and imaging process in IEROM produces images with fixed width and height. The Image Stitcher block creates a stack of images with the highest resolution possible for any specimen. Input for the Sub-Sampler block is the image stack directory created by the Image Stitcher block in the previous chapter (`MOU1_BRA_IND_2008_04_9600x12000` in my case), which will be referred as *original stack* in this chapter for the ease of understanding.

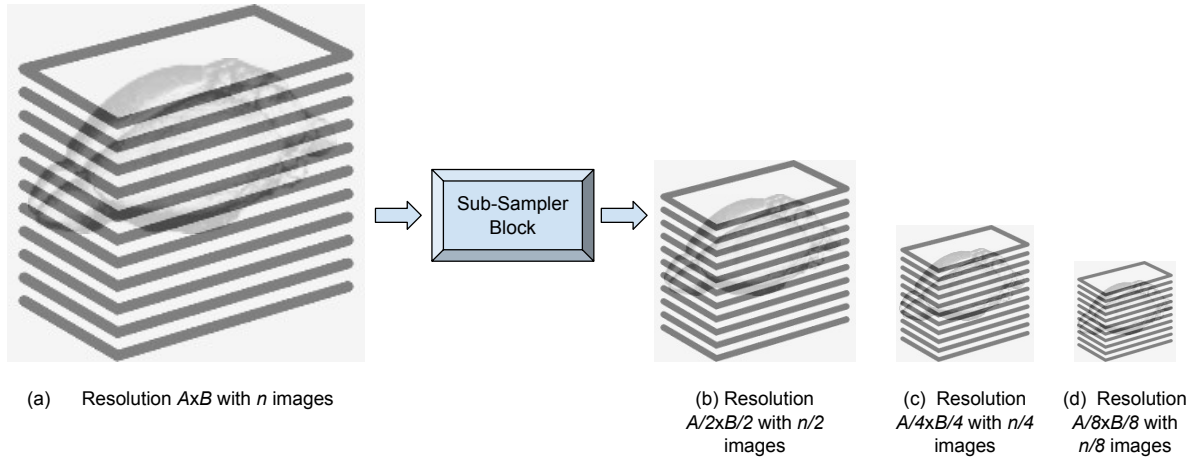


Figure 4.1: Sub-sampler block overview.

(a) Original image stack input to the sub-sampler block. (b) First sub-sampled image stack. (c) and (d) are further sub-sampled image stacks.

4.3 Sub-Sampler

For any input image stack, this block will create a new image stack with images half the resolution of input images selected alternatively from the stack.

Sub-Sampler Controller

This *Controller* simply picks every alternate file from the input image stack and calls the *worker* to down-scale that image by half. It also passes the destination directory path to the *worker* for saving the down-scaled images. The *Controller* creates a destination directory, and labels it with the metadata information (taken from the input stack) and resolution of the output images. For example, if the input stack is `MOU1_BRA_IND_2008_04_9600x12000` then the output image stack will be labeled as `MOU1_BRA_IND_2008_04_4800x6000`.

Sub-Sampler Worker

The *Worker* receives an input image from the *Controller* and shrinks it using an ITK image filter called `ShrinkImageFilter()`. It then saves the output image in the destination directory specified by the *Controller*. The shrink factor for this filter is set to a value of 2, which means the width and height of the output image are half that of the input image. The output image size in each dimension is given by:

```
outputSize[j] = max( std::floor(inputSize[j]/shrinkFactor[j]), 1 );
```

When the shrink factor is 2, starting from the first pixel, alternate pixels are selected from both x & y dimensions of the input image to make the output image. Note that the physical centers of the input image and output image will be the same, due to which the origin of the output image may not be the same as the origin of the input image.

One cycle of the *Sub-Sampler Controller and Worker* creates half resolution image stack. The cycle repeats until an image stack of resolution lesser than 512×512 is achieved (See Fig.4.2). This restriction of selecting the smallest resolution is to retain the entire organ structure in the smallest resolution image stack. Down-scaling this resolution by half will end up with a resolution of 256×256 , which is the size of a unit image (will be explained in the next chapter).

4.4 Output of the Sub-Sampler

The output of the sub-sampler block is a set of multi-resolution image stack directories. Each directory is labeled with its metadata information to indicate the ID of the biological organ used for the experiment, type of staining, date of scanning and the resolution of images in the stack. Table 4.1 summarizes the results of my experiment. The idea is to retain the complete organ structure in the smallest resolution, so in my case, I ended up with a resolution of 300×375 . Further sub-sampling, would decimate some tissue traces from the images. This creates a limiting factor on the number of sub-sampling processes that can take place.

Sub-sampled Directories Created	No. of files in the directory
MOU1_BRA_IND_2008_04_4800x6000	4813
MOU1_BRA_IND_2008_04_2400x3000	2407
MOU1_BRA_IND_2008_04_1200x1500	1204
MOU1_BRA_IND_2008_04_600x750	602
MOU1_BRA_IND_2008_04_300x375	301

Table 4.1: Output of the sub-sampler block for the vascular networks dataset.

All these directories cumulatively occupy a hard disk space of ≈ 70 GB.

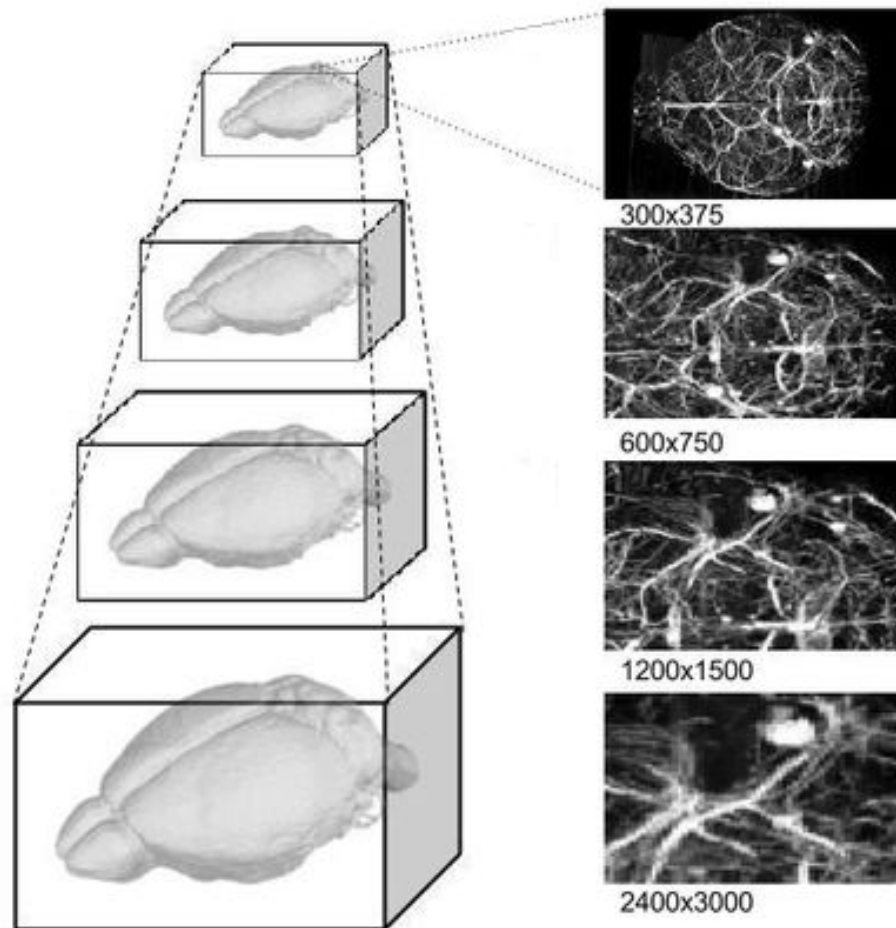


Figure 4.2: Theoretical representation of the sub-sampler output.

The left side represents the sub-sampled mouse brain image stacks, and the right side represents images from each sub-sampled stack.

4.5 Challenges

Overcrowding of Data caused by Sub-Sampling:

After performing the sub-sampling of image stacks, the sub-sampled images of the lower resolution stacks suffer from overcrowding of data. This could be due to the binarization of images performed during the image stitching. This overcrowding could be very well displayed in the *unit-volume meshes* created later. A lot of points in the *volume mesh* were observed to be unconnected, and they simply appeared as chunks of dots. So, I had to process

these images either using some ITK filters or by adjusting their brightness values. Due to the shrinking operation performed, there is a large difference between the intensities of the background and foreground data. Adjusting the brightness of these images, removed the background data and reduced the overcrowding resulting in cleaner *Volumetric Images*. (See Fig.4.3).

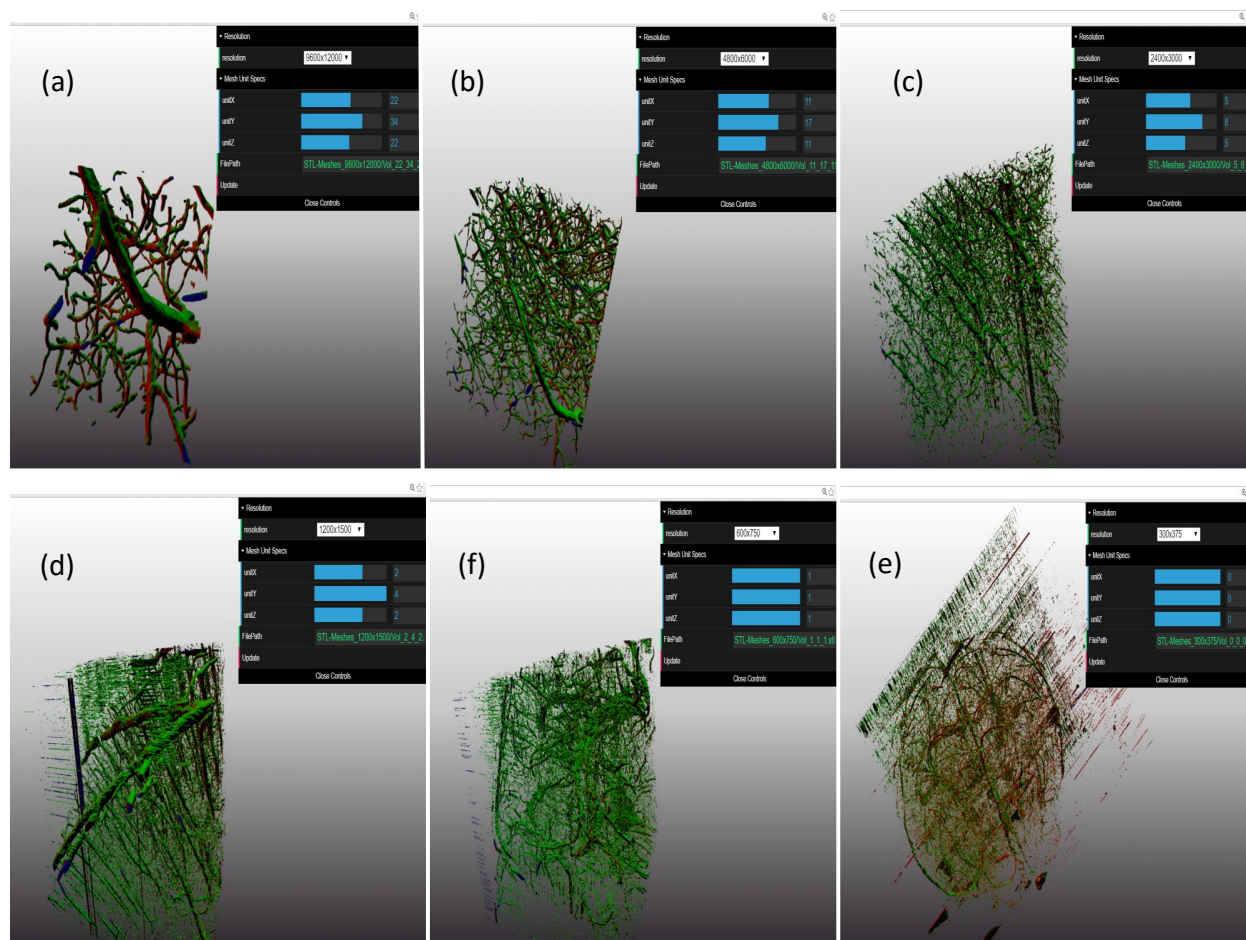


Figure 4.3: Overcrowding of data caused by binarization and sub-sampling seen during volume visualization.

(a) *unit-volume* selected in the highest resolution i.e. 9600×12000 , (b) *unit-volume* of resolution 4800×6000 , (c) *unit-volume* of resolution 2400×3000 , (d) *unit-volume* of resolution 1200×1500 , (e) *unit-volume* of resolution 600×750 and (f) *unit-volume* of resolution 300×375 . *Unit-Volumes* selected in the lower resolutions appear to be more overcrowded.

Chapter 5

Unit-Volume Creation

5.1 Overview

The Unit-Volume Creator block crops out *unit-image* stacks or *unit-stacks* from the image stack directories created in the previous chapters. In short, they prepare the dataset for generating 3D models for visualization.

Handling 3D models of higher resolution image stacks to develop a 3D visualization method for the detailed study of the whole mouse brain structure, could be computationally challenging. However, proper division and categorization of data sets can resolve data management issues; making the process more flexible. This chapter explains a cropping mechanism implemented to extract unit volumes of size $256 \times 256 \times 256$ from the 2D image stacks. The value for the resolution standard is selected to be able to view the tissue details clearly in every volume. The result of the process is a set of multi-resolution unit volume meshes. It is important to create such multiscale models, to visualize and analyze different sections of the mouse brain vascular data at various resolutions, facilitating a better understanding of the morphology.

To create *unit-volumes*, I crop out stacks of 256 images each of resolution 256×256 from an original image stack of a particular resolution. Consecutive 2D images of resolution 256×256 , referenced as *unit-images* are cropped and extracted from each image of an input image stack. Each *unit-image* is labeled with its *unit-x* and *unit-y* coordinates. Where, *unit-x* and *unit-y* mark 256 pixels in *x* and *y* direction. Each image in an input image stack points to a coordinate in the *z* direction, which is used to name the directory storing all the *unit-images* for that image. Now, these directories save the *unit-images* temporarily, until they are moved to their respective *unit-volume* image stack directories (explained in sections below). Every 256 images in the input image stack mark a unit in *z* direction. Starting from the first image in the input image stack, a set of 256 images are taken in sequence, to create 256 temporary directories. These 256 temporary directories will create *unit-volume* image stacks of the same *unit-z* coordinate. This process is repeated for all the images in the input image stack, taken in a set of 256 files at once. Table 5.1 can be referenced for

understanding the common terms used in this chapter.

Terms	Definition
<i>Unit</i>	A unit is defined as 256 pixels
<i>Unit-Image</i>	An Image file having a resolution of 256×256
<i>Layer</i>	A unit along the Z direction or a set of 256 image files
<i>Unit-Stack</i>	A directory with 256 unit-images
<i>Unit-Volume</i>	A Volume file having a resolution of $256 \times 256 \times 256$

Table 5.1: Common terms used with respect to volume maker block

5.2 Input for Unit-Volume Creator

The image directories created by the Image Stitcher and Sub-Sampler blocks are the input to the Unit-Volume Creator. The Unit-Volume Creator is executed once for each image directory, starting from the highest resolution.

5.3 Unit-Volume Creator

For any input image stack, this block will create *unit-image* stacks which are a pre-requisite for the next chapter. The next chapter will explain how to start building the *3D Models* or *unit-volumes* from the *unit-image stacks*.

Let's illustrate the process of building *unit-image stacks* through my experiment as an example. In my case, the original image stack had 9626 images each of resolution 9600×12000 followed by all the sub-sampled image stacks created in the previous chapter. Starting from the highest resolution, the *Unit-Volume Controller* is called once for each image stack.

Unit-Volume Controller

Firstly, the controller creates a text file to save all the original z coordinate values from the image stack. For example, as the image stack contains 9626 images (in my case), corresponding 9626 z coordinate values are indexed in a file, which will be used later to retrieve the original z coordinate values while performing volume rendering (explained in later sections).

Then, the *Controller* calls the *Worker* once for each file in the image stack.

Unit-Volume Worker

The *Worker* receives a single file at a time from the controller. Since a file name is uniquely identified by its z coordinate value or its z position in the image stack. The *worker* is

designed to create a directory labeled with this z coordinate value, to store all the cropped *unit-images* extracted from the input image file (See Fig. 5.1). This directory is created temporarily to be used later while making the *unit-volumes*.

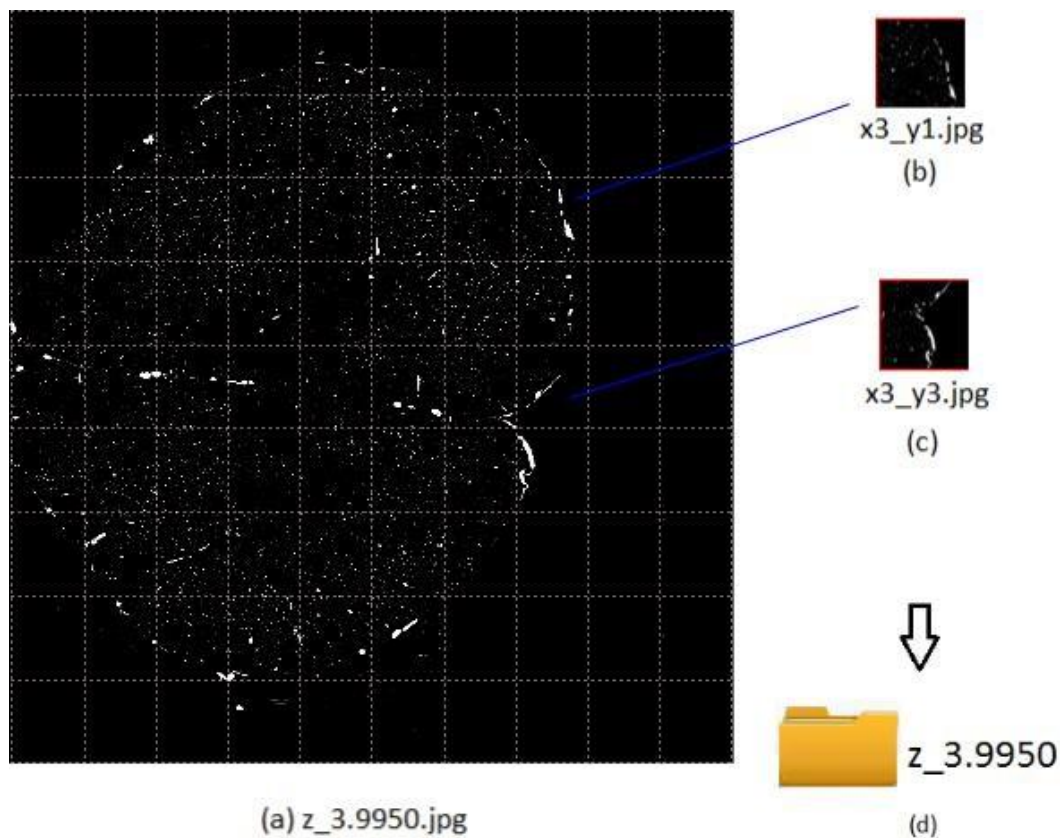


Figure 5.1: Unit-images created from an input image.

(a) The original image is divided into units of 256 pixels each in x and y directions. (b) shows how the unit images of resolution 256×256 are cropped and extracted from the original image. (d) Temporary directory where all the unit images are stored.

To create *unit-images*, the input image is passed through an ITK filter called **ExtractImageFilter()**. This filter crops and extracts *unit-images* of resolution 256×256 pixels. By definition, the **ExtractImageFilter()** decreases or changes the image boundary of an image by removing pixels outside the target region. I define the boundary image width and height as 256, so starting from the first pixel, it will crop out the image after 255 consecutive pixels, in both x and y directions.

For example, for an input image file of resolution 9600×12000 , the filter divides the 9600 pixels along the x direction and 12000 pixels along the y direction into units of 256 pixels each. This results in 37 *unit-x* and 46 *unit-y* coordinates. The *unit-images* cropped out are labeled with their *unit-x* and *unit-y* coordinates such as: `x0_y0.jpg`, `x0_y1.jpg`,

`x36_y45.jpg`. All these *unit-images* corresponding to a single image file are stored in the temporary directory created by the *worker* labeled with the z coordinate value of the image.

This process is repeated for all the images in the input image stack by the *controller*, resulting in a set of temporary directories, one for each file in the input stack. So, for 9626 images in the input stack, 9626 temporary directories are created.

A *Layer* marks 256 image files corresponding to a *unit* along the z direction. For example, for 9626 images in the input stack, 38 sets of 256 *unit-z* coordinates can be created, resulting in 38 layers. The temporary directories corresponding to a single layer, creates *unit-stacks* with the same *unit-z* coordinate value. The *unit-images* labeled with same *unit-x* and *unit-y* coordinate values across a set of 256 temporary directories, result in a *unit-stack* directory. These directories are labeled with their *unit-x*, *unit-y* and *unit-z* co-ordinates such as: `Vol_0_0_0`, `Vol_0_1_0`, `Vol_0_2_0`, , `Vol_36_45_37` (See Fig.5.2).

For example: all *unit-images* labeled as `x0_y0.jpg`, moved out from the 1st *layer* of temporary directories, will create a *unit-volume* image stack called `Vol_0_0_0`. A *unit-image* moved out of a temporary directory is renamed with its original z coordinate value, when saved in the *unit-stack* directory.

A single temporary directory stores *unit-images* for a single image file in the input stack. So temporary directories for all the input images means immensely sized data set (E.g., 9626 temporary directories for each image, in my case). Creating all these temporary directories at once and then making *unit-stacks* out of it, will be a time-taking process and also will exhaust the disk space resulting in lower processing speeds. To avoid that, while creating the *unit-volume* image stacks or *unit-stacks*, I create only 256 temporary directories at a time. As soon as a temporary directory is created, *unit images* corresponding to their respective *unit-stacks*, are moved out and stored in their *unit-stack* directories. While a temporary directory is being created, all the directories for the *unit-stack* in the same *layer* are created simultaneously. So at once, only 256 temporary directories are created and utilized. After all the *unit-images* are moved out of the temporary directories, these empty directories are deleted. This process avoids creating multiple copies of the images and eventually saves processing time and hard disk space (See Fig. 5.3).

5.4 Output of the Unit-Volume Creator

The *Unit-Volume* Creator block basically outputs *Unit-Stacks* i.e. directories of 256 *unit-images*, which is a pre-requisite for creating *Unit-Volumes* or *3D Models* (explained in the next chapter).

The *Controller-Worker* model is called for all the sub-sampled image stacks, resulting in a huge pile of multi-resolution *unit-stacks*. Each file in the input image directory contributes to a set of *unit-stacks*. Thus, the output of this complete block is a set of directories, one for each input image directory containing *unit-stacks*. However, I do not create *unit-stacks* for the lowest resolution image stack which contains 300 images of resolution 300×375 . If I sub-sample this image stack, I will create an image stack of dimension $150 \times 187 \times 150$,

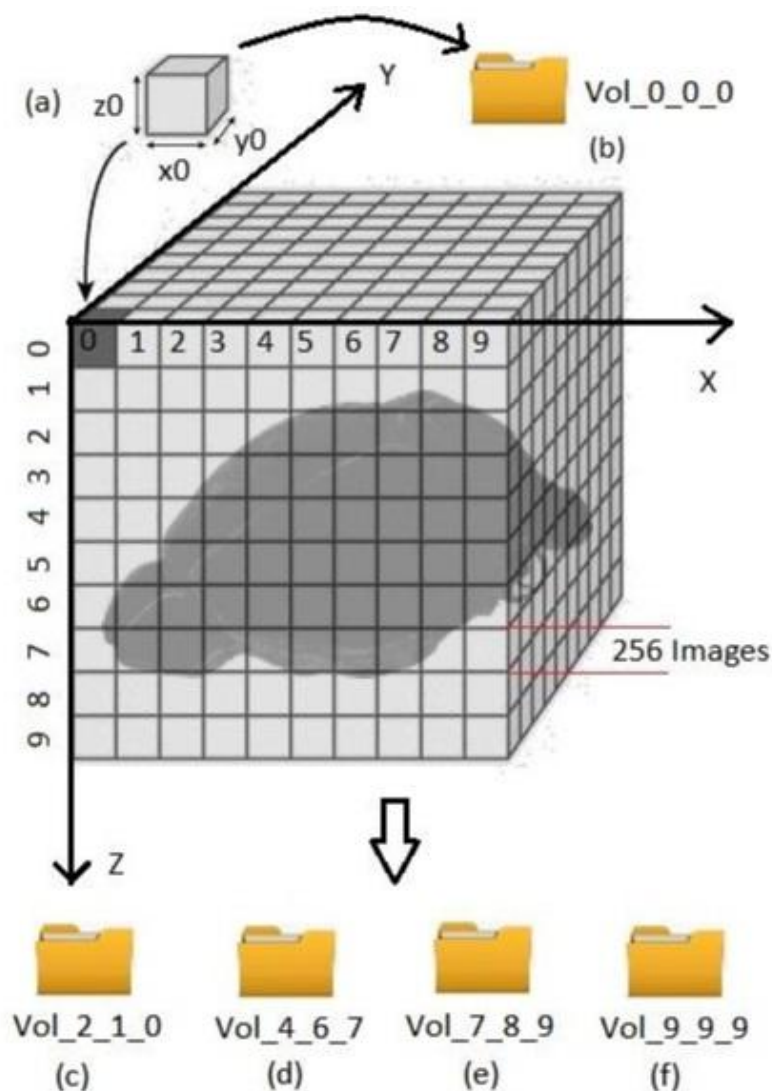


Figure 5.2: Unit-volume image stack creation.

(a) represents a unit-volume image stack of dimension $256 \times 256 \times 256$. Each unit in the z direction marks a layer of 256 images. Each unit in x and y directions mark 256 pixels. (b) shows the directory that stores the *unit-volume* image stack for unit coordinates 0,0,0. (c), (d), (e), (f) represent unit-volume directories containing unit images mapped and moved out from the temporary directories. These *unit-volume* directories contains 256 images each of resolution 256×256 .

which is even smaller than the *unit-volume* dimension i.e., $256 \times 256 \times 256$. The framework application requires to be able to visualize the whole-mouse-brain structure at first, which can only be done in the smallest resolution. Thus, for clear visualization, I consider the

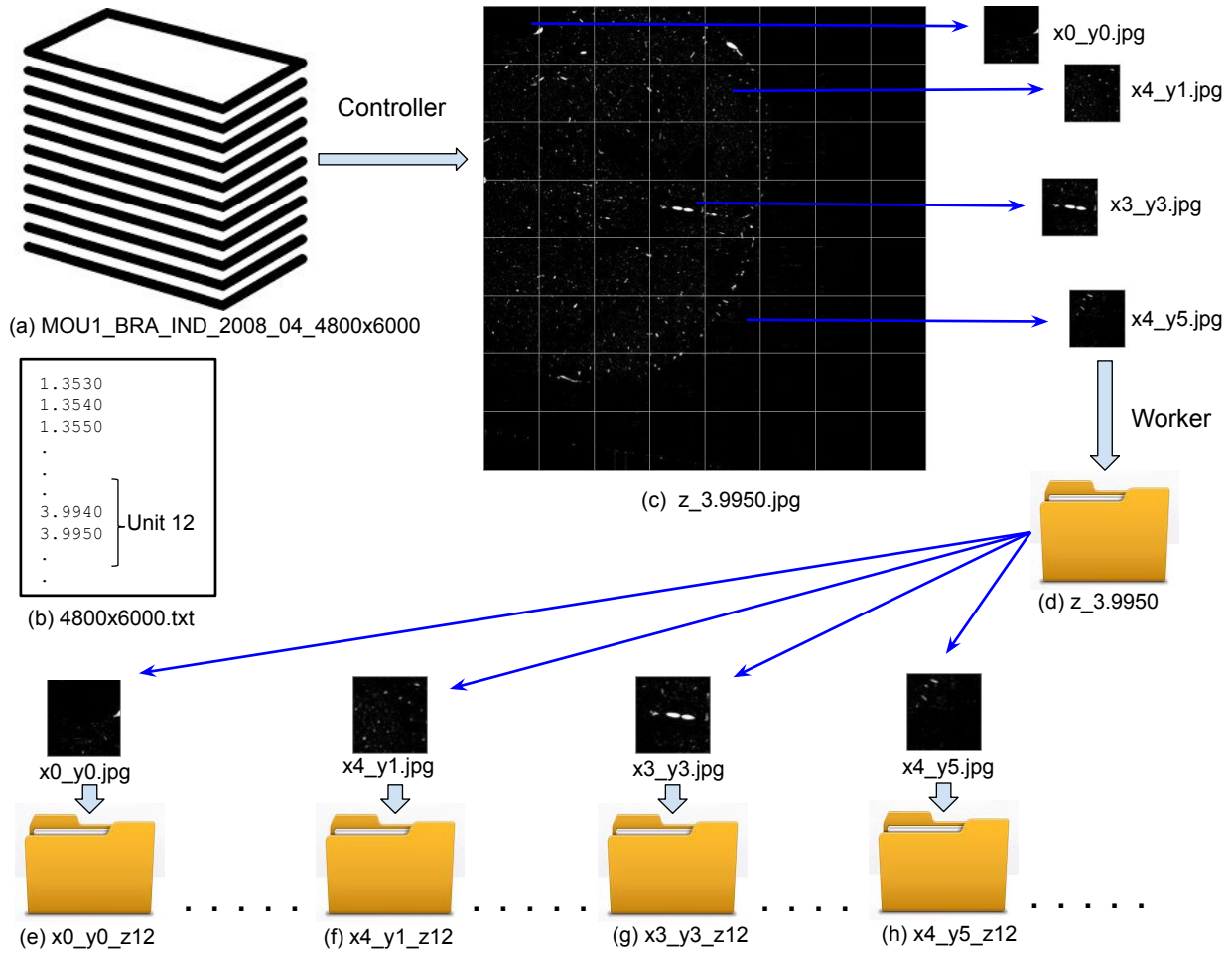


Figure 5.3: Creation of one temporary directory and corresponding unit-stack directories.

(a) Input image stack for the *Controller*. *Controller* passes one file at a time to the *Worker*. (b) Text file created by the *Controller* to store all the z coordinates of the input image stack. Defining a layer of 256 consecutive coordinates is easier with the help of this text file. (c) An image from the input stack sent by the *Controller* to the *Worker*. (d) Temporary directory created to store all the *unit-images* cropped and extracted from the input image. (e), (f), (g), and (h) are the *unit-stack* directories created for the layer to which the input image belongs. The *Worker* takes the *unit-z* value for the input image defined in the text file and uses it to label the *unit-stack* directories.

smallest resolution image stack of dimension $300 \times 375 \times 300$ as one complete *unit-stack*.

Table 5.2 summarizes the results of the *Unit-Volume Creator* block for my experiment.

Resolution of Images in the Source Image Stack	No. of Unit-Stacks Created
9600×12000	57944
4800×6000	7866
2400×3000	990
1200×1500	80
600×750	8
300×375	1 <i>stack</i> of 300 <i>unit-images</i>

Table 5.2: Output of the unit-volume maker for the vascular networks dataset.

All these *unit-stacks* cumulatively occupy a hard disk space of ≈ 94 GB.

5.5 Challenges

Insufficient Pixels in the Images causing Data Loss:

While cropping and extracting *unit-images* from the image files, it was seen that if any of the image resolution parameters (i.e. image width in pixels and image height in pixels) were not a multiple of 256, that resulted in data loss. For larger resolution image stacks, the organ structure traces are in the centre of the image. So, there is no tissue areas in the end pixels of the image thus, these pixels can be ignored. However, when dealing with smaller sub-sampled resolution image stacks, some tissue area traces are seen in the end pixels of the image files. So, I created dummy pixels of intensity value equal to the background intensity of the original images to substitute the missing ones.

Insufficient Images in the Image Stack causing Data Loss:

While creating the *unit-volume* image stacks, it was observed that if the number of files in the original image stack was not a multiple of 256. Then, the *unit-stacks* for the last unit or *layer* in the z direction is never created, leading to loss of data. To resolve this issue, I implemented a workaround. First, I calculated the number of files undershot in the last *layer*, to make the total number of files in the original stack as a multiple of 256. By doing this, I now know how many files are required to be added. Then, I created *dummy image files* of the same resolution as that of the images in the original stack. These *dummy images* are images with a constant background intensity value as explained in the previous section.

Chapter 6

Making 3D Models and Meshes

6.1 Overview

In this chapter, the *unit-stacks* created earlier will be converted into actual volumes files. The aim is to create 3D STL (Standard Tessellation) meshes which can be loaded easily to a Web-based framework. I choose the volume output format as STL because it is supported by the XTK APIs. XTK or the *X Toolkit* is a WebGL based scientific visualization toolkit. I use this platform to create a web-based 3D visualization framework (explained in the next chapter). At first, using the ITK classes, I create 3D volumetric images from the *unit-stacks*. These 3D volumetric images generate *unit-volumes* and are expected to be isotropic in all three directions. Iso-surfaces for each *unit-volume* are found using the Marching Cube algorithm in VTK, and are then saved as a 3D mesh in an STL file format. A *STL Mesh* file is labeled with the name of its *unit-stack* directory. So, for the highest resolution image stack, I create *Meshes* from *Vol_0_0_0.stl*, *Vol_0_1_0.stl*, . . . to *Vol_36_45_37.stl*. This process is repeated for all the sub-sampled *unit-stacks*, resulting in a set of multi-resolution *unit-volume meshes*. The *Iso-Surfaces* are the distribution of scalar data in a volumetric image. Marching Cube algorithm uses patterned cubes or isosurfaces to approximate contours in a volumetric image. VTK supports the marching cubes algorithm with *VtkMarchingCubes* class, which requires a volumetric image input as a VTK data object, and creates an output in VTK poly data format. The threshold value and the number of contours can be specified while using *VtkMarchingCubes*, to generate the 3D surface of the object. *3D Model Maker* is the last block of the IEROM image processing pipeline.

6.2 Input for the 3D Model Maker

The directories containing *unit-stacks* created in the previous chapter are the source for this block. Each directory contains *unit-stacks* of a particular resolution. These directories are fed one by one to the *3D Model Maker Controller*, so the *Controller-Worker* model is called once for each resolution.

6.3 3D Model Maker

This block creates 3D models or meshes from the *unit-stacks* fed to it. The block is currently capable of producing three different formats of volume files: TIFF (Tagged Image File Format), and STL (Standard Tessellation Language). The user can select the output file format. Different file formats are produced for different use cases.

The 3D Model Maker block utilizes two major toolkits: ITK and VTK. The ITK filters are used to process 2D images and the VTK filters are used for creating the 3D meshes.

3D Model Controller

The *Controller* receives a directory containing *unit-stacks* for a single resolution at a time as input. It will call the *worker* once for every *unit-stack* in that directory. A user needs to specify the source directory path and output file format as input arguments to make a call to the *controller*. The *controller* will first create an output directory and set it as the destination directory for the *worker* to save all the output volume files.

3D Model Worker

The *Worker* will create one volume file every time it is called and will save it in the destination directory path provided by the *controller*. The tasks performed by the *worker* are explained in the following steps:

Create Sequential File Names

The process of generating a volume file from slices or 2D images, requires to have the input image files in an ordered sequence. The *Name Generator* will convert the file names in the *unit-stack* into an ordered sequence of file names. For example: initially a *unit-stack* labeled as `Vol_0_0_0` have files named as `z_0.1325.jpg`, `z_0.1335.jpg`, ... `z_0.3875.jpg`. When this *unit-stack* is passed through the *Name Generator* block, it generates file names as `0.jpg`, `1.jpg`, ... `255.jpg`. I utilize an ITK filter called **NumericSeriesFileNames** to perform this task.

As a next step the *worker* will convert these sequence of files into 3D Models and Meshes. According to users choice, it can either be a TIFF, or STL file format.

TIFF Model Generation

For generating the TIFF files, I use an ITK filter called **TIFFImageIO**, that combines all the sequence files and writes them into an output TIFF volume format. **ImageFileWriter()** is an ITK class that interfaces with this **ImageTIFFIO()** class and writes the data to a single output file.

STL Mesh Generation

For creating STL files, I first convert the ITK image to a VTK image using an ITK filter called **ImageToVTKImageFilter()**. This filter will convert an ITK data pipeline to a VTK data pipeline and will take care of the details of the connection of the two pipelines. After this step, I end up with a 3D structured point set.

As a second step, I convert these 3D structured point set to one or more isosurfaces using a VTK filter called **vtkMarchingCubes()**. By definition, this filter requires specification of one or more contour values to generate the isosurfaces. Alternatively, one can specify a min/max scalar range and the number of contours to produce a series of evenly spaced contour values. For ease of reference, I call this value as the *iso-surface value*; this value is directly proportional to the scalar values extracted. Higher values of this parameter denote a greater number of scalar data set extraction leading to lesser data loss. However, a higher value also means that the *marching cube algorithm* will repeat the generation of iso-surfaces for a larger number of times, resulting in higher computational time. Therefore a balance is to be maintained. I choose the iso-surface value as 100 for our data set.

As a the third step, I compute normals for the polygonal mesh using a VTK filter **vtkPolyDataNormals()**. By definition, this filter computes points and/or cell normals for a polygonal mesh. The user specifies if they would like the point and/or cell normals to be computed by setting the *ComputeCellNormals* and *ComputePointNormals* flags. The computed normals (a `vtkFloatArray`) are set to be the active normals (using `SetNormals()`) of the `PointData` and/or the `CellData` (respectively) of the output `PolyData`. The filter can reorder polygons to insure consistent orientation across polygon neighbors. Sharp edges can be split and points can be duplicated with separate normals to give crisp (rendered) surface definition. It is also possible to globally flip the normal orientation. The algorithm works by determining normals for each polygon and then averaging them at shared points. When sharp edges are present, the edges are split and new points are generated to prevent blurry edges.

As a the fourth step, the polygonal data created is mapped to the graphics primitives using a VTK class called **vtkPolyDataMapper()**. This class maps polygonal data to the rendering/graphics hardware/software. Then I use the **vtkActor()** class to represent the object in a rendered scene. By definition, it inherits functions related to the actors position, and orientation and has scaling and maintains a reference to the defining geometry (i.e., the mapper), rendering properties, and possibly a texture map. `vtkActor` combines these instance variables into one 4x4 transformation matrix as follows: $[x \ y \ z \ 1] = [x \ y \ z \ 1]$ Translate(-origin) Scale(scale) Rot(y) Rot(x) Rot (z) Trans(origin) Trans(position).

Finally I use a **vtkSTLWriter()** to write stereo lithography (.stl) files in binary form. Stereo lithography files only contain triangles. If polygons with more than three vertices are present, only the first three vertices are written.

6.4 Output of the 3D Model Maker

The *3D Model Maker* is executed for all the different resolution directories, where for each directory it converts all its *unit-stacks* into volume files. So, the output of this complete block is a set of directories with multi-resolution 3D models/meshes.

The iso-surfaces are only generated for volumetric images with tissue areas, as only those areas have the scalar data values. Thus, the number of STL Meshes created is not always equal to the number of *unit-stacks*. In my case, the *3D-Model-Maker* converts the multi-resolution *unit-stacks* created for the vascular network of a mouse brain into *STL-Meshes*.

Resolution of Images in the Source Image Stack	No. of STL Meshes Created
9600 × 12000	49884
4800 × 6000	7055
2400 × 3000	904
1200 × 1500	74
600 × 750	8
300 × 375	1

Table 6.1: Results of the 3D model maker block for the vascular network dataset.

All the STL's cumulatively occupy a hard disk space of ≈ 1 TB.

6.5 Challenges

Unequal Spacing in the 3D Meshes Created

The three-dimensional serial sectioning performed in IEROM is not spaced equally in the x , y , z directions. The spacing ratio maintained by the instrument is 0.625: 0.7: 1 in the x , y and z directions respectively. This unequal spacing obstructs the construction of volume meshes of exact 256^3 size. The data doesn't align properly in the volume mesh and appears stretched in one direction. To overcome this issue, I set the spacing ratio of the 3D volumetric image as 1: 1: 1 before creating iso-surfaces using marching cube algorithm (See Fig.6.1).

Selecting a Proper Iso-Surface Value

For creating the iso-surfaces with the marching cube algorithm, its important to set the min/max scalar range and the number of contours to generate a series of evenly spaced contour values. While creating the unit-volume STL meshes, one needs to be careful in selecting a proper value for the number of contours to be generated. Since the marching cube

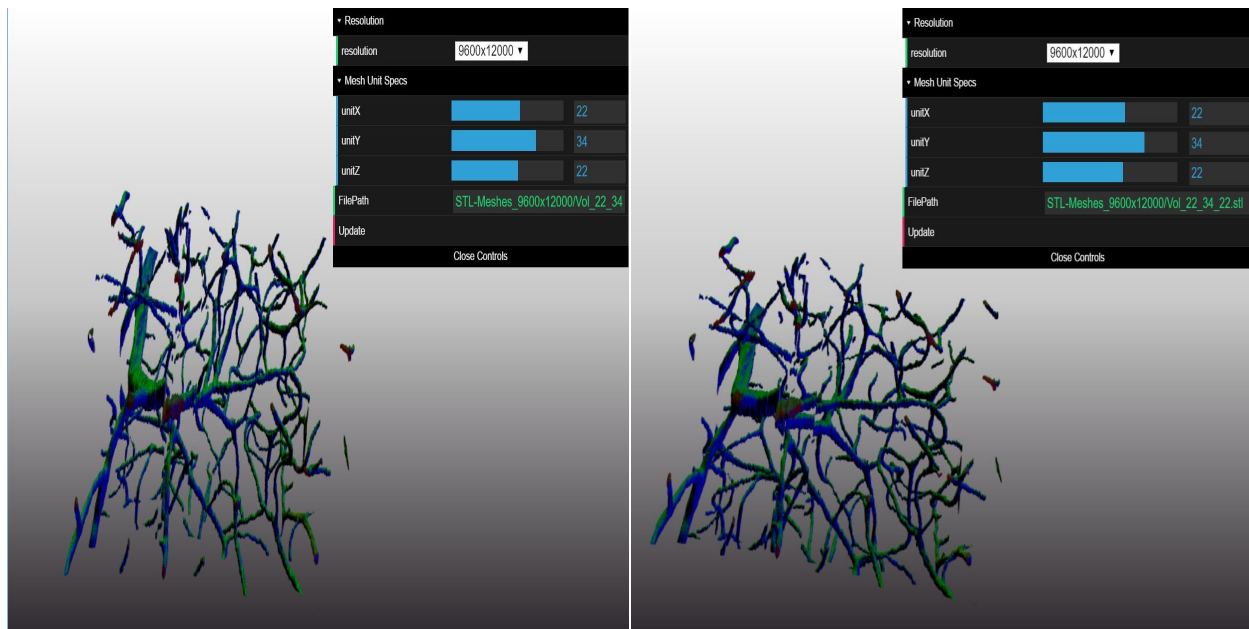


Figure 6.1: Unequal spacing observed in the 3D STL meshes.

(a) Proper cubical volume followed with the spacing ratio set as 1:1:1 *unit-volume* selected in the highest resolution, (b) The same volume appears like a cuboid when the spacing ratio is 0.625:0.7:1.

algorithm will make repeated generation of iso-surfaces for that number of times. For higher resolutions, creation of STL meshes will be a time consuming task. Keeping a lower value of contour number will take lesser time to create the meshes. So, it is required to consciously choose a value which is neither too low nor too high to maintain the complete data visibility for higher resolutions. However, the same value might not work for lower resolutions as it will lead to data losses in them. So, one needs to select different values of *contour number* for creating multi-resolution volume meshes. In my case, it has been observed that a contour value of 100 works well for *unit-volumes* image stack of 9600×12000 resolution, and a value of 180 works well for the *unit-volume* image stack of 300×375 resolution. I somehow maintain values between 100 and 180 for the *unit-volume* between these two resolutions (See Fig 6.2).

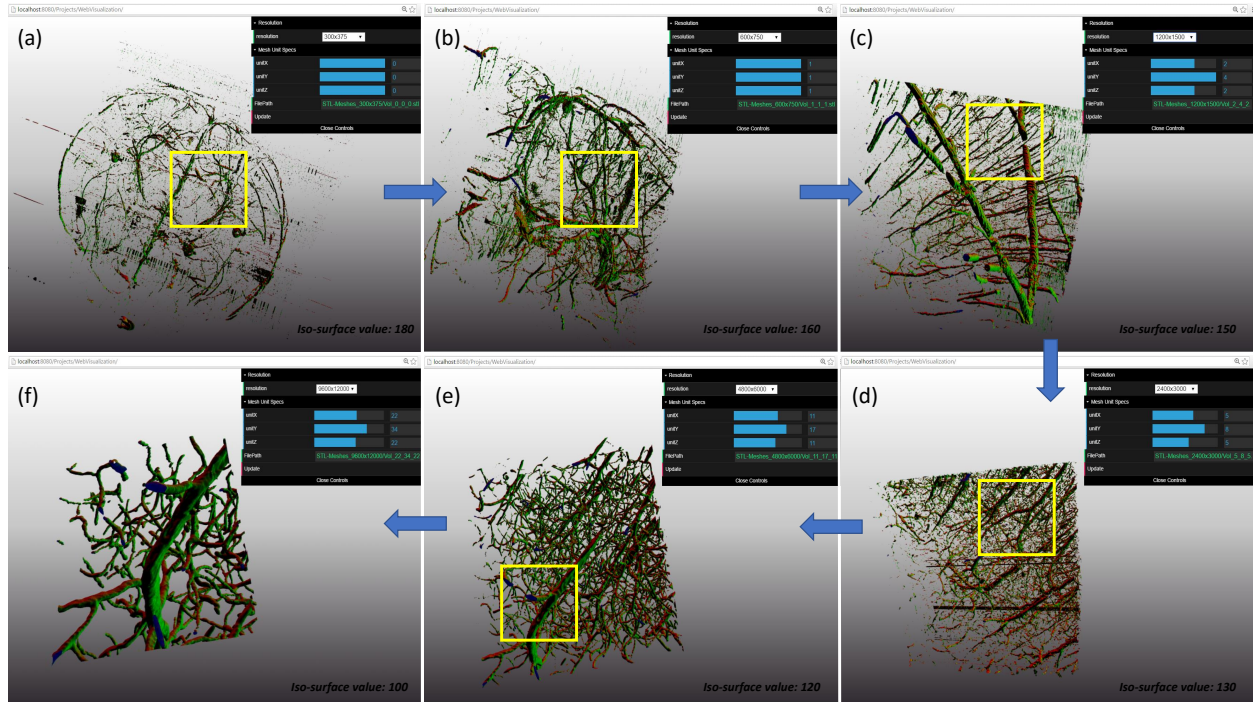


Figure 6.2: Iso-surface selection for the multiple resolution *unit-volumes*.

A *unit-volume* loaded with *unit x-y-z* coordinates as 0,0,0 and resolution 300×375 with an iso-surface value of 180, (b) *Unit-volume* loaded with *unit x-y-z* coordinates as 1,1,1 and resolution 600×750 with an iso-surface value of 160, (c) *Unit-volume* loaded with *unit x-y-z* coordinates as 2,4,2 and resolution 1200×1500 with an iso-surface value of 150, (d) *Unit-volume* loaded with *unit x-y-z* coordinates as 5,8,5 and resolution 2400×3000 with an iso-surface value of 130, (e) *Unit-volume* loaded with *unit x-y-z* coordinates as 11,17,11 and resolution 4800×6000 with an iso-surface value of 120, and (f) *Unit-volume* loaded with *unit x-y-z* coordinates as 22,34,22 and resolution 9600×12000 with an iso-surface value of 100.

Part III

Web-Based 3D Visualization Framework : Implementation

Chapter 7

3D Brain Atlas: Web-Based Real-Time 3D Visualization Framework

7.1 Overview

For biomedical data visualization, most users are required to have an appropriate software installed on their local desktop computer, which may involve a lengthy download or installation process. In this model, software developers have to cater for different operating systems when writing these programs. When they have finished an update, it will again have to be delivered to the user (usually via download) and installed. To circumvent these issues, the goal of this chapter is to provide a 3D web-based image viewer. This web-based application will aim to provide the same functionality as a desktop solution without being tied to a particular operating system or computer architecture.

3D Brain Atlas is a web-based real-time 3D visualization framework designed to study the morphology of the mouse brain vascular networks and to analyze it at multiple resolutions. With the IEROM Image Processing Pipeline explained in the previous chapters, it is possible to acquire teravoxel sized three-dimensional microvascular images of the whole mouse brain with sub-micrometer resolution. This web-based framework is designed, to be able to visualize and share these teravoxel volumes across research communities efficiently. I believe that this novel framework for real-time 3D visualization can facilitate data sharing of terabyte-sized three-dimensional images easily. Although this framework is created for the IEROM dataset but the implementation can be utilized to visualize any other multi-resolution biomedical teravoxel sized dataset.

In this chapter, I will explain the design of the Web-Based Application created for managing visualization and interaction with the 3D meshes. I utilized the X Toolkit (XTK); *a WebGL for scientific visualization* [39], to make the web-based 3D visualization framework for teravoxel volumes. A simple web server is implemented by using *Node.js* [29]. Then

through a custom javascript code, I designed the graphical user interface to control the whole functionality of the web application. The graphical user interface (GUI) is designed using a JavaScript controller library called *dat.GUI* [10]. The graphical user interface is used to display the details of the volume loaded and to interact with it: x, y, z unit coordinates and the resolution (see Fig. 7.1). The URL of this web-based visualization framework for vascular network data set is <http://jrkwon.com/3dbrainatlas>.

7.2 Tools and Environment Settings

To create an interactive browser-based application which is useful for displaying biomedical image data, the available tools for creating 3D graphics in a web browser have to be considered. Generally, in the past, web browsers have provided several different methods to display 2D and 3D graphics on screen, and only recently with the introduction of HTML5 and WebGL a widely-conformed standard has emerged. At a very basic level, a website can be written with just *HTML* (Hyper Text Markup Language) code. HTML is written with tags such as `<html>`, `<body>`, `</body>`, `</html>` and then the code is converted into a tree format of JavaScript node objects or Document Object Model (DOM) by the web browser. The purpose of this is to provide a programmatic interface for scripting (removing, adding, replacing and modifying) this live document using *JavaScript*. Different tags can be added to an HTML element, such as the class tag, which gets used to hook extra attributes into the element. For adding attributes such as font, color, dimensions and many more, *CSS* is used. With CSS an HTML element can be assigned a class (via the class tag), which will refer it to specific set of CSS rules for setting style and look. I used the above basics of developing web applications for designing the *3d Brain Atlas*.

The web-server is implemented using *Node.js* which is a JavaScript runtime built on Chrome's V8 javascript engine. As an asynchronous event driven JavaScript runtime, Node is designed to create scalable network applications. HTTP is a first class citizen in Node, designed with streaming and low latency in mind; this makes Node well suited for the foundation of my web framework. I installed an HTTP server in Node and started it. The web-page could be easily accessed with the url- <http://jrkwon.com/3dbrainatlas>. In my case, I could use the localhost url- <http://localhost:8080>, since I was using the computer on which the server was running.

WebGL is a 3D graphics API for the Web and I utilized *XTK* which is a WebGL framework that provides easy-to-use APIs for scientific data visualization on the web. I used some basic APIs such as **X.renderer3D()** for creating a new 3D renderer inside a given DOM element and **X.mesh()** to create a mesh or displayable object loaded from an .STL file.

I designed a lightweight GUI for my web framework using a JavaScript controller library called *dat.gui*. This library creates an interface to easily change variables in JavaScript. The easiest way to use *dat.gui* in my code is by using the built-in source at *build/dat.gui.min.js*. These built JavaScript files bundle all the necessary dependencies to run *dat.gui*.

7.3 Input Data Set

The web-based framework is a WebGL based application built using the X Toolkit. This toolkit supports many different surface models/mesh file formats such as .STL (Standard Tessellation), .VTK (Visualization Toolkit poly data), .OBJ (Wavefront format) and .FSM, .INFLATED, .SMOOTHWM, .SPHERE, .PIAL, .ORIG (Freesurfer meshes). It also supports volume files such as .DICOM, .DCM (Multi file DICOM). However, surface models/meshes provide better architectural rendering and define the shape of the polyhedral object in 3D computer graphics and modeling. Thus, for the detailed study and analysis of the structure of the mouse brain vascular networks, I prefer rendering surface models/meshes.

The idea is to drop the files on the web server and have them ready for rendering. Therefore, I selected a file format which is supported by XTK for fast loading and can correctly regenerate the mouse brain vasculature data points. An STL file describes a raw unstructured triangulated surface by the unit normal and vertices (ordered by the right-hand rule) of the triangles using a three-dimensional Cartesian coordinate system. STL coordinates must be positive numbers, there is no scale information, and the units are arbitrary. I used the STL Meshes created by the 3D Model Maker block in the IEROM image processing pipeline, as the input data set to the web-based framework. The STL meshes can be directly uploaded to the web-server from the local disk space.

7.4 Graphical User Interface Design

Before I step into the GUI Design of the *3D Brain Atlas*, let's understand the basics of 3D graphics which is important to design this framework. 3D Graphics are usually defined by a space in Cartesian coordinates in which resides three-dimensional objects, as well as a camera object through which the scene is viewed with help of a projection matrix. 3D graphics is computationally much more expensive than 2D graphics due to its more complex mathematics. On top of that, rendering a 3D scene can mean that the image should be refreshed 60 times a second, which poses a challenge for many web browsers.

Now let's describe the implemented features of the **3D Brain Atlas** Graphical User Interface in steps:

Main Page Layout

The main view that the user is presented with shows a data display pane with a mesh loaded and control panels on the right side of the page as shown earlier in Figure 7.1). The web page opens with the smallest resolution STL mesh data file i.e. $300 \times 375 \times 301$ resolution volume, loaded at the onset of the page. The background properties of the *CSS* are modified to give it a 3D rendering background effect. The linear gradients are set to change from the top of the page, with color-stop values of `rgba(255, 255, 255, 1)`, `rgba(199, 199, 199, 1)` and `rgba(48, 43, 48, 1)`.

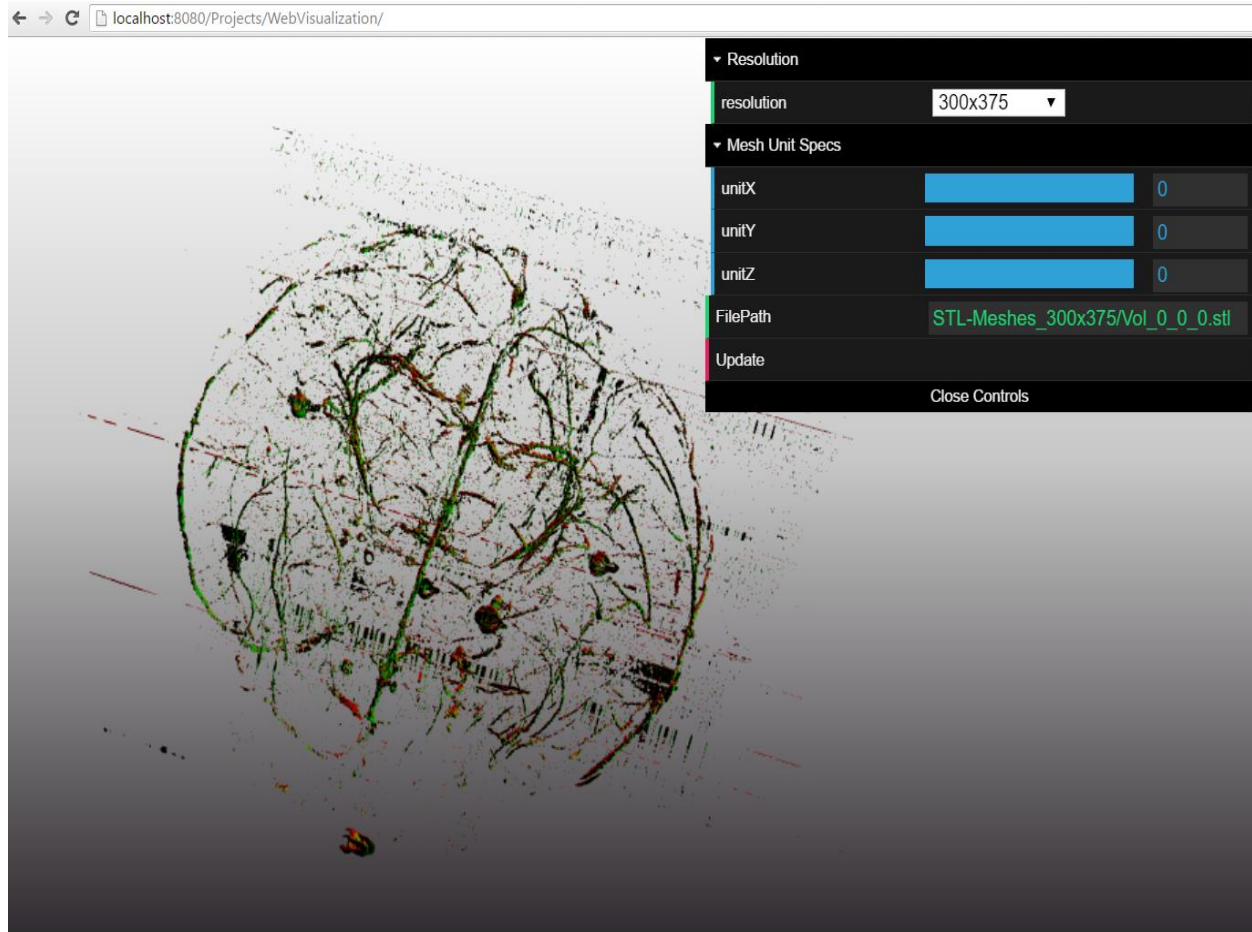


Figure 7.1: 3D Brain Atlas loaded with the smallest resolution volume file.

Control Panel

Resolution Tab

I added controls using the *dat.gui* library, to be able to switch resolutions and display different STL meshes. For my mouse brain vascular dataset, I added a drop-down menu for selecting the desired resolution, where the drop-down is a list of strings with pre-loaded values: 300×375 , 600×750 , 1200×1500 , 2400×3000 , 4800×6000 and 9600×12000 . These values could change depending upon the dataset used and IEROM image processing pipeline output resolutions. At an instance, only an STL mesh of *unit-volume* i.e. of 256^3 dimension is loaded, according to the user scroll input depending upon their region-of-interest and angle-of-perspective.

Mouse Interaction	Type of Graphics Interaction
LEFT CLICK + MOVE	Rotate the scene or Window/Level adjustment in 2D
SHIFT + LEFT CLICK or MIDDLE CLICK	Pan the scene
MOUSE WHEEL UP	Zoom In, fast
MOUSE WHEEL DOWN	Zoom Out, fast
RIGHT CLICK + MOVE UP	Zoom In, fine
RIGHT CLICK + MOVE DOWN	Zoom Out, fine

Table 7.1: List of mouse control modes used for interacting with the renderer. I used the above mouse control modes for panning, zooming in and zooming out operations.

Mesh Unit Specs Tab

A user can manually select the *unit-x*, *unit-y* and *unit-z* coordinates for a particular resolution from the drop down menus. If a valid STL mesh file for such a combination exists, it will be loaded to the web framework. The *unit-x*, *unit-y* and *unit-z* coordinate entries provided by the user are taken as input for framing a file name appending the string `Vol_(unit-x)_(unit-y)_(unit-z).stl`. This file name is then searched in the respective directory for the selected resolution.

FilePath

This tab will display the complete path name of the mesh file currently loaded in the visualization pane. It would show the user if the mesh were loaded from the local disk or the cloud space. For initial development stage, I used files from the local disk space but later after uploading all the mesh data files in the cloud data space, they can be used from the cloud space which will make the loading and caching process faster.

Rotate Tab

For better visualization and understanding of the architecture of the mouse brain vascular networks, it is important that the user can interact with it. Interaction with the 3D graphic model/mesh means that the user should be able to perform Rotate, Zoom, and Pan operations on the model/mesh at least. The X Toolkit supports a list of control modes to interact with renderers. Tables 7.1 and 7.2 enlists the types of control modes defined by the X Toolkit. They are enabled by default but can be disabled on request.

The *Pan* and *Zoom* operations are same for 3D and 2D renderers. However, the *Rotate* operation using either the mouse or keyboard is mostly for 2D renderers. Thus I disabled the control modes for *Rotate* operations and built my own control mode for rotation in all three directions. The **Rotate Tab** consists of three controllable *checkboxes* which can be

Keyboard Interaction	Type of Graphics Interaction
ARROW KEYS	Rotate the scene
SHIFT + ARROW KEYS	Pan the scene
ALT + UP	Zoom In, fast
ALT + DOWN	Zoom Out, fast
ALT + LEFT	Zoom In, fine
ALT + RIGHT	Zoom Out, fine
r	Reset the view to default based on bounding box of all visible objects or a manual configured camera position

Table 7.2: List of keyboard control modes used for interacting with the renderer. When multiple renderers exist in the document, the one under the mouse listens to the keyboard interaction.

used for both monitoring and control. Each checked-box will overwrite the previous rotate operation.

Update

After the user makes any changes to any of the above tabs either the *Resolution* or the *Mesh Unit Specs*, this *Update* button will actually perform the changes. The user can switch to other resolutions or change the unit specs of the STL mesh for the selection, and then click *update*. This will upload the corresponding mesh file into the renderer. If there is no file available for the combination selected, the same data will continue to be rendered in the visualization pane.

7.5 Results

The framework automatically loads the smallest resolution volume when first launched. The resolution and *unit-x*, *unit-y*, *unit-z* coordinates can then be selected to load the other higher resolution volume *Meshes* (See Fig.7.2). It is observed that without caching, the time taken to display the data is about 10-15 seconds. The URL of the Web-based visualization for the IEROM vascular network data set is <http://jrkwon.com/3dbrainatlas>.

7.6 Challenges

Slow loading of the STL Meshes

The whole mouse brain vascular network dataset is a set of complex meshes. The STL meshes created for a single *unit-volume* have around 2,400,000 vertices and are approximately of

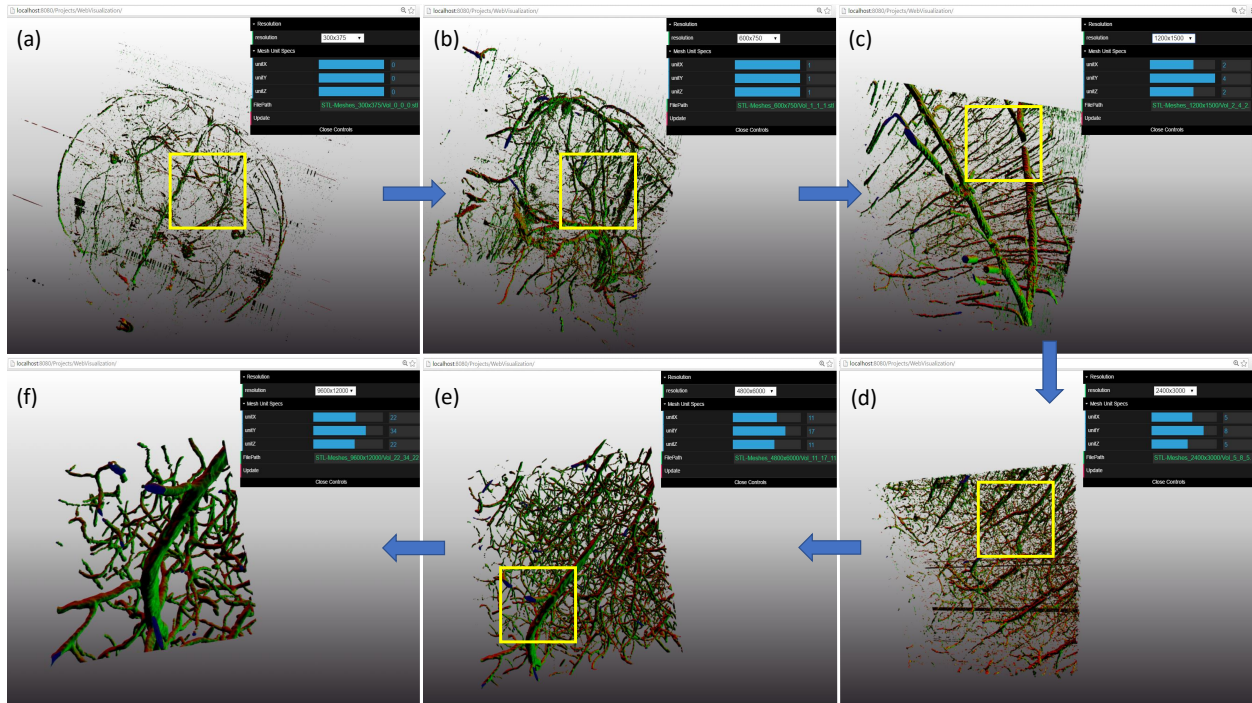


Figure 7.2: STL meshes of different resolutions loaded according to the region of interest selected by the user.

size 42000 KB. Loading and rendering such huge STL mesh files from the local disk space is a time-consuming task, leading to slow loading of the STL meshes in the display pane. Therefore to avoid such latency, I uploaded all the STL files created by the 3D Model Maker block to a cloud based data storage space, so the web-based application directly fetches the mesh data files from the same web data storage space instead of the local computer disk. This process speeds up the loading and unloading of the large mesh data files on the web-application and also enables collaboration among research groups across the globe.

Part IV

Virtual Reality Framework : Methods and Implementation

Chapter 8

Virtual Reality for Mouse Brain Vascular Network Study

8.1 Overview

Virtual Reality (VR) is an emerging computer technology to enable a user to be physically present in a virtual environment. It requires a special set of hardware that includes Virtual Reality headsets in combination with physical spaces or multi-projected environments to simulate audio, visual and other sensations for a real life-like experience. With a headset and motion tracking, VR lets you look around a virtual space as if you're actually there.

Biomedical image visualization has been struggling with the need to accurately analyze and decipher information from the vast volumes of data generated by multiple imaging modalities that exist today. VR has a variety of potential benefits for many aspects of biomedical imaging. Fusing the evolution of advanced biomedical imaging systems and VR, has lead to the development of powerful computational techniques to visualize, analyze and use these images for advanced use in medical practice.

IEROM research work aims to study the mammalian (Mouse) brain morphology to be able to compare a diseased brain with a healthy one. The whole mouse brain vasculature data acquired by the IEROM is a motley bunch of interconnected blood vessels. To properly study and analyze the architecture of such data sets, there is a need of sophisticated visualization methods which can deduce even minor morphological details accurately. With the advancement of VR in the field of biomedical image visualization, it is now possible to design VR frameworks to visualize and interact with 3D biomedical images. The idea is to use VR to visualize and comprehend large and complex biomedical datasets for better detailed understanding. Therefore, in this chapter, I will explain my approach to create such a VR framework for the study and analysis of mouse brain vascular networks through better visualization and interaction techniques. The aim is to load the mouse brain vascular volumes created earlier (explained in previous chapters) in a virtual reality space and be able to walk-through the structure and interact with it.

8.2 Tools and Environment Settings

To achieve the aim of visualizing and interacting with the whole mouse brain vascular data models in Virtual Reality, it is first important to get the right tools and setup the right environment.

Selecting the VR Headset

There are many VR headsets available in the market today from leading companies like HTC, Sony, Oculus, Google, Samsung, etc. However Virtual Reality can be best realized with an Oculus Rift. Oculus Rift in comparison with other headsets has a better per eye resolution of 1080×1200 , refresh rate of 90 Hz and a wider field of view of 110 degrees. Developing a VR framework on a PC using an Oculus platform is also easy to integrate with most of the modern game engines and SDKs. Powerful game engines like *Unity* and *Unreal* come with out-of-the-box support for the Oculus hardware, such as Platform SDK, tutorials, sample scenes, custom utility packages, and more. Therefore, I select the **Oculus Rift** Headset for developing and realizing my VR framework.

Leap-Motion Controller

To be able to interact with 3D models in the virtual reality with our bare hands, I mount a *Leap Motion Controller* onto the Oculus Rift Headset. Leap Motion's hand tracking technology is designed to be embedded directly into VR/AR headsets. It is a hardware sensor device that supports hand and finger motions as input analogous to a mouse but requires no hand contact or touching. The device consists of two cameras and three infrared LEDs that track infrared light with a wavelength of 850 nanometers, which is outside the visible light spectrum. The Leap Motion Controller comes with an easy and flexible VR integration packages for game engines like *Unity* and *Unreal*.

Unity Game Engine

Unity is a cross-platform game engine developed by Unity Technologies. It is an all purpose game engine, and supports both 2D and 3D graphics, drag and drop functionality and scripting through C# and UnityScript. UnityScript is a proprietary scripting language which is syntactically similar to JavaScript.

Oculus VR Headset Support in Unity

Unity has built-in support for certain VR devices including Oculus Rift and Oculus Development Kit2 (DK2). Oculus Utilities Unity Package assists all VR development needs, including assets, scripts, and sample scenes (see Table 8.1). The sample scenes are helpful for developers to have a starting reference.

Unity Utilities	Usage
OVRManager	An interface for controlling VR camera behavior
OVRPlayerController	A VR first-person control prefab
OVRInput	A unified API for Xbox controllers, Oculus Touch, and Oculus Remote
OVRHaptics	An API for Oculus Touch haptic feedback
OVRScreenshot	A tool for taking cubemap screenshots of Unity applications
Adaptive Resolution	Automatically scales down resolution as GPU exceeds 85

Table 8.1: List of Unity Utilities to support Oculus VR devices.

Leap-Motion Controller Support in Unity

Unity provides Core Assets and Modules for Leap Motion to make it easy to design hands, user interfaces, and interactions. Leap Motion’s Core Assets provide the foundation for VR applications with a minimal interface between Unity and the Leap Motion Controller. With Core, you can render a basic set of Leap hands or attach arbitrary objects to hand joints. Unity Modules are extensions built on top of the Unity Core Assets to provide additional features and capabilities.

Unity Editor Interface Basics

When you open a project in Unity, the main editor window opens which is made up of tabbed windows which can be rearranged, grouped, detached and docked. The default arrangement of windows gives you practical access to the the most common windows (see Fig.8.1).

- *Project Window*: Displays library of assets that are available to use in the project. The imported assets of the project appear here.
- *Scene View*: Allows to visually navigate and edit scenes. The scene view can show a 3D or 2D perspective, depending on the type of working project.
- *Hierarchy Window*: A hierarchical text representation of every object in the scene. Each item in the scene has an entry in the hierarchy, so the two windows are inherently linked. The hierarchy reveals the structure of how objects are attached to one another.
- *Inspector Window*: Allows to view and edit all the properties of the currently selected object. Because different types of objects have different sets of properties, the layout and contents of the inspector window will vary.

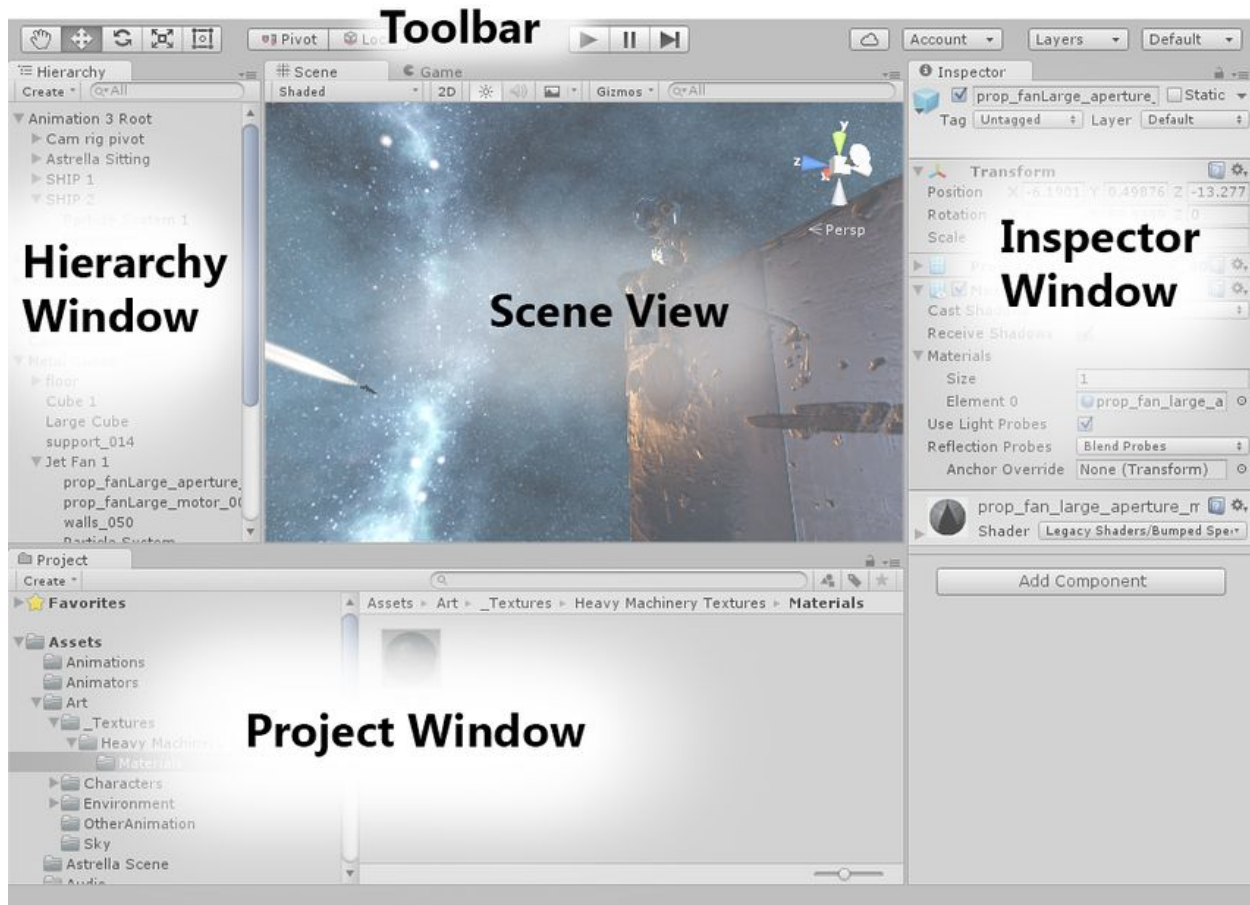


Figure 8.1: Unity default setup with different views and windows [36].

- **Toolbar**: Provides access to the most essential working features. On the left it contains the basic tools for manipulating the scene view and the objects within it. In the centre are the play, pause and step controls. The buttons to the right give access to Unity Cloud Services and Unity Account, followed by a layer visibility menu, and finally the editor layout menu (which provides some alternate layouts for the editor windows, and allows to save our own custom layouts). The toolbar is not a window, and is the only part of the Unity interface that you can't rearrange.

Asset

An *Asset* is a representation of any item that can be used in the game or project. An asset may come from a file created outside of Unity, such as a 3D model, an audio file, an image, a mesh, or any of the other types of file that Unity supports.

Scenes

Scenes contain the environments and menus of a game. Think of each unique Scene file as a unique level. In each Scene, you place your environments, obstacles, and decorations, essentially designing and building your game in pieces. When you create a new Unity project, your scene view displays a new Scene. This Scene is untitled and unsaved. The Scene is empty except for a Camera (called **Main Camera**) and a Light (called **Directional Light**) (see Fig.8.2).

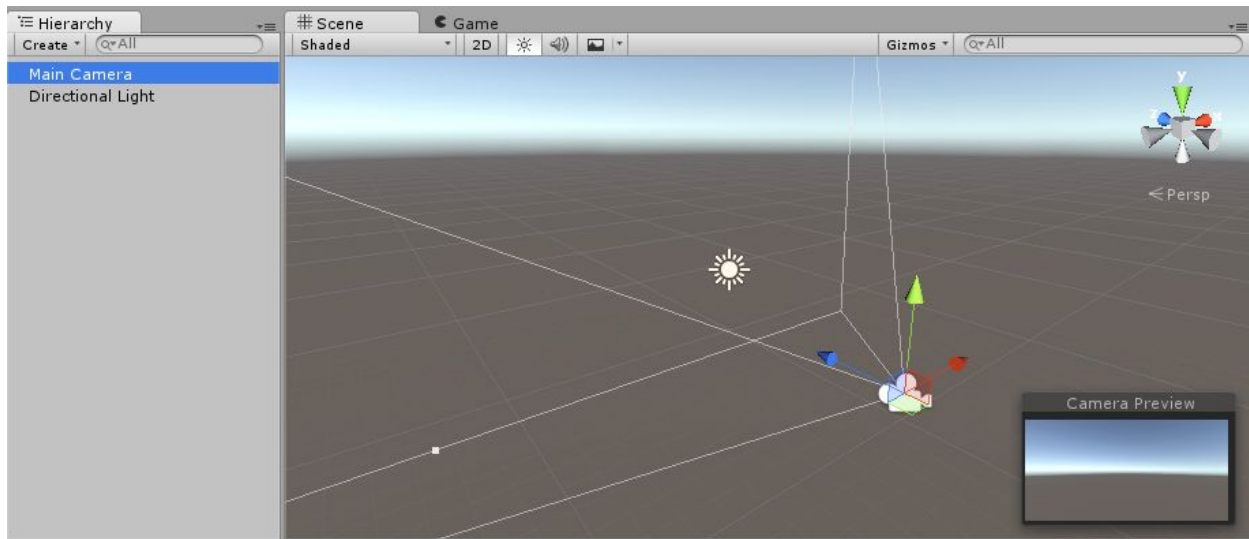


Figure 8.2: A default scene in *Unity* with the *main camera* and *directional light* [36].

GameObjects

The *GameObject* is the most important concept in the Unity Editor. Every fundamental object in a game is a *GameObject*, from characters, props, and collectible items to lights, cameras, special effects and scenery. They do not accomplish much in themselves but they act as containers for **Components**, which implement the real functionality.

A *GameObject* always has a *Transform* component attached (to represent position and orientation) and it is not possible to remove it. The other components that give the object its functionality can be added from the editor's Component menu or from a script (see Example Fig.8.3).

Transforms

The *Transform* is used to store a *GameObject*'s position, rotation, scale and parenting state and is thus very important. A *GameObject* will always have a *Transform* component attached, it is not possible to remove a *Transform* or to create a *GameObject* without one. A *Transform* can be edited in the Scene View or by changing its properties in the Inspector.

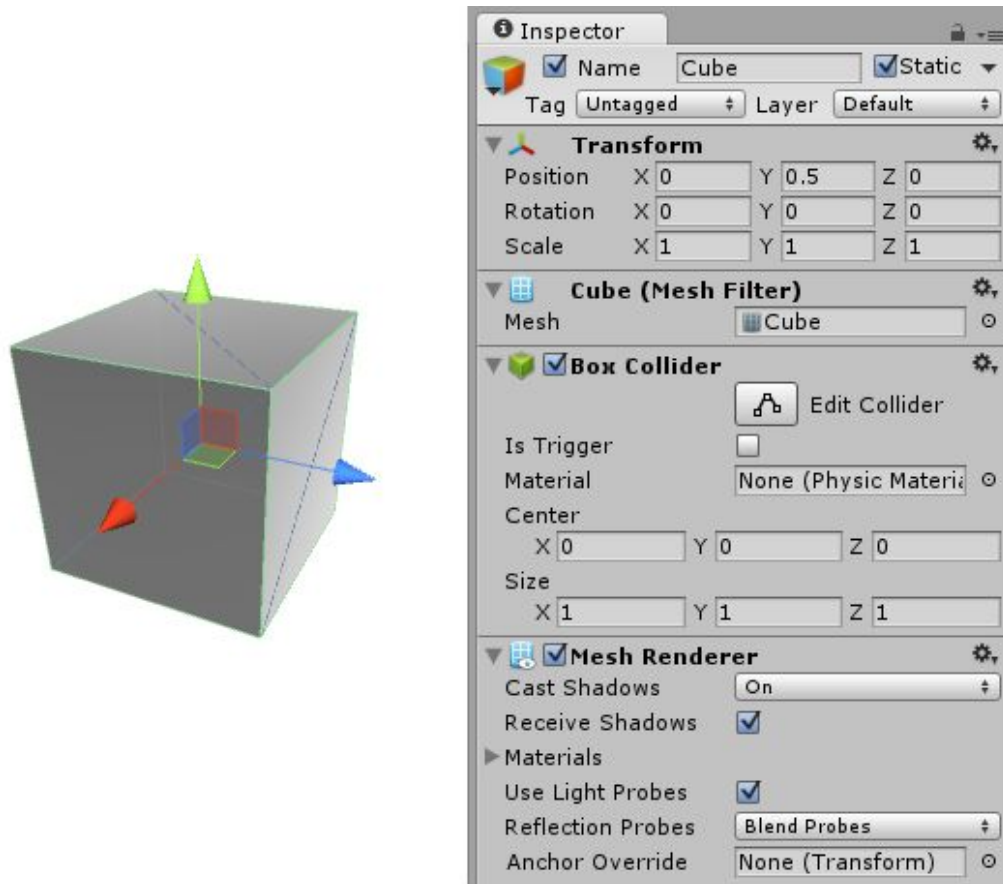


Figure 8.3: A sample gameobject in *Unity* called *Cube* and its inspector window options [36].

Lights

Lights are an essential part of every scene. While meshes and textures define the shape and look of a scene, lights define the color and mood of the 3D environment.

Cameras

Cameras in Unity are used to display the game world to the player. You will always have at least one camera in a scene, but you can have more than one. I used the Leap Motion Head Mounted camera in the scene enabled with VR support.

Required Hardware Setup

System Prerequisites

To power up an Oculus Rift and design VR frameworks with Rift and Leap Motion Controller, the host computer needs to meet or exceed some system specifications as mentioned in Table 8.3. I used an Oculus recommended desktop; *Alienware X51 R3 i5 Desktop*. It has Intel core i5 6400 2.7 GHz, 16GB RAM, 256GB Solid-State Hard Drive, and NVIDIA GeForce GTX970 graphics card.

Oculus Rift Hardware Setup

- Unbox the Oculus Rift kit that contains: Oculus Rift Headset with Quick Start Guide, Oculus Camera Sensor with Built-in Stand, Small Plastic Tool for Integrated Headphone Removal, Oculus Remote with Integrated Battery, Xbox One Wireless Gamepad controller, Xbox One USB Wireless Receiver for Gamepad and Instructions, 2 x AA Batteries for Gamepad, 2 x Oculus Logo Stickers, and Oculus Lens Wipe Cloth (See Fig. 8.4).



Figure 8.4: Oculus Rift Kit [30].

- Remove the protective films from the headset lenses and from the sensor lens (shiny side of the sensor body).
- Connect the HDMI end of the headset cable to the HDMI port on your graphics card. Note: Don't use the HDMI port on your motherboard, if you have one. If you're not sure which HDMI port to use, try the one on the narrower and simpler panel on the back of your computer.
- Connect the USB end of the headset cable to a USB 3.0 (blue) port on your computer.

Oculus Remote Buttons	Usage
Navigation disk	Move up, down, back, or forward through menu options
Select button	Select a menu option, or to select an item in a game or app
Back button	Cancel an option, or move back a screen
Volume Down and Volume Up	Control the volume in the On-Ear Headphones
Oculus button	Press to access the Universal Menu from almost anywhere in Rift

Table 8.2: List of Oculus Remote button's functionalities.

- Connect the sensor cable to another USB 3.0 (blue) port on your computer.
- You'll see three green icons in the lower left of the Oculus screen indicating that the headset and sensor have both connected successfully. Note: If you see red or yellow warning icons or have any other issues try [Rift Hardware Troubleshooting](#).
- Follow the link: <https://www3.oculus.com/en-us/setup/>. Download and run the Rift's setup tool, which will automatically install all the software required to use the Rift. It will further guide the user to setup and configure the Rift headset, sensor and other hardware.
- Gently pull the clear plastic tab out from the battery door on the back of the Oculus Remote. This tab keeps the batteries from running down during shipping. Press and hold the select button, which is in the center of the navigation disk, to pair the remote with your headset. See Table 8.2 and Figure 8.5 to know how to use the Oculus Remote.
- The Oculus sensor makes sure what the user is seeing in Rift tracks their position and movement. While setting up the Oculus sensor, I need to enter the correct height of placement when asked. This helps make sure that the VR environment looks right towards the user. Entering your standing height lets Rift calculate the distance to the floor. This makes your experience in VR feel more realistic. You only need to set your height once, even if you decide to sit or let someone else use your Rift.
- To make sure your sensors can accurately track your movement, it is required to find a good place for placing them:
 - Place the sensors between 3 feet (1 m) and 6 feet (2 m) away from your head.
 - Make sure nothing is blocking the line of sight between your headset and the sensors. Try crouching and stepping sideways to make sure the edges of the desk or shelf you're using won't block your view of the sensor. Don't use an area where people will be walking between you and the sensor.



Index

1	Up	8	Volume Up
2	Status LED	9	Back Button (B Button)
3	Left	10	Volume Down
4	Select Button (A Button)	11	Oculus Button
5	Right	12	Battery Door
6	Navigation Disk	13	Lanyard
7	Down		

Figure 8.5: Oculus *Remote Controller* specifications [14].

- Place in a direction where you’ll normally be facing. Keep the sensor inside your starting field of view. Check to make sure the glossy side of the sensor lens is pointing towards your play area.
- Put them on a stable surface. Don’t put the sensor on top of your monitor or computer, or anywhere else it will vibrate or wobble.
- Make sure to adjust them slightly above your headset. If that’s not possible, it’s fine to have it below your head instead.
- Make sure your play area is at least 3 feet by 3 feet (1 meter by 1 meter). If you’re only using 2 sensors, try to put your sensors 3-6.5 feet (1-2 meters) in front

of where you'll be wearing your headset.

- If your sensors are close together, rotate them so that they face forward. If your sensors are wide apart, rotate them towards the center of your play area.
- The sensor's general field of view (See Fig. 8.6) is 100 degrees horizontal and 75 degrees vertical. Notice that if you get really close to a sensor, it'll generally be difficult for it to see more than the middle of your body—so you won't get great tracking within about a foot and a half of it.

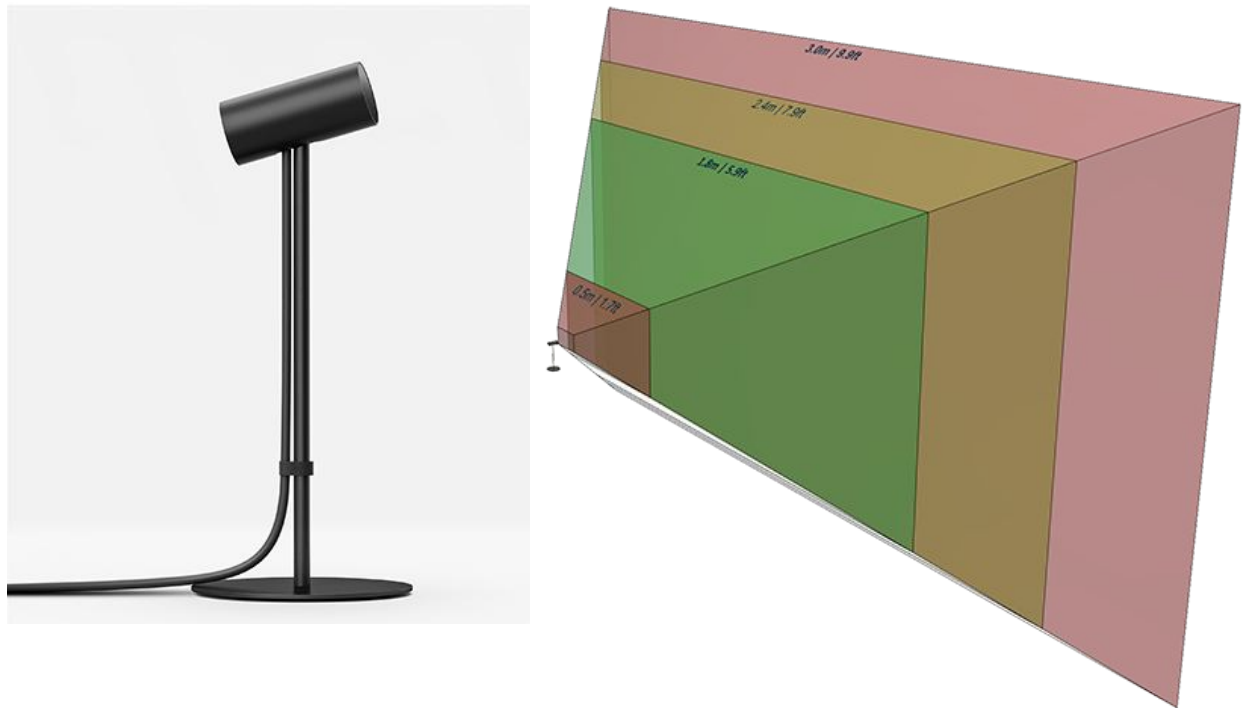


Figure 8.6: Oculus Sensor and its field of view [30].

- In cases where two sensors can see the Touch controller, you should get ideal tracking up to at least 10 feet. Figure 8.7 illustrate how the ideal tracking volume of two sensor configurations look when placed on a six-foot desk inside a 12-foot by 12-foot room.
- Take the Rift headset to the spot where you plan to use it. Make sure the sensor lens (the shiny side) is pointing at your head.
- Gently adjust the angle of the sensor body on the sensor stand if necessary.
- Hold the headset just in front of you and move it slowly side to side. You may also need to swing it gently down toward the floor and back up in front of your head. You'll be notified when the Oculus sensor has found your headset.

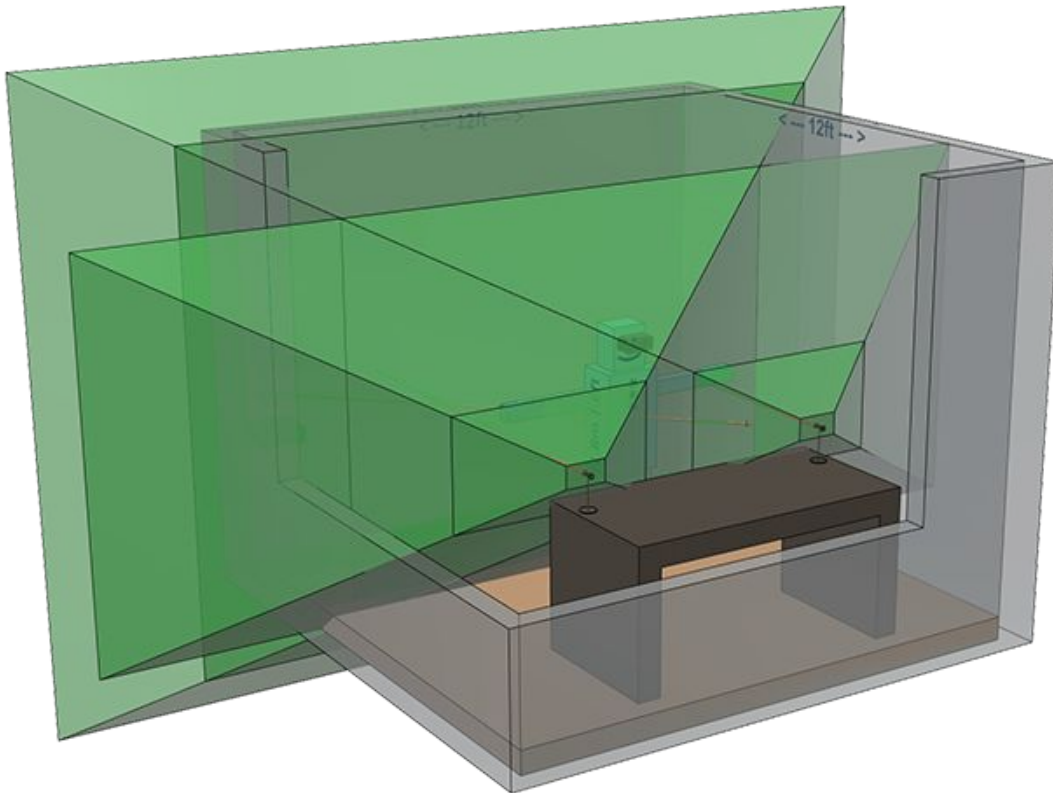


Figure 8.7: Combined optimal tracking volume when two sensors can see the headset controller [30].

- After your Rift headset fits you properly, it will be quick and easy to put it on from now on (Refer Fig. 8.8).
 - Open the side tabs on the main strap. Fasten the tabs to the middle of the strap arms as a starting point.
 - Open the top tab, loosen the top strap all the way, and leave it loose. Angle the On-Ear Headphones outward.
 - Hook the tracking triangle on the back of your head. Tighten the side tabs slightly and tighten the top strap until you feel the weight balanced around your head.
 - Rotate the headphones into position and push them onto your ears.
 - Find the lens slider on the underside of the headset. It controls lens spacing inside the headset. Push and hold it into the headset, then slide it to get the sharpest possible image



Figure 8.8: Oculus Headset Specifications [30].

- Clear the surrounding area where you stand wearing the VR headset, at least a few feet in all directions. Move anything that might get in your way, like furniture or other objects. Always be aware of your surroundings while using the Rift.
- Once the hardware setup for the Oculus Rift is completed:
 - Stand in the spot where you'd like to use Rift and face the Oculus sensor
 - Slide your wrist through the Oculus remote's lanyard
 - Put on the Rift headset
 - Move the headset very slightly up and down on your face until the image is sharpest
 - Then push in the lens slider on the bottom of the headset and slowly slide it from side to side until the image is sharpest
 - Press the select button on the Oculus remote. You'll see a few short experiences to get you started in VR.

Leap Motion Controller Hardware Setup

- Peel Off Sticker: Remove the Sticker from the top of the controller.
- Plug into the Computer: Use the USB cable included in the box. Shiny side of the controller faces up and the green light faces towards you (see Fig. 8.9).

System Specs	Recommended	Minimum
Graphics Card	NVIDIA GTX 1060 / AMD Radeon RX 480 or greater	NVIDIA GTX 1050 Ti / AMD Radeon RX 470 or greater
Alternative Graphics Card	NVIDIA GTX 970 / AMD Radeon R9 290 or greater	NVIDIA GTX 960 4GB / AMD Radeon R9 290 or greater
CPU	Intel i5-4590 equivalent or greater	Intel i3-6100 / AMD FX4350 or greater
Memory	8GB+ RAM	8GB+ RAM
Video Output	Compatible HDMI 1.3 video output	Compatible HDMI 1.3 video output
USB Ports	3×USB 3.0 ports, plus 1×USB 2.0 port	1×USB 3.0 port, plus 2×USB 2.0 ports
OS	Windows 10	Windows 8.1 or newer

Table 8.3: System Specifications of a computer required to power-up the connected Oculus VR device.



Peel off sticker

Plug into your computer

Get ready

Figure 8.9: Leap Motion Controller Setup [19].

- Clean the Headset: Make sure that the surface on the Oculus VR headset is fully cleaned. It is recommended using rubbing alcohol and a clean cloth.
- Align the mount: align the angled sides of the adhesive mount with the angled details on the Rift.
- Fix the mount: Attach the VR Developer Mount to your headset. Firmly press the adhesive mount into place pressuring full contact over the entire surface. Allow at least 1 hour for the mount to adhere to the surface. Then use the free cable extender bundled with the mount to connect the controller directly to the computer. Make sure the orientation of the mount is as shown in Figure 8.10. For more details follow the LeapMotion Setup video <https://youtu.be/OUdL3y-mrFM>.



Figure 8.10: Leap Motion Controller mounting on the Oculus Rift [37].

Software Setup

Unity Game Engine Installation

Game Engines can significantly reduce the time and effort it takes to build Virtual Reality experiences with Oculus devices like Rift. *Unity* well supports Oculus devices. I downloaded the latest version of Unity Installer. The installer uses a *Download Assistant* which will direct a user to install correctly. It provides options to install specific components of the Unity Editor, according to user's requirements.

There is a need to import Unity Packages for specific applications that is planned to use in the project, like Oculus and Leap Motion. To import any package, it is required that any previous version of the same package is deleted, then either a new project is created or the current scene is saved. For importing any package: Select *Assets* → *CustomPackage* → and select the *Utilities Unity Package* to import it. Alternately, one can locate the *.unityPackage* file in your file system and double-click it to launch.

Oculus Software Setup

- Unlike Oculus DK2, Oculus Rift comes with an easy software installation process. After the user has successfully connected and completed the hardware setup, *Rift's Setup Tool* will automatically install all the software required to use it.
- The list of software's that the tool will install includes the *Oculus Runtime* and *Oculus App*. I need to have this App and calibrate the Rift. A user needs to create an Oculus

Account to use the Rift. After all the software is installed correctly. Test the Rift by opening any example scene or movie from the Oculus App.

- Each VR device requires appropriate runtime installed on the machine. To develop and run Oculus within Unity, one needs to have the *Oculus runtime*.
- For any project in Unity, Oculus support is enabled by checking *Virtual Reality Supported* in the *Edit* → *ProjectSettings* → *Player* → *OtherSettings Configuration tab* (See Fig. 8.11). Unity automatically applies position and orientation tracking, stereoscopic rendering, and distortion correction to your main camera when VR support is enabled.

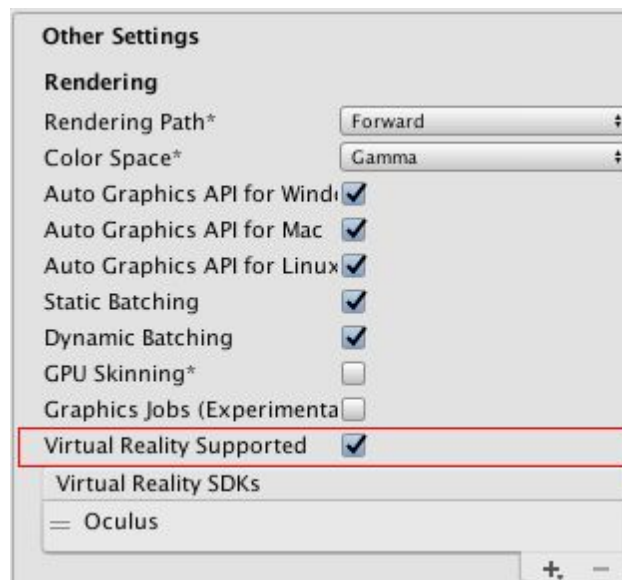


Figure 8.11: Enabling VR option in Unity [36].

- The *Unity Utilities Package* is easy to download and contain useful prefabs, C# scripts, and other resources to support VR projects in Unity. The package includes an interface for controlling VR camera behavior, a first-person control prefab, a unified input API for controllers, advanced rendering features, object-grabbing and haptics scripts for Touch, debugging tools, and more.
- The *Oculus Unity Sample Framework* includes sample scenes and scripts illustrating common VR features such as locomotion, in-app media players, crosshairs, UI, interaction with Game Objects with Oculus Touch, and more.

When Unity virtual reality support is enabled, any camera with no render texture is automatically rendered in stereo to the device. Positional and head tracking are automatically applied to the camera, overriding the camera's transform. Unity uses head tracking to

the VR camera within the reference frame of the camera's local pose when the application starts. If one is using *OVRCameraRig*, that reference frame is defined by the Tracking Space GameObject, which is the parent of the *CenterEyeAnchor* GameObject that has the Camera component. The Unity Game View does not apply lens distortion. The image corresponds to the left eye buffer and uses simple pan-and-scan logic to correct the aspect ratio.

Leap Motion Software Setup

- Download the Orion software and run the installer.
- Right-click on the new *Leap Motion* system tray icon and click Settings. Go to the Troubleshooting tab and select *Recalibrate Device*. A calibration of 90% is recommended.
- On the General tab, check Allow Images. This allows apps to access the infrared video pass through.
- Download the *Unity Core Assets for Leap Motion* to program the Leap Motion in Unity. In Unity, go to File and click New Project. Name your project and click Create Project. Right-click in the Assets window, go to Import Package and left-click Custom Package. Find the *Core Unity package* and import it.
- Core Assets import three folders in the Assets window – the *Plugins* folder and *LeapC* folder which contain all of the API bindings, and the *LeapMotion* folder, which contain all of the Prefabs, Scripts, and Scenes (see Table 8.4).
- Once the Core Assets are set, go to LeapMotion/Core/Prefabs in the Asset window. From there, drag a **LMHeadMountedRig** into the scene. In the hierarchy for the LMHeadMountedRig, I have a **LeapHandController**.
- From the LeapMotion/Prefabs/HandModelsNonhuman folder, drag a *CapsuleHand_L* and a *CapsuleHand_R* to the scene's hierarchy window and make them children of the LeapHandController.
- From the LeapMotion/Prefabs/HandModelsPhysical folder, drag a *RigidRoundHand_L* and a *RigidRoundHand_R* to the scene's hierarchy window and make them children of the LeapHandController.
- Locate the HandPool component attached to the LeapHandController. Set the Model Collection value to 4. Then move your two graphics hands and two physics hands from the Hierarchy view to the four empty slots.
- On the LeapHandController GameObject you'll see a LeapProvider component. For VR, make sure that "*Is Head Mounted*" is enabled (see Fig. 8.12).

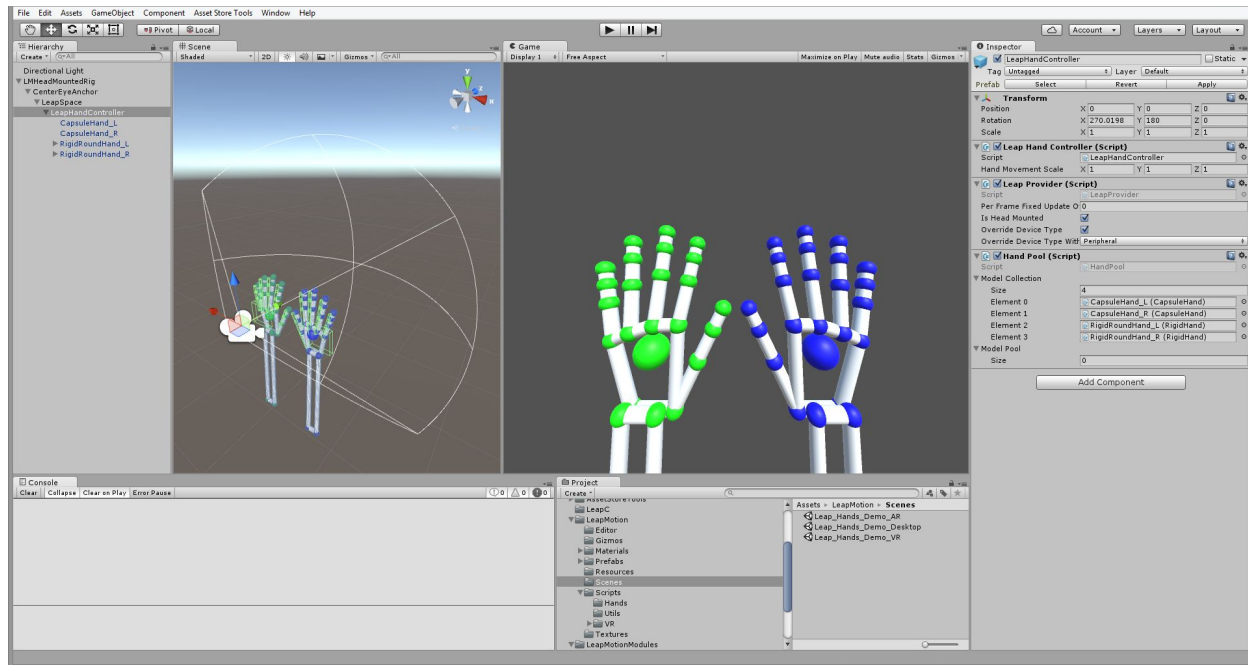


Figure 8.12: Using the Leap Motion core assets in Unity [18].

8.3 Input Data Preparation

The mouse brain vascular network's 3D models created by the IEROM image processing pipeline is loaded into the Unity Editor as an Asset. Unity can read .fbx, .dae (Collada), .3ds, .dxf, .obj, and .skp model files. I decided to use .OBJ file format for this application. OBJ is a geometry definition file format developed by Wavefront Technologies. The OBJ file format is a simple data-format that represents 3D geometry alone — namely, the position of each vertex, the UV position of each texture coordinate vertex, vertex normals, and the faces that make each polygon defined as a list of vertices, and texture vertices. Vertices are stored in a counter-clockwise order by default, making explicit declaration of face normals unnecessary. OBJ coordinates have no units, but OBJ files can contain scale information in a human readable comment line.

I converted the .STL files created by the IEROM image processing pipeline into .OBJ files, using a converter tool called *3D Tool*. The converter tool maintains the STL structure and order of the faces, vertices and normals in the model.

8.4 Mouse Brain as a GameObject in Unity

At first, a new 3D project is created in Unity which will open the basic settings for a scene. The basic settings of a scene include a *Main Camera* and a *Directional Light*. The Oculus

Prefab/ Components	Use Case
<i>LMHeadMountedRig</i> Prefab	A full VR rig that combines cameras and hand tracking. This prefab is designed to work with Unity's built-in VR Support. To use the <i>LMHeadMountedRig</i> to a scene, one needs to remove any existing camera or camera rigs from the scene
<i>LeapHandController</i> Prefab	Queries the Leap Motion service for tracking data and uses it to place hands in the scene. The tracking data from the service is transformed relative to the prefab's position and orientation in the scene. The scripts in the controller manage the hand objects that represent the physical hands detected by the Leap Motion device.
<i>Leap Service Provider</i> Component	The connection point between the Leap Motion service and the rest of the Unity assets. The service provider gets frames and images from the service and provides them other parts of your application.
<i>Hand Pool</i> Component	Manages the representation of the hands in a scene. A single tracked hand can have any number of task-specific Unity game objects associated with it.

Table 8.4: Leap Motion Core Asset Prefabs and their Use Cases.

support is enabled by checking the *Virtual Reality Support* option in project settings (as described in the *Oculus Software Setup* section above.

Camera in the Scene

I replaced the *Main Camera* in the scene hierarchy with a *Leap Motion Prefab* called *LMHeadMountedRig*. It is a combination of camera and hand-tracking, and works well with Unity's built-in VR support. The *LMHeadMountedRig* has three parts namely: *CenterEyeAnchor*, *LeapSpace*, and *LeapHandController*. The scripts in the *LMHeadMountedRig* automatically adjust the stereo camera positions to the correct interpupillary distance and automatically compensate for video lag in VR scenes. The default settings are typically correct for the default *LMHeadMountedRig* as used in a VR scene. I didn't have to change the position or orientation of the Rig for my scene, the Rig is set to have the hands in the field of view. The default *Transform* position is set to $(\mathbf{x}=\mathbf{0}, \mathbf{y}=\mathbf{0}, \mathbf{z}=\mathbf{0})$, which is the origin of the world space coordinate system (Table 8.5). This means the user's vision is centered at the origin of the 3D space and is looking along the positive *z direction*.

The *CenterEyeAnchor* has the camera component and the *Leap VR Camera Control* component. The camera component has the *Player Settings* of the project included in

User's Movement in Virtual Reality	3D Space Translation
Right	Positive X direction
Left	Negative X direction
Up	Positive Y direction
Down	Negative Y direction
Forward	Positive Z direction
Backward	Negative Z direction

Table 8.5: 3D space translation of the user's movement in virtual reality framework.

the *Rendering Path*. So, the camera, like the Leap Motion Controller, also follows the orientation and positional tracking of the Oculus SDK. The *LeapSpace* has the *Leap VR Temporal Warping* component which interpolates the position of the cameras to compensate for differences between the captured Leap Motion frame time and the current Unity update time. The *LeapHandController* has the *Leap Service Provider* component, which is the connection point between the Leap Motion service and the rest of the Unity assets. The service provider gets frames and images from the service and provides them to the other parts of the application. The Leap Service Provider is an important component and the following options are enabled:

- *Is Head Mounted* is enabled for proper hand tracking when the Leap Motion hardware is mounted on an HMD (Oculus Rift).
- *Override Device Type* is checked to enable the use of a specific Leap Motion hardware profile (i.e. Leap Motion Controller)

Directional Light

Directional lights are very useful for creating effects such as sunlight in the scenes. Behaving in many ways like the sun, directional lights can be thought of as distant light sources which exist infinitely far away. A directional light does not have any identifiable source position and so the light object can be placed anywhere in the scene. All objects in the scene are illuminated as if the light is always from the same direction. The distance of the light from the target object is not defined and so the light does not diminish. The *Transform* component of this Gameobject is modified such as the position is set to face the positive *y-axis*.

Mouse Brain as the Target Object

Unity allows importing 3D models by either dragging the model file from the file browser straight into the Unity project window or by copying the 3D model file into the Project's Assets folder. I imported the Unit Mouse Brain Vasculature Model as an .OBJ file into

the Assets Folder of the project. The import settings of the model file is selected from the importer's inspector window (see Fig.8.13). Some of the import settings enabled are as follows:

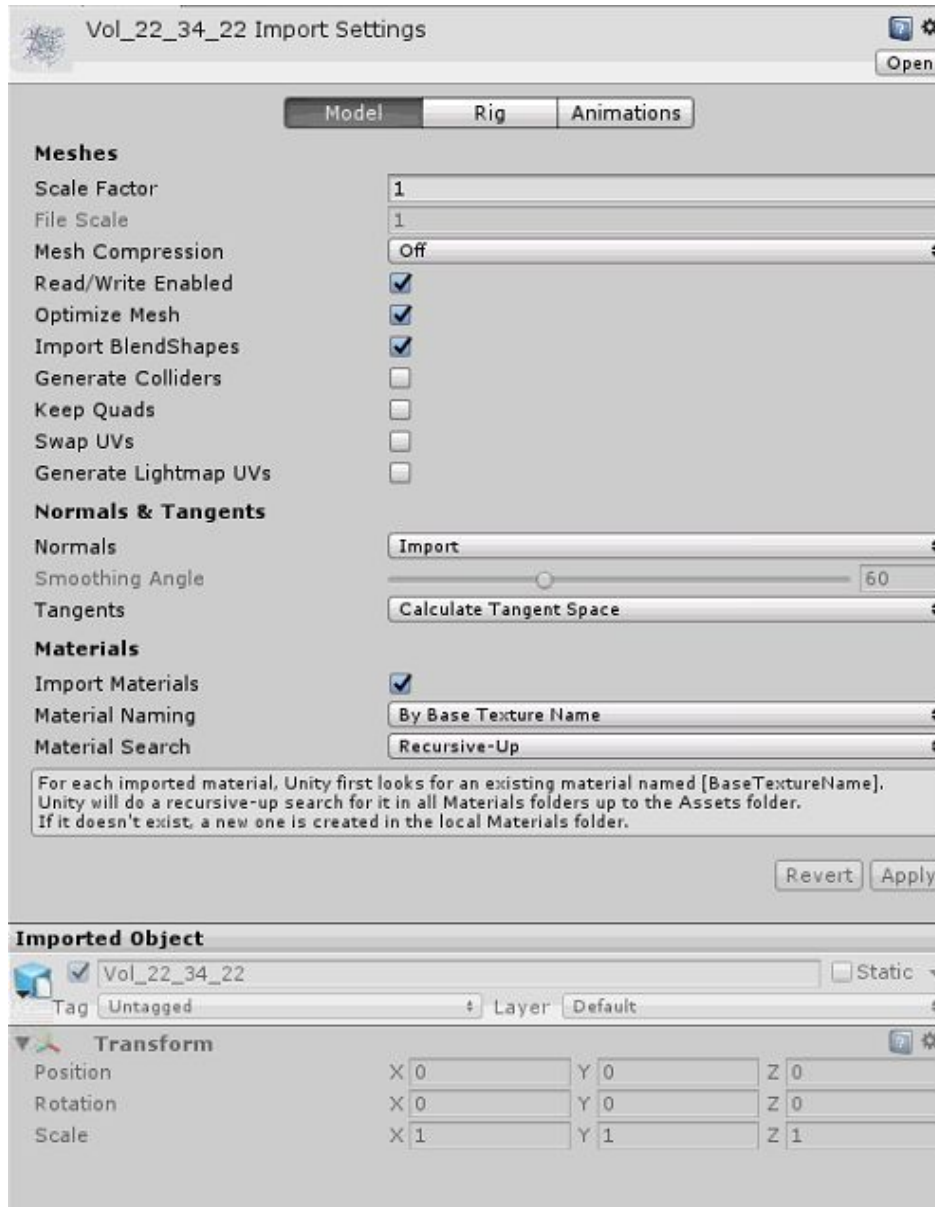


Figure 8.13: Imported mouse brain model settings.

- Default *Scale Factor* of the imported .OBJ model is 1 unit. Unity's physics system expects 1 meter in the game world to be 1 unit in the imported file.

- *Read/Write Enabled* option is checked so the Mesh data is kept in memory due to which a custom script can read and change it.
- *Optimize Mesh* option is enabled, so that Unity determines the order in which triangles are listed in the Mesh.
- *Import Blendshapes* checked, allows Unity to import BlendShapes with the Mesh.
- *Normals* are imported and *Tangents* are calculated.
- *Materials* are imported by default. Material Naming is *by Base Texture Name* which means the name of the diffuse Texture of the imported Material is used to name the Material in Unity. Material is searched *recursively*, which means Unity tries to find existing Materials in all Materials subfolders in all parent folders up to the Assets folder.

Model files placed in the Assets folder of the Unity project are automatically imported and stored as Unity Assets. A model file containing a 3D model, such as a Mouse Brain Vasculature Mesh is imported in the project as a .OBJ file. In the Project window, the primary imported object appears as a model Prefab. Usually, several Mesh objects are referenced by the model Prefab. In my case, the model prefab was split into 8 Mesh Objects, each representing a part of the original model (See Fig. 8.14). While importing, Unity breaks up any high-poly model prefabs into sub-models based on the maximum vertex limit of each mesh. The maximum vertex limit for one imported model is 65535.

This imported model is added to the scene as a Gameobject and also the only target object in the scene. The *Transform* parameters of the Gameobject was modified to fit it into the VR camera's/ user's field of view (see Fig. 8.15):

- *Scale Factor* is reduced to 0.1 unit as the model is too big to visualize.
- *Rotation* value is unchanged and is by default as $\mathbf{x}=0^\circ$, $\mathbf{y}=0^\circ$, $\mathbf{z}=0^\circ$.
- *Position* is changed to $\mathbf{x}=12.8$, $\mathbf{y}=-12.8$, $\mathbf{z}=2$ from the default values i.e. $\mathbf{x}=0$, $\mathbf{y}=0$, $\mathbf{z}=0$. Originally when the model is loaded into the scene, only one corner end of the mesh is visible. This is because the of the pivot point of the Gameobject is at that vertex. A pivot point of the any model/mesh in its local space is the first vertex point ($x=0.0$, $y=0.0$, $z=0.0$). In the world space, the pivot point acts as the center of the object and is placed at the origin of the world space coordinate system.

The imported OBJ models are created originally from the STL meshes, which sets a starting point or vertex for the meshes. This starting point is retrieved by the OBJ file and is transferred as the pivot point of the imported model. The volumetric dimension of the original model loaded into the scene is $256 \times 256 \times 256$ units. After the reduction of the *Scale Factor* to 0.1 unit, the reference dimensions of the model becomes $25.6 \times 25.6 \times 25.6$. To set the center of the model as the visualization starting

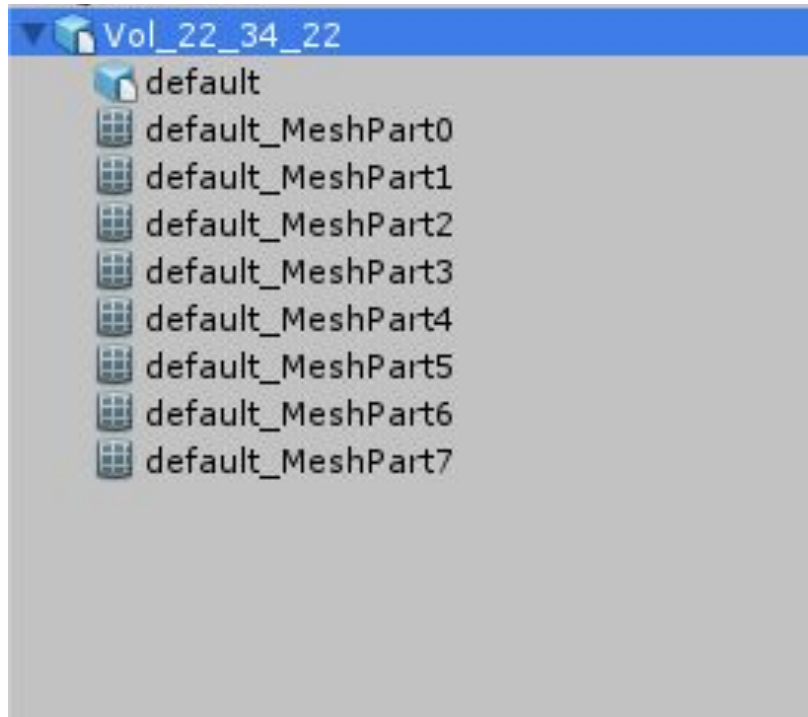


Figure 8.14: Unity breaks up any high-poly model prefab into sub-models based on the maximum vertex limit.

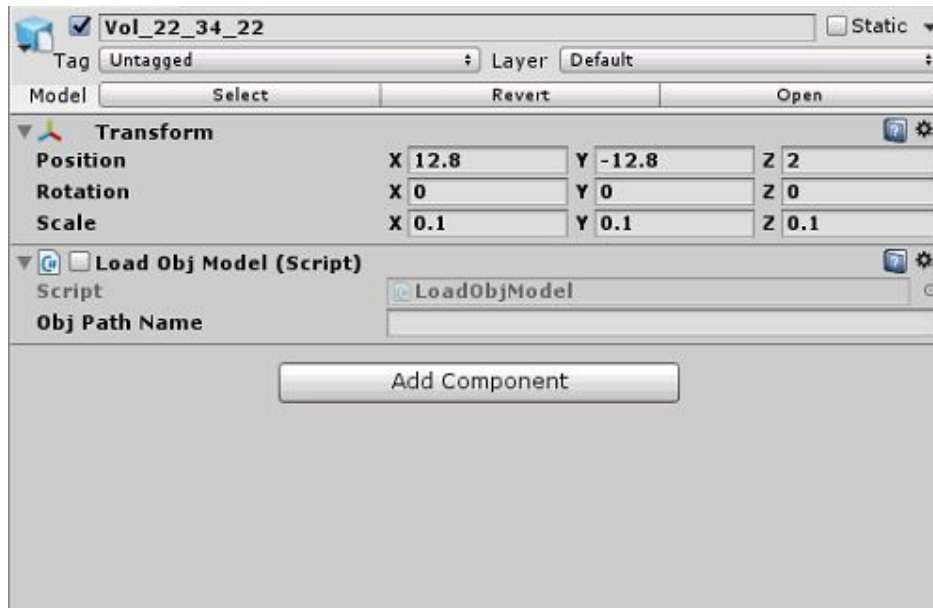


Figure 8.15: Transform settings of the imported mouse brain model.

point, I shifted the position transform of the model along the x and y directions to get the center of x - y plane first; ($\mathbf{x}=\mathbf{12.8}$, $\mathbf{y}=-\mathbf{12.8}$). This implies I moved the pivot point 12.8 units to the right and 12.8 units down, so the user sees the center of the plane. The position of the camera is the position of the user in Virtual Reality. At start, the aim is to visualize the whole Mouse Brain model in front of the user at a distance that corresponds to distinct vision. I pushed the model 2 units away from the user to visualize it clearly from the outside.

8.5 Challenges

Missing OBJ File Writer in ITK

In the ITK library there is no API to support writing .OBJ file format. Since, in *Unity* framework, it is easier to load .OBJ format files as Gameobjects. I decided to use a third-party tool called Meshlab to convert the STL mesh files into OBJ files.

Chapter 9

Gesture Controlled Navigation Method

9.1 Overview

In the previous chapter, I explained how to setup the Virtual Reality framework and how to load the mouse brain vasculature meshes in the framework as mere `GameObjects`. In this chapter, I will design a primary use case for this VR framework implementation. Zooming in and Zooming out in 3D space provides a good way to visualize and analyze a biological mesh. However, virtual reality provides an upper hand advantage of being able to walk-through and move around in the structure providing a better-detailed understanding of the different parts of the meshes. While studying the architecture of the mouse brain vasculature using different 3D visualization methods, it is always observed that we can't walk into the structure and see the inner parts of the blood vessels. With this VR framework, one can easily walk into the structure and visualize any part of the model. Thus, to better study and analyze the morphology of the mouse brain vasculature in VR, I designed this *Gesture Controlled Navigation* method to navigate inside out the mouse brain volume. It allows the user to visualize from every angle and distance. This method is developed to navigate inside a single unit volume model loaded as a `GameObject` in Unity.

9.2 Required Input

Gesture Controlled Navigation method uses our hand gestures as controllers for navigation. I captured the right-hand gestures as input and transformed those gestures into events. These events, in turn, trigger the control algorithm implemented for camera movements. The Leap Motion Controller tracks the hand gestures and provides input to the Leap Service Provider, which is fed in a script for further implementation. The *Leap Service Provider* is a major component of the *Leap Hand Controller* in the *LMHeadMountedRig* prefab. The Leap Service Provider is the connection point between the Leap Motion service and the rest of

the Unity assets. The service provider gets frames and images from the service and provides them to the other parts of the application.

9.3 Basics of Scripting in Unity

Scripting is an essential ingredient in Unity; it can control objects created in Unity Editor. Although Unity uses an implementation of the standard Mono runtime for scripting, it still has its practices and techniques for accessing the engine from scripts. The behavior of Game Objects is controlled by the Components that are attached to them. However, Unity allows creating Components using scripts extrapolating the provided features. These allow to trigger game events, modify Component properties over time and respond to user inputs. Unity supports two programming languages: C# (pronounced C-sharp), an industry-standard language similar to Java or C++; and UnityScript, a language designed specifically for use with Unity and modeled after JavaScript. A user can create a new script from the Create menu at the top left of the Project panel or by selecting *Assets* → *Create* → *C# Script* (or JavaScript) from the main menu. Unity uses *MonoDevelop* script editor, but any editor can be selected from the External Tools panel in *Unity's Preferences*.

A script can be attached by dragging it from the asset window to a GameObject in the hierarchy panel or to the inspector of the GameObject that is currently selected. There is also a Scripts sub menu on the Component menu which will contain all the scripts available in the project, including the one created by the user.

A script makes its connection with the internal workings of Unity by implementing a class which derives from the built-in class called *MonoBehaviour*. A class is a kind of blueprint for creating a new Component type that can be attached to GameObjects. Each time a script component is attached to a GameObject, it creates a new instance of the object defined by the blueprint. The name of the class is taken from the name you supplied when the file is created. The class name and file name must be the same to enable the script component to be attached to a GameObject.

MonoBehaviour is the base class for all new Unity scripts, the *MonoBehaviour* reference provides a list of all the functions and events that are available to standard scripts attached to Game Objects. It is the starting reference for any kind of interaction or control over individual objects in the game.

In Unity scripting, there are a number of event functions that get executed in a predetermined order as a script executes (see Table 9.1). Two basic functions exist in any script by default when it is created namely: *Start()* and *Update()*.

- The *Start()* function will be called by Unity before gameplay begins (i.e., before the Update function is called for the first time) and is an ideal place to do any initialization. It is called before the first frame updates only if the script instance is enabled.
- The *Update()* function is the place to put code that will handle the frame update for the GameObject. This might include movement, triggering actions and responding to

Event Functions	Execution Order
Awake()	This function is always called before any Start functions and also just after a prefab is instantiated. (If a GameObject is inactive during start up Awake is not called until it is made active.)
OnEnable()	This function is called just after the object is enabled. This happens when a MonoBehaviour instance is created, such as when a level is loaded or a GameObject with the script component is instantiated.
OnApplicationPause()	This is called at the end of the frame where the pause is detected, effectively between the normal frame updates. One extra frame will be issued after OnApplicationPause is called to allow the game to show graphics that indicate the paused state.
FixedUpdate()	It is often called more frequently than Update. It can be called multiple times per frame, if the frame rate is low and it may not be called between frames at all if the frame rate is high. All physics calculations and updates occur immediately after FixedUpdate. When applying movement calculations inside FixedUpdate, you do not need to multiply your values by Time.deltaTime. This is because FixedUpdate is called on a reliable timer, independent of the frame rate.
LateUpdate()	LateUpdate is called once per frame, after Update has finished. Any calculations that are performed in Update will have completed when LateUpdate begins. A common use for LateUpdate would be a following third-person camera. If you make your character move and turn inside Update, you can perform all camera movement and rotation calculations in LateUpdate. This will ensure that the character has moved completely before the camera tracks its position.
OnDestroy()	This function is called after all frame updates for the last frame of the object's existence (the object might be destroyed in response to Object.Destroy or at the closure of a scene).

Table 9.1: Execution order of some editable event functions while scripting in Unity.

user input, basically anything that needs to be handled over time during gameplay. To enable the Update function to do its work, it is often useful to be able to set up variables, read preferences and make connections with other GameObjects before any game action takes place.

9.4 Gesture Controller

I created a C# script to detect hand gestures and control the physical movement of the camera, named *Gesture Controller*. This script will act as a new component for the Mouse Brain GameObject in the scene. I added some public variables to examine better the features of the component and some private variables for taking inputs from other Unity Assets for internal implementation.

The public variables can be viewed under the *Gesture Controller* component in the inspector window and are useful for debugging while the scene is running (see Fig.9.1):

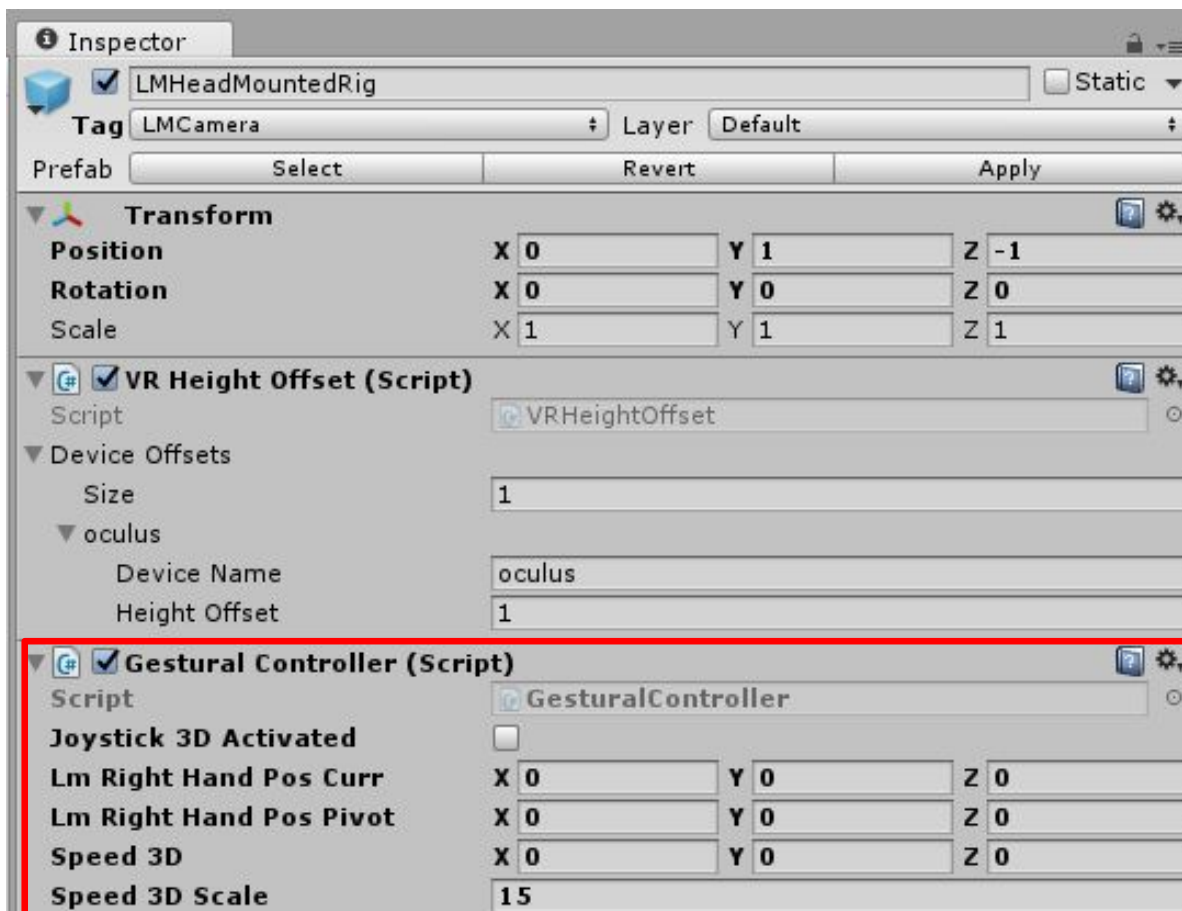


Figure 9.1: Gesture Controller Component options open in the inspector window.

- *Joystick 3D Activated*: This is a flag controlled by the right-hand gestures. The status of this flag activates or deactivates the camera movement in the 3D space. This flag is unchecked by default and is checked only when the right-hand in front of the Leap Tracker makes a transition from an *Open Palm* to a *Closed Fist*. (see Fig. 9.2) If the hand remains open, this flag remains unchecked leading to deactivated movement of the camera.

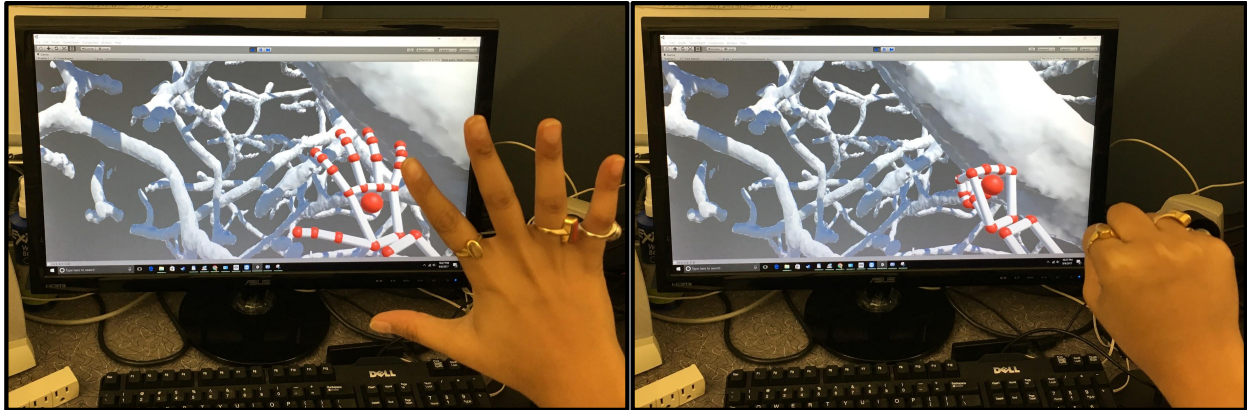


Figure 9.2: Right hand gesture change required to activate the 3D joystick.

- *LM Right Hand Pos Curr*: This is a 3D vector value indicating the current position of the right-hand in the 3D space relative to the Leap Motion Camera. This value keeps changing with the hand movements and is tracked every frame.
- *LM Right Hand Pos Pivot*: This is a 3D vector value indicating the position of the right-hand at the beginning of the control implementation, relative to the Leap Motion Camera. This value is updated only when the camera movement is active and stores the reference current position of the right-hand after each frame as the pivot.
- *Speed 3D*: This is a 3D vector which stores the difference between the right-hand's current position and the pivot position and is tracked once per frame in the *LateUpdate()* function. This value is used to move the camera after it has tracked the position of the hand in the *Update()* function.
- *Speed 3D Scale*: This is an editable floating value which is used to decide the speed of camera's movement. The value is calibrated between 1.0 to 1.5 units to experience a firm, steady camera movement, comforting the user.

The private variables are used to provide input from other GameObjects in the scene, for the computation of gesture control algorithm:

- *LM Service Provider*: It is a Leap Service Provider instance for creating a controller in the scene. It provides leap hands and images in the scene.

- *LM Camera*: It is the Leap Motion Camera GameObject in the scene i.e., *LMHeadMountedRig*. The user looks through this camera in the scene and the movement of this camera is controlled through the *Gesture Controller*. In the script, I access the *LMHeadMountedRig* GameObject via a Tag called *LMCamera*.
- *LM Right Hand Detected*: It is a flag to detect if the Leap Motion Controller is tracking the right-hand in the scene in the field of view of the user.
- *LM Right Hand Closed*: It is a flag to detect if the Leap Motion Controller is tracking the right-hand as a fist or a closed-palm.

With the above defined variables I first track the right-hand gestures and then set flags to perform camera movements accordingly. The following steps are performed to compute the gesture change of the right-hand in the scene:

- Step 1: In the *Update()* function which is called once per frame, I first read the current frame from the Leap Service Provider.
- Step 2: Detect all hands in the current Leap Motion frame and then get the current hand instance.
- Step 3: Check performed to see if the current hand is a right-hand.
- Step 4: Get the current position of the right-hand in the scene relative to the Leap Motion Camera position, and store it in the 3D vector *LM Right Hand Pos Curr* variable.
- Step 5: Store the previous right-hand status which includes the flags for right-hand detection in the scene and right-hand closed.
- Step 6: Update the right-hand status with current values. To find out if the right-hand detected in the scene is an open palm or a closed fist, the *Grab Angle* of the hand is measured. If the *Grab Angle* is more than 90° , the hand is considered to be closed.
- Step 7: If previously right-hand was detected with an open palm status and the current right-hand is detected with a closed fist. Then, the camera movement is activated which can be reviewed through the *Joystick 3D Activated* variable in the Gesture Controller Component. The current right-hand position is stored as the pivot in the *LM Right Hand Pos Pivot* variable.
- Step 8: The camera movement remains deactivated if the right-hand is detected as an open palm.

Further, after the gesture change of the right-hand is captured for a frame, I perform the camera movement accordingly in the *LateUpdate()* function. In this function, I will change the transform position of the Leap Motion Camera only if the *Joystick 3D Activated* flag is checked. The distance to move is retrieved from the *Speed 3D* value. This value is multiplied

with the *Time.deltaTime* and *Speed 3D Scale* values. The *Speed 3D Scale* will maintain the steady camera movement and the *Time.deltaTime* will make the movement frame rate independent. The camera moves *Speed 3D* distance per second and not per frame, at a speed defined by *Speed 3D Scale* value. Thus, the camera movement is smooth and steady and is not delayed due to frame loses. In this way, the user can activate the camera movement by the gesture transition and then quickly move inside out of the mouse brain vasculature model (see Fig. 9.3).



Figure 9.3: Different gestures used to navigate inside the unit volume loaded to the VR framework.

(a) First open palm gesture to initiate right hand recognition. (b) Closed fist gesture change to activate the 3D joystick. (c) With a closed fist moving away from the leap motion tracker or towards the screen, enables moving forward in the VR space. One could move left or right while moving forward and the hand in the VR space will move accordingly. (d) At any point, an open palm gesture will deactivate the 3D joystick to stop the navigation, enabling analysis of a ROI in the dataset. (e) Moving forward with a closed fist will take the user inside the unit volume in the VR space and (f) moving backwards with a Closed fist will take the user outside the unit volume in the VR space.

Chapter 10

User-Interface for the Virtual Reality Framework

10.1 Overview

The previous chapter serves a major use case of the Virtual Reality framework but navigates within a single Mouse Brain model loaded in the scene. This chapter extends the capability of the framework by implementing a way to change the model loaded into the scene and be able to visualize and study the mouse brain vasculature in different resolutions. I created a user-interface for performing this switching of data set. This user-interface will allow the user to visualize a section of the mouse brain in multiple resolutions, helping to study the biological organ in detail. Again, the framework is explained using the mouse brain vasculature dataset but it can be used for any other large biomedical dataset created in the same fashion.

10.2 Required Input

The user-interface for this framework appears as an overlay screen space with some controls. The screen space is not visible to the user by default or at the start of the scene. It appears only when the left-hand is detected in the scene, and it makes a gesture transition from a *closed fist* to an *open palm*.

To switch to different resolution models, it is required to have the 3D models loaded into the scene as and when called by the user. The *OBJReader* asset will allow loading of 3D models during run-time. I load these models directly from the local computer disk. The idea is to convert all the STL meshes created by the image processing pipeline to OBJ models. Thus ending up having similar directory structure for different resolution OBJ models.

10.3 Basics of UI Designing in Unity

The UI appears as a overlaid screen space or a ”*canvas*” in Unity’s language. All UI elements reside inside the Canvas. A Canvas is a Game Object with a Canvas component on it, and all UI elements are children of the Canvas. The Canvas area is shown as a rectangle in the Scene View and uses the *EventSystem* object to help the Messaging System. UI elements in the Canvas are drawn in the same order they appear in the Hierarchy.

The Canvas has a Render Mode setting (see fig. 10.2) which can be used to make it render in screen space or world space.

- *Screen Space - Overlay* render mode places UI elements on the screen rendered on top of the scene. If the screen is resized or changes resolution, the Canvas will automatically change size to match this.
- *Screen Space - Camera* is similar to Screen Space - Overlay, but in this render mode the Canvas is placed a given distance in front of a specified Camera. The UI elements are rendered by this camera, which means that the Camera settings affect the appearance of the UI.
- In *World Space* render mode, the Canvas will behave as any other object in the scene. The size of the Canvas can be set manually using its Rect Transform, and UI elements will render in front of or behind other objects in the scene based on 3D placement. This is useful for UIs that are meant to be a part of the world. This is also known as a *diegetic interface*.

The *Rect Transform* is a new transform component that is used for all UI elements instead of the regular Transform component. Rect Transforms have position, rotation, and scale just like regular Transforms, but it also has a width and height, used to specify the dimensions of the rectangle.

10.4 Walk-Through the User-Interface Design

I created a canvas with *screen space overlay* rendering mode. I added a set of interactive UI elements such as buttons to the canvas (see Fig. 10.1):

- *Resolution Buttons*: One button for each resolution is added to the canvas for switching to that resolution 3D models during run-time.
- *Reset*: This button is used to reset the camera’s position at the starting point. While navigating inside a structure, I might get to random locations in the 3D space. So, in any situation, if a user wants to come back to the point from where they started navigating, they can click this button to do so.
- *Exit*: This button is used to exit the user-interface screen space overlay.

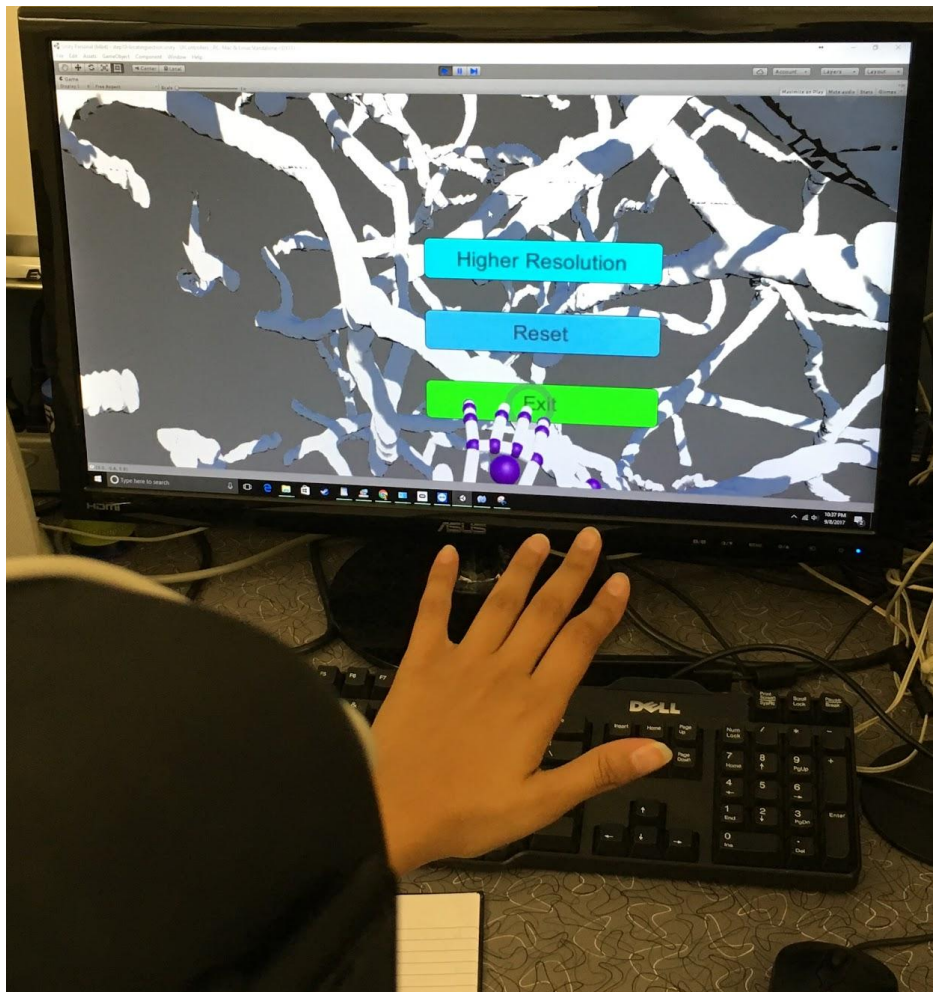


Figure 10.1: Canvas options appearing on the detection of left hand gesture change from closed fist to open palm.

Enabling/Disabling the UI Control Panel

I created a component called *UIController* through a C# script for this implementation (see Fig.10.2). This component is attached to the Canvas and has following variables:

- *UI Controller Visible*: A public variable flag that is controlled by the left-hand gestures and is used to show or hide the user-interface Control Panel.
- *LM Service Provider*: A private variable and Leap Service Provider instance to create a controller and supply leap hands as inputs.
- *Control Panel*: Private variable to hold the *canvas* instance. This instance is disabled by default and is enabled only when the *UI Controller Visible* flag is checked. When the *Exit* button is clicked, the canvas is disabled again.

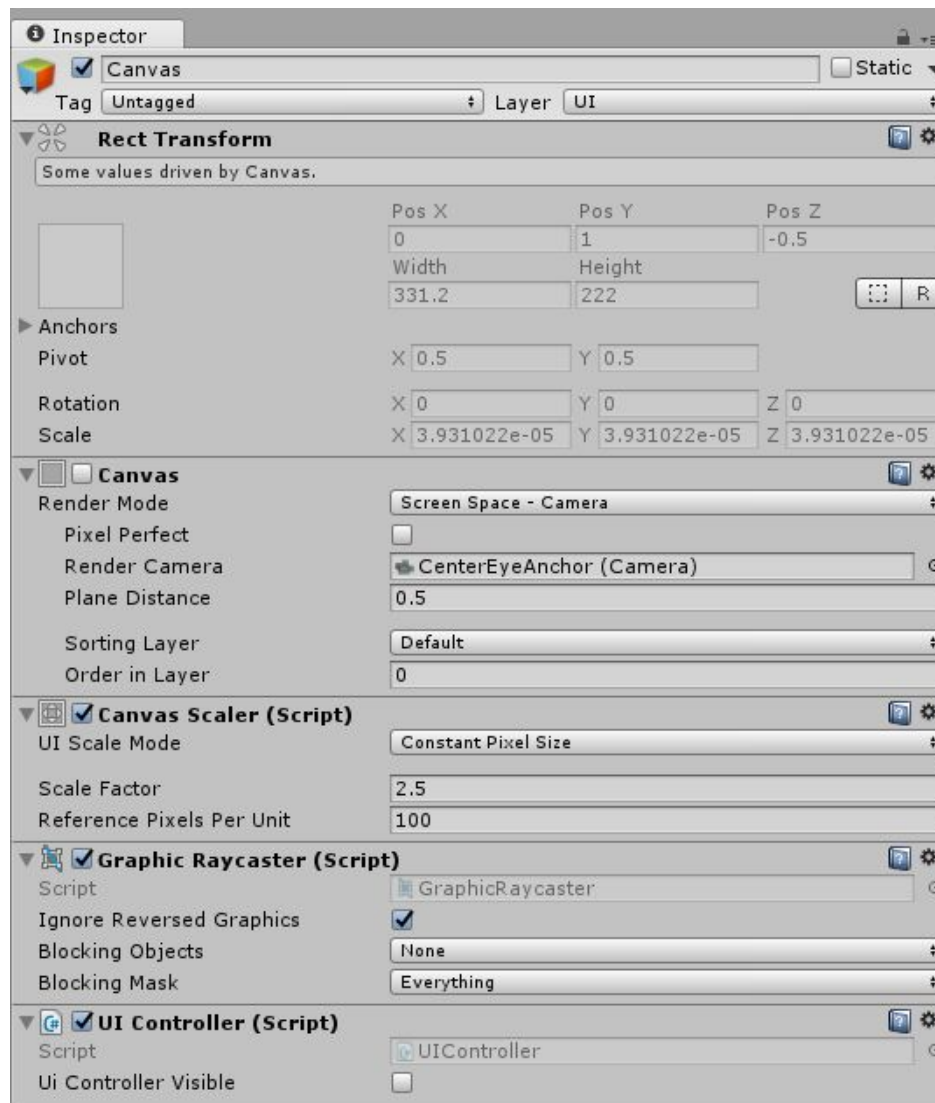


Figure 10.2: UI Controller component options and the main canvas options.

The left-hand gestures are tracked for each frame in the same way as done in the *Gesture Controller* component. However, the interpretation is different. In this case, if the left-hand previously detected was in a *closed fist* situation and current left-hand gesture is detected as an *open palm*, the *UI Controller Visible* flag is checked and the *Control Panel* is enabled.

Loading the 3D Models

I created another component called *Object Manager* for switching and loading different resolution data sets from the local disk space during run-time. This script exploits a unique *Data Mapping* method to select the 3D model to be loaded (explained below). It then

implements the *OBJReader* method to load the selected 3D model in the scene during run-time. This component contains variables to display the loaded .OBJ file name and file path. It also shows the material and texture details used in the .mtl file (see Fig.10.3).

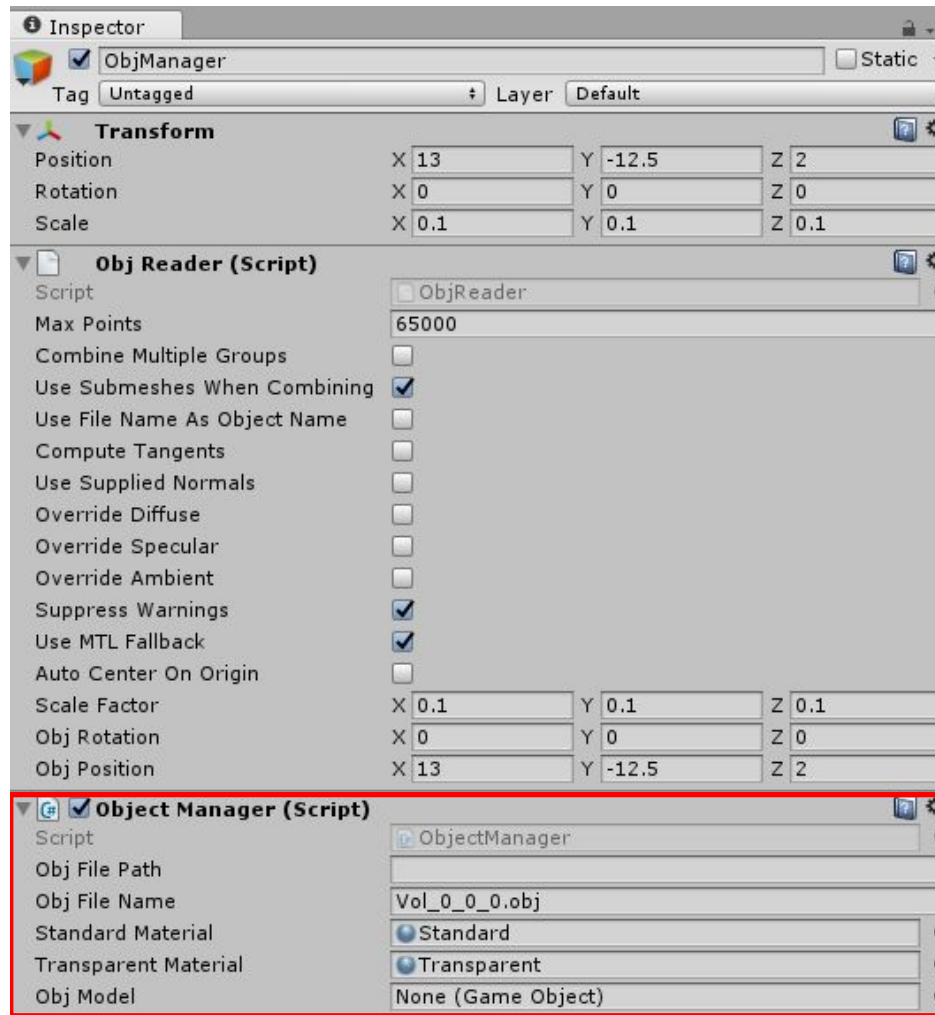


Figure 10.3: Object Manager component options for the lowest resolution volume loaded in the scene in Unity.

Proposed Data Mapping Technique

Let's explain this with an example: If a user is visualizing a part of a model in a lower resolution i.e., $300 \times 375 \times 301$ and wants to switch to visualize a section of that model in the next higher resolution i.e., $600 \times 750 \times 602$. First, the user needs to navigate to that section of the model and then open the *UI Control Panel* and select the desired higher resolution.

Sections of the Lower Resolution	Corresponding Range of Coordinates in the 3D Model	Mapped Higher Resolution File
Part_000	x:(0 → 15.0), y:(0 → 18.75), z:(0 → 15.5)	Vol_0_0_0.0bj
Part_001	x:(0 → 15.0), y:(0 → 18.75), z:(15.5 → 30.1)	Vol_0_0_1.0bj
Part_010	x:(0 → 15.0), y:(18.75 → 37.5), z:(0 → 15.5)	Vol_0_1_0.0bj
Part_011	x:(0 → 15.0), y:(18.75 → 37.5), z:(15.5 → 30.1)	Vol_0_1_1.0bj
Part_100	x:(15.0 → 30.0), y:(0 → 18.75), z:(0 → 15.5)	Vol_1_0_0.0bj
Part_101	x:(15.0 → 30.0), y:(0 → 18.75), z:(15.5 → 30.1)	Vol_1_0_1.0bj
Part_110	x:(15.0 → 30.0), y:(18.75 → 37.5), z:(0 → 15.5)	Vol_1_1_0.0bj
Part_111	x:(15.0 → 30.0), y:(18.75 → 37.5), z:(15.5 → 30.1)	Vol_1_1_1.0bj

Table 10.1: The 8 split parts of the lower resolution mapped to the 8 unit volume models in the higher resolution.

The *Object Manager* component will perform the following steps to select the appropriate 3D Model to be loaded:

- Step 1: It will first capture the coordinates of the current position of the user (or LM Camera) inside the lower resolution model, and store this coordinate in a temporary vector3 variable. Let's say the user is at position $\mathbf{x}=3.5012$, $\mathbf{y}=21.4562$, $\mathbf{z}=8.9275$.
- Step 2: A 3D model in its lower resolution is internally split into 8 parts to map to 8 higher resolution data sets. The 3D models created by the IEROM image processing pipeline are unit volumes labelled with their *unit-x*, *unit-y*, *unit-z* coordinates. The lowest resolution i.e., $300 \times 375 \times 301$ has only one 3D model volume i.e., Vol_0_0_0.0bj. Splitting this model into 8 parts means bi-sectioning the model in each direction (see Table 10.1). So the 8 parts created are: part_000, part_001, part_010,..., part_111. These parts are mapped to the 8 unit volume models in the next higher resolution i.e., $600 \times 750 \times 602$.
- Step 3: As per the Table 10.1, the current position of the LM Camera inside the model lies in the range x:(0 → 15.0), y:(18.75 → 37.5), z:(0 → 15.5), corresponding to Part_010. Thus, the higher resolution model to be loaded is Vol_0_1_0.0bj.

OBJReader

OBJReader can load 3D models at run-time from local files or web storage space. It requires only a file name or a string for the .Obj file, and automatically loads the model as a GameObject. It works with most .obj files from a variety of sources, and has .mtl file support for materials and textures. Includes various options such as generate tangents, position/rotate/scale, and combine groups into a single mesh or generate one mesh per group,

using submeshes or not. Plus it's fast...a 4MB .obj file will typically generate a mesh in less than 0.5 second, depending on CPU speed.

When I import the OBJReader asset to use in my project, a GameObject named *ObjManager* is added to the hierarchy window. This GameObject has *Obj Reader* component which has the following public variables (see Fig.10.4) :

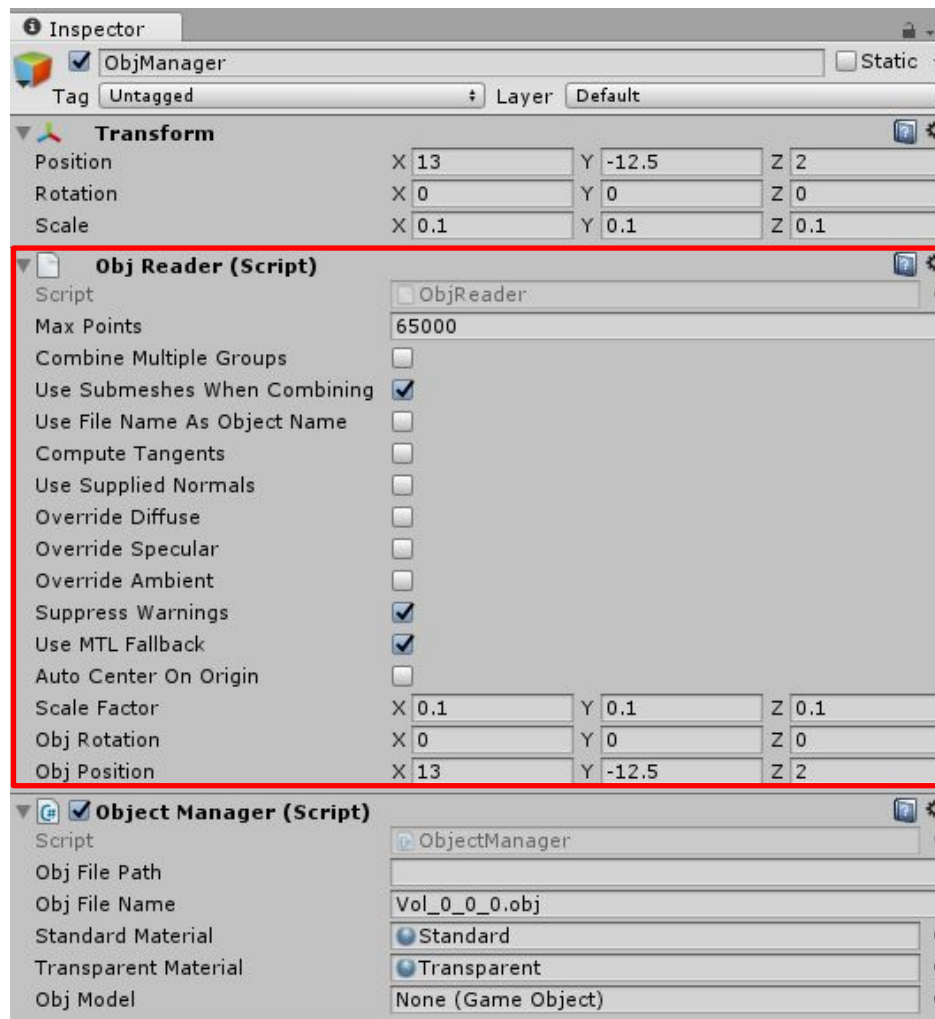


Figure 10.4: Obj Reader component options selected for the unit volume loaded.

- *MaxPoints*: Maximum number of vertices that the ObjReader will accept per group. The .obj file can exceed this limit by using multiple groups, as long as each group is under the vertex limit. The MaxPoints is clamped to 65,534 as the maximum regardless of what is set by the user. Since, that is the most Unity will accept for one mesh.
- *CombineMultipleGroups*: If checked, will combine all groups found per .obj file into one mesh as a single GameObject. Otherwise each group will result in a separate

GameObject. Combining multiple groups into one object will fail if it causes the number of vertices to exceed MaxPoints.

- *UseSubmeshesWhenCombining*: It is only used if *CombineMultipleGroups* is checked. It makes each group into a submesh on a single GameObject. If it's not checked, then using *CombineMultipleGroups* will result in a single mesh with a single material, regardless of what an associated .mtl file might contain.
- *UseFileNameAsObjectName*: It will cause any generated GameObjects to be named with the actual file name of the .obj file (without extension). If unchecked, the GameObjects will be named by group names that are supplied in the .obj file.
- *ComputeTangents*: If checked, will cause tangents to be calculated for each object.
- *UseSuppliedNormals*: It will cause ObjReader to use any normals that may be supplied by the .obj file. Otherwise, normals are calculated instead (using Unity's *RecalculateNormals* function).
- *OverrideDiffuse*: If checked, will discard any diffuse color supplied by MTL files in favor of the Main Color used on any materials that you supply.
- *OverrideSpecular*: If checked, will discard any specular color supplied by MTL files in favor of the Specular Color used on any materials that you supply.
- *OverrideAmbient*: If checked, will discard any ambient color supplied by MTL files in favor of the Emissive Color used on any materials that you supply.
- *SuppressWarnings*: It will prevent any standard ObjReader warnings from being printed.
- *UseMTLFallback*: If checked, will use the standard material in such case as an MTL file is specified in the OBJ file, but is missing. If *useMTLFallback* is not checked, then missing MTL files will generate an error.
- *AutoCenterOnOrigin*: If checked, will physically move the vertices so the object is centered on (0, 0, 0).
- *ScaleFactor*: It is a Vector3 that scales the resulting object meshes by the specified amount on the x, y, and z axes.
- *ObjRotation*: It will rotate the resulting object meshes around the specified x, y, and z axes.
- *ObjPosition*: It does the same thing for the position of object meshes. If the .obj file is off-center, you can compensate by using *ObjPosition* to move the mesh to the desired location.

The Object Manager uses the *OBJReader* method to load the file `Vol_0_1_0.obj` into the scene. It will first remove the 3D model loaded in the scene and then simply pass this file name to the *OBJReader*.

Reset Camera

This is the simplest component created to Reset the Leap Motion Camera Position to the starting point from where the user started navigating. This component is attached to the *Reset* button in the *UI Control Panel*. It implements a function which changes the position transform of the Leap Motion Camera i.e., *LMHeadMountedRig* back to origin of the 3D space i.e., $x=0.0$, $y=0.0$, $z=0.0$ (see Fig. 10.5).

10.5 Challenges

Importing all the 3D models in the Project Window

To switch to different resolution models, it is important that I have those models loaded in the Project window like imported Assets. However, the 3D models created by the Image Processing Pipeline for the whole mouse brain structure is a huge amount of data. Unity cannot accommodate such a huge number of models. Thus, I loaded the models into the scene directly without importing them. I loaded the models from the local disk of the computer where all the 3D models of all the resolutions are stored. The loading happens during run-time using an imported *OBJReader* Asset. *OBJReader* allows to load 3D models in a scene at run-time from local files or the web.

Loading the huge Mouse Brain models into the scene

The *OBJReader* can load the 3D models into the scene during run-time. However, it has a limitation to the number of vertices to be loaded in one model, i.e., 65000. All the 3D models created for the Mouse Brain Vasculature has a lot more than 65000 vertices. This poses a big problem of improper data input for the *OBJReader*. This issue is resolved by splitting the 3D models into separate sections, each section having a maximum of 65000 vertices. Usually, Unity performs this splitting when a 3D model is imported in the project window. But since I am directly loading the models from the local disk space at run-time, Unity's mesh splitting is overridden. I performed the splitting of OBJ models using a third-party tool called *Blender*. It is a time-taking, complicated and manual process of splitting in *Blender*, but this was the only solution feasible in the available time.

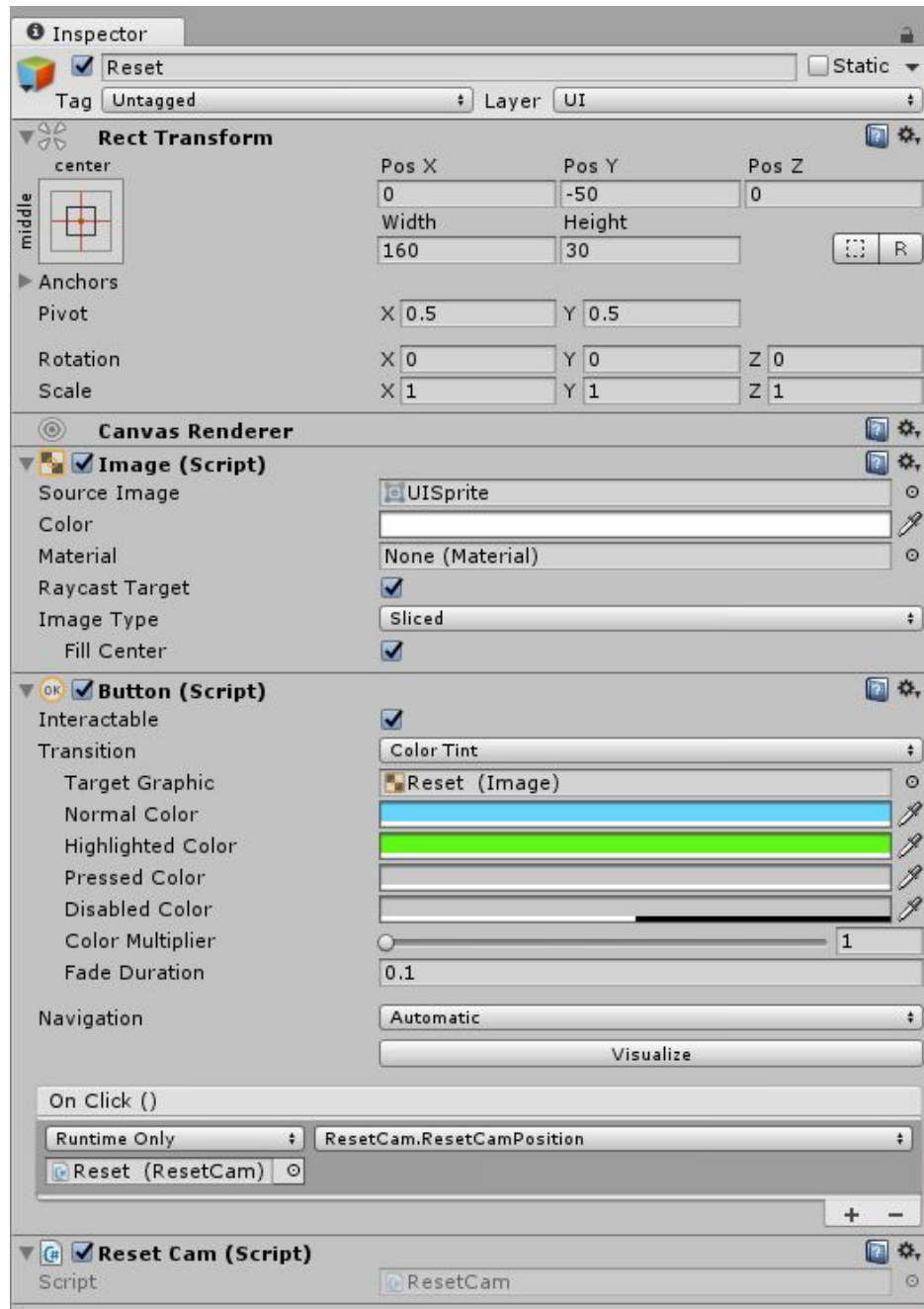


Figure 10.5: Reset Camera component options in the inspector window.

Part V

Conclusion and Future Work

Chapter 11

Conclusion and Future Work

11.1 Image Processing Pipeline Improvement

Although the design of the IEROM image processing pipeline explained in this thesis, performs all the necessary steps to produce a meaningful dataset for biomedical research and study. However, the pipeline still needs correction to incorporate ways to create much clearer datasets. It was observed that the use of *Binary Filter* during the image stitching process, had a bad impact (overcrowding issue) later on the lower resolution image stacks or volumes. Therefore, it is required to find a different approach in the future, to get a clear contrast between the background noise and foreground data without hampering the image quality in total.

The 3D Model Maker block in the image processing pipeline needs the further additional implementation to support creating other volume file formats like OBJ (Wavefront .obj), VTK (Visualization Toolkit), etc. Being able to create different file formats provides more options to use different platforms for visualization, for a much comprehensive study of teravoxel volumes of multi-modalities. OBJ file formats are also required to support VR framework development in Unity.

11.2 Web-Based Framework Additions

The 3D Brain Atlas created for the 3D real-time visualization of the teravoxel volumes loads a particular data or volume file at a time and performs basic interaction with it. However, the web-page needs the additional implementation to be able to show the morphological details of the STL mesh loaded to the renderer.

Addition of a Mesh Details Tab

This tab could be read-only for the user to learn more about the morphological details of the mesh loaded by the renderer. As a part of previous research work done in my lab, a research

student had worked on extracting details of the *unit-volumes* of the mouse brain vasculature using a 3D Analysis Software called Vaa3D [32]. The details of the extracted features were saved in .JSON files, one file per *unit-volume*. The *Mesh Details* tab could showcase that information such as number of branches, number of nodes, number of compartments in a segment, etc. In short, the .JSON file data could be used as input to this tab and be displayed in the web-page every time an STL mesh is loaded.

11.3 Virtual Reality Framework Additions

Dataset Creation

The VR framework designed for the course of this thesis lacks enough dataset. I manually created some OBJ files from the STL meshes generated by the IEROM image processing pipeline, using a tool called "Meshlab". Either the IEROM image processing pipeline needs an additional implementation to generate 3D models of OBJ format to support VR framework development in Unity. Or, using a third-party tool like Meshlab, all the STL meshes have to be converted manually into OBJ models.

Even when we can generate all the OBJ models, we cannot import them as assets in Unity, due to memory constraints (as explained in Chapter 10). So, the idea proposed was to be able to load the OBJ models directly from the local disk space by the *OBJReader*. While doing that, Unity's way of mesh splitting is overwritten. So, it is required to make sure the models are split into sections of 65000 vertices (at max.) before they are loaded in the scene. I used a tool called *Blender*, to manually perform the splitting, but I could only do it for two models to be able to finish my experiment in the available time and provide a proof-of-concept. In the future, it is required to implement a way to perform the splitting for all the multi-resolution OBJ models in a more time-efficient way.

Data Mapping for Higher Resolutions

The Data Mapping concept proposed in Chapter 10 is without an actual implementation due to lack of dataset. It needs to be implemented in the future to be able to switch between multi-resolution dataset and be able to have a fully-realized interactive analysis method in the VR space.

11.4 Conclusion

In conclusion, during the course of this thesis, a complete image processing pipeline was proposed, designed and utilized for generating the meaningful dataset. This pipeline was tested with IEROM output raw data for the study and analysis of the mouse brain vasculature networks. The pipeline converted the raw images into teravoxel-sized volumes. However, the

proposed pipeline can be executed for any large biomedical dataset. Two methods of 3D real-time visualization methods are proposed and implemented:

- 3D real-time web-based visualization method is proposed and implemented to be able to visualize and analyze the teravoxel-sized biomedical datasets, and at the same time, be able to study and collaborate with research communities across the globe.
- Virtual Reality framework is proposed and implemented for 3D visualization and much real interaction with the teravoxel-sized volumes. One can walk through inside-out the volume model and select a region-of-interest for the study and analysis.

Part VI
Appendix

Appendix A

Image Processing Pipeline Code

A.1 Image Stitcher block

ImageStitcher

- ImageStitcher is a C++ program, written using QtCreator 3.5.1
- Repository: <https://github.com/akankshaashwini/ImageStitcher>

A.2 Sub Sampler block

DownScaler

- SubSampler worker program written in C++, using QtCreator 3.5.1
- Repository:
<https://github.com/akankshaashwini/SubSampler/tree/master/DownScaler>

DownScalerController

- SubSampler controller program written in C++, using QtCreator 3.5.1
- Repository:
<https://github.com/akankshaashwini/SubSampler/tree/master/DownScalerController>

A.3 Unit Volume Maker Block

VolumeMaker

- VolumeMaker worker program written C++, using QtCreator 3.5.1

- Repository:
<https://github.com/akankshaashwini/UnitVolumeMaker/tree/master/VolumeMaker>

VolumeMakerController

- VolumeMaker controller program written C++, using QtCreator 3.5.1
- Repository:
<https://github.com/akankshaashwini/UnitVolumeMaker/tree/master/VolumeMakerController>

A.4 3D Model Maker Block

3DModelMaker

- 3DModelMaker worker program written C++, using QtCreator 3.5.1
- Repository:
<https://github.com/akankshaashwini/ModelMaker/tree/master/3DModelMaker>

3DModelMakerController

- 3DModelMaker controller program written C++, using QtCreator 3.5.1
- Repository:
<https://github.com/akankshaashwini/ModelMaker/tree/master/3DModelMakerController>

Appendix B

Web-based GUI Code

B.1 3D Brain Atlas

- Web-based 3D visualization framework written in Javascript
- Webpage: <http://jrkwon.com/3dbrainatlas>
- Repository: <https://github.com/akankshaashwini/3DBrainAtlas>

Appendix C

Virtual Reality Framework Code

- Gesture controlled navigation and GUI based data switching
- Scripts are written in C#, using monoscript editor
- Scenes are designed in Unity
- Respository: https://github.com/akankshaashwini/VR_GCNavigation

Bibliography

- [1] James Ahrens et al. *36-ParaView: An End-User Tool for Large-Data Visualization*. 2005.
- [2] Akanksha Ashwini and Jaerock Kwon. “Image Processing Pipeline for Web-Based Real-Time 3D Visualization of Teravoxel Volumes”. In: *International Conference on Data Mining and Big Data*. Springer. 2018, pp. 203–212.
- [3] Vadim Astakhov et al. “Data integration in the biomedical informatics research network (BIRN)”. In: *International Workshop on Data Integration in the Life Sciences*. Springer. 2005, pp. 317–320.
- [4] *Brain Networks Laboratory*. URL: <http://research.cs.tamu.edu/bnl/static/home.html>.
- [5] Alessandro Bria, Giulio Iannello, and Hanchuan Peng. “An open-source VAA3D plugin for real-time 3D visualization of terabyte-sized volumetric images”. In: *Biomedical Imaging (ISBI), 2015 IEEE 12th International Symposium on*. IEEE. 2015, pp. 520–523.
- [6] Yoonsuck Choe et al. “Complete submicrometer scans of mouse brain microstructure: neurons and vasculatures”. In: *Neuroscience Meeting Planner, Chicago, IL: Society for Neuroscience*. 2009.
- [7] Yoonsuck Choe et al. “Multiscale imaging, analysis, and integration of mouse brain networks”. In: *Neuroscience Meeting Planner*. Society for Neuroscience San Diego, CA. 2010.
- [8] Yoonsuck Choe et al. “Specimen preparation, imaging, and analysis protocols for knife-edge scanning microscopy”. In: *Journal of visualized experiments: JoVE* 58 (2011).
- [9] Ji Ryang Chung et al. “Multiscale exploration of mouse brain microstructures using the knife-edge scanning microscope brain atlas”. In: *Frontiers in neuroinformatics* 5 (2011).
- [10] *dat.GUI A lightweight graphical user interface for changing variables in JavaScript*. <http://workshop.chromeexperiments.com/examples/gui/#1--Basic-Usage>. Accessed: 2016-06-11.
- [11] Ciro Donalek et al. “Immersive and collaborative data visualization using virtual reality platforms”. In: *Big Data (Big Data), 2014 IEEE International Conference on*. IEEE. 2014, pp. 609–614.

- [12] David A Gutman et al. “Web based tools for visualizing imaging data and development of XNATView, a zero footprint image viewer.” In: *Frontiers in neuroinformatics* 8 (2013), pp. 53–53.
- [13] Daniel Haehn et al. “Neuroimaging in the browser using the x toolkit”. In: *Frontiers in Neuroinformatics* 101 (2014).
- [14] *How to use Oculus Rift remote*. URL: <https://www.vrfocus.com/2017/07/a-guide-to-the-oculus-remote-for-oculus-rift/>.
- [15] G Allan Johnson et al. “Waxholm space: an image-based reference for coordinating mouse brain research”. In: *Neuroimage* 53.2 (2010), pp. 365–372.
- [16] David B Keator et al. “A national human neuroimaging collaboratory enabled by the Biomedical Informatics Research Network (BIRN)”. In: *IEEE Transactions on Information Technology in Biomedicine* 12.2 (2008), pp. 162–172.
- [17] Jaerock Kwon et al. “Automated lateral sectioning for knife-edge scanning microscopy”. In: *Biomedical Imaging: From Nano to Macro, 2008. ISBI 2008. 5th IEEE International Symposium on*. IEEE. 2008, pp. 1371–1374.
- [18] *Leap Motion Asset in Unity*. URL: <http://blog.leapmotion.com/unity-core-assets-101-start-building-vr-project/>.
- [19] *LeapMotionController*. URL: <https://youtu.be/OUdL3y-mrFM>.
- [20] Ed S Lein et al. “Genome-wide atlas of gene expression in the adult mouse brain”. In: *Nature* 445.7124 (2007), pp. 168–176.
- [21] David Lesage et al. “A review of 3D vessel lumen segmentation techniques: Models, features and extraction schemes”. In: *Medical image analysis* 13.6 (2009), pp. 819–845.
- [22] Fuhui Long, Jianlong Zhou, and Hanchuan Peng. “Visualization and Analysis of 3D Microscopic Images”. In: *PLOS Computational Biology* 8 (6 2012). DOI: [10.1371/journal.pcbi.1002519](https://doi.org/10.1371/journal.pcbi.1002519).
- [23] Allan MacKenzie-Graham et al. “The informatics of a C57BL/6J mouse brain atlas”. In: *Neuroinformatics* 1.4 (2003), pp. 397–410.
- [24] David Mayerich, L Abbott, and B McCormick. “Knife-edge scanning microscopy for imaging and reconstruction of three-dimensional anatomical structures of the mouse brain”. In: *Journal of microscopy* 231.1 (2008), pp. 134–143.
- [25] David Mayerich, Bruce H McCormick, and John Keyser. “Noise and artifact removal in knife-edge scanning microscopy”. In: *Biomedical Imaging: From Nano to Macro, 2007. ISBI 2007. 4th IEEE International Symposium on*. IEEE. 2007, pp. 556–559.
- [26] Bruce H McCormick et al. “Construction of anatomically correct models of mouse brain networks”. In: *Neurocomputing* 58 (2004), pp. 379–386.
- [27] Shawn Mikula et al. “Internet-enabled high-resolution brain mapping and virtual microscopy”. In: *Neuroimage* 35.1 (2007), pp. 9–15.

- [28] Xing Ming et al. “Rapid reconstruction of 3D neuronal morphology from light microscopy images with augmented rayburst sampling”. In: *PloS one* 8.12 (2013), e84557.
- [29] *Node.js is a JavaScript runtime built on Chrome’s V8 JavaScript engine*. <http://nodejs.org>. Accessed: 2016-06-11.
- [30] *Oculus Setup Documentation*. URL: https://www.oculus.com/rift/setup/?locale=en_US.
- [31] Hanchuan Peng et al. “Extensible visualization and analysis for multidimensional images using Vaa3D”. In: *Nature protocols* 9.1 (2014), pp. 193–208.
- [32] Shruthi Raghavan and Jaerock Kwon. “Fully Automated Image Preprocessing for Feature Extraction from Knife-Edge Scanning Microscopy Image Stacks”. In: ().
- [33] F. Ritter et al. “Medical Image Analysis”. In: *IEEE Pulse* 2.6 (Nov. 2011), pp. 60–70. ISSN: 2154-2287. DOI: [10.1109/MPUL.2011.942929](https://doi.org/10.1109/MPUL.2011.942929).
- [34] Glenn D Rosen et al. “The mouse brain library@ www. mbl. org”. In: *Int Mouse Genome Conference*. Vol. 14. 2000, p. 166.
- [35] Tarek Sherif et al. “BrainBrowser: distributed, web-based neurological data visualization.” In: *Frontiers in neuroinformatics* 8 (2013).
- [36] *Unity Documentation*. URL: <https://docs.unity3d.com/Manual/UnityOverview.html>.
- [37] *VR Setup for Leap Motion Controller*. URL: <https://developer.leapmotion.com/vr-setup>.
- [38] Mingrui Xia, Jinhui Wang, and Yong He. “BrainNet Viewer: a network visualization tool for human brain connectomics”. In: *PloS one* 8.7 (2013), e68910.
- [39] *XTK The X Toolkit: WebGLTM for Scientific Visualization*. <http://github.com/xtk/X>. Accessed: 2016-06-11.